

**Discriminant Training of Front-End and Acoustic Modeling Stages to
Heterogeneous Acoustic Environments for Multi-stream Automatic
Speech Recognition**

by

Michael Lee Shire

B.S. (University of California, San Diego) 1991

M.S. (University of California, Berkeley) 1997

A dissertation submitted in partial satisfaction of the
requirements for the degree of
Doctor of Philosophy

in

Engineering - Electrical Engineering and Computer Science

in the

GRADUATE DIVISION

of the

UNIVERSITY OF CALIFORNIA, BERKELEY

Committee in charge:
Professor Nelson Morgan, Chair
Professor David Wessel
Professor Hynek Hermansky
Professor Jitendra Malik
Professor Steven Greenberg

Fall 2000

The dissertation of Michael Lee Shire is approved:

Chair

Date

Date

Date

Date

Date

University of California, Berkeley

Fall 2000

**Discriminant Training of Front-End and Acoustic Modeling Stages to
Heterogeneous Acoustic Environments for Multi-stream Automatic
Speech Recognition**

Copyright 2000

by

Michael Lee Shire

Abstract

Discriminant Training of Front-End and Acoustic Modeling Stages to Heterogeneous Acoustic Environments for Multi-stream Automatic Speech Recognition

by

Michael Lee Shire

Doctor of Philosophy in Engineering - Electrical Engineering and Computer Science

University of California, Berkeley

Professor Nelson Morgan, Chair

Automatic Speech Recognition (ASR) still poses a problem to researchers. In particular, most ASR systems have not been able to fully handle adverse acoustic environments. Although a large number of modifications have resulted in increased levels of performance robustness, ASR systems still fall short of human recognition ability in a large number of environments. A possible shortcoming of the typical ASR system is the reliance on a single stream of front-end acoustic features and acoustic modeling feature probabilities. A single front-end feature extraction algorithm may not be capable of maintaining robustness to arbitrary acoustic environments. Acoustic modeling will also degrade due to distributional changes caused by the acoustic environment. This thesis explores the parallel use of multiple front-end and acoustic modeling elements to improve upon this shortcoming. Each ASR acoustic modeling component is trained to estimate class posterior probabilities in a particular acoustic environment. In addition to discriminative training of the probability estimator, existing feature extraction algorithms are modified in such a way as to improve class discrimination in the training environment. More specifically, Linear Discriminant Analysis provides a mechanism for obtaining discriminant temporal basis functions that can replace components of the existing algorithms that were designed in either an empirical or intuitive manner. Probability streams are generated using multiple front-end acoustic modeling stages trained to heterogeneous acoustic environments. In new sample acoustic environments, simple combinations of these probability streams give rise to word

recognition rates that are superior to the individual streams.

Professor Nelson Morgan
Dissertation Committee Chair

*For my mother Arsenia,
my father Arlen
my sister Miriam
and my brother Aaron*

Contents

List of Figures	vi
List of Tables	ix
1 Introduction	1
1.1 Multi-Stream ASR	3
1.2 Acoustic Environments	7
1.3 Overview	9
2 Automatic Speech Recognition	11
2.1 Probability Estimation	15
2.2 Speech Feature Extraction	17
2.2.1 Time-Frequency Analysis	18
2.2.2 Feature Orthogonalization	21
2.2.3 Frequency Smoothing	24
2.2.4 Temporal Processing	26
2.2.5 Complete Algorithms	29
2.3 Acoustic Environments	34
2.4 Experimental Setup	39
2.4.1 Speech Corpora	40
3 LDA Temporal Filters for RASTA-PLP	42
3.1 Temporal Filter Design with Linear Discriminant Analysis	42
3.2 Temporal LDA Filters in Varying Acoustic Conditions	44
3.2.1 Clean Speech Data	44
3.2.2 Reverberated Speech Data	45
3.2.3 Speech Data With Added Noise	46
3.2.4 Varying Noise SNR and Reverberation Parameters	46
3.3 Recognition Results	51
3.3.1 Initial Experiments	51
3.3.2 Recognition with Local Normalization	56
3.3.3 Performance of Individual LDA Filters	61
3.4 Discussion	64

4	LDA temporal filters with PLP and MSG	68
4.1	Logarithm of the Power Spectra	68
4.2	Delta Calculation with Perceptual Linear Prediction	71
4.3	Temporal Filtering with the Modulation-Filtered Spectrogram	77
4.4	Discussion	81
5	Multi-Stream Recognition Tests	85
5.1	Simple Combination Strategies	86
5.2	Multi-Stream Experiments with RASTA-PLP	90
5.2.1	Combining Heterogeneously Trained MLPs with Identical Feature Processing	91
5.2.2	Training an MLP on Data from Two Conditions	92
5.3	RASTA-PLP with Different LDA Filters	93
5.3.1	Dual LDA Filter Sets with Common MLP Training Environment	94
5.3.2	Matched LDA Filter and MLP Training Environments	96
5.4	PLP and MSG	99
5.4.1	Dual-stream PLP and MSG with Common MLP Training Environment	100
5.4.2	PLP and MSG with Heterogeneously Trained MLPs	100
5.4.3	Four Stream Combination	103
5.5	Weighted Stream Combinations	104
5.5.1	Weighting Based on Frame-Level Confidence	106
5.6	Final Tests with Unseen Conditions and Best Stream Combination	111
5.7	Discussion	115
6	Conclusion	119
6.1	Discriminant Feature Extraction	120
6.2	Multi-Stream Combinations	121
6.3	Contribution and Future Work	123
A	Recognition Units	125
B	Temporal LDA Filters with Phonetic Units	128
C	Temporal LDA Filters with Syllabic Units	132
D	Temporal LDA Filters for PLP	135
E	Correlating Frame Accuracy and Word Error	137
E.1	Method	138
E.2	Experiments	139
E.3	Discussion	147
	Bibliography	148

List of Figures

1.1	The typical ASR system relies on a single stream of probability estimates based on a fixed preprocessing.	2
1.2	New ASR systems will incorporate a variety of knowledge sources to aid in speech recognition. This system has multiple front-end acoustic modeling stages.	3
1.3	Speech features from different acoustic environments can exhibit different feature distributions.	7
1.4	In addition to the non-linear discrimination used in the MLP along the frequency-related dimension, we apply discriminant training along the time dimension.	8
2.1	Abstract depiction of a typical ASR system.	12
2.2	Hidden Markov Model.	13
2.3	Fully connected multi-layer perceptron.	16
2.4	Integration windows of critical-band-like ranges spaced at 1 Bark intervals.	20
2.5	Dimensions of maximum variance and linear separability may not coincide.	24
2.6	Impulse and frequency response for standard RASTA filter.	28
2.7	Processing steps for RASTA-PLP.	30
2.8	Processing steps for the MSG features.	32
2.9	Processing diagram for online normalization.	34
2.10	Processing schematic for AGC.	35
2.11	Log-power trajectory of 3 seconds of the same utterance under the original <i>clean</i> condition, with added <i>factory</i> noise at 10 dB SNR, and lightly reverberated with a characteristic reverberation time of 0.5 seconds. The utterance is of a male speaker saying “Well, uh, maybe I should tell ya about how...”	35
2.12	Log-power trajectory of same utterance as in Figure 2.11 under severely reverberated condition (characteristic reverberation time of 2.5 seconds).	36
2.13	Average spectral power for <i>car</i> and <i>factory</i> noise.	38
3.1	LDA is applied to the temporal trajectories of the log-critical-band energy. Linguistic classes are assigned to the center of relatively long time spanning windows of trajectories. Means μ and covariances Σ are collected for each class.	43

3.2	Averaged impulse and frequency responses for LDA filters derived with <i>clean</i> data.	45
3.3	Impulse and frequency responses for averaged LDA filters derived with reverberated data.	47
3.4	Impulse and frequency responses for filters derived from speech data with added noise.	48
3.5	Impulse and frequency responses for filters derived with varying <i>car</i> noise SNR, reverberation T60, reverberation DTR, and reverberation T60 and DTR.	50
3.6	Impulse and frequency responses when varying the proportion of <i>clean</i> and <i>heavy</i> reverberated training data.	52
3.7	The RASTA filter is replaced by filters derived from LDA based on the Stories corpus. Recognition tests used the NUMBERS corpus.	53
3.8	Feature distributions from speech distorted by environmental conditions can be warped to match an undistorted distribution.	57
3.9	Examples of the histogram distribution of first cepstral coefficient for PLP and RASTA-PLP before and after per-utterance local normalization.	58
4.1	Histogram distributions of the critical-band output centered at 570 Hz, and subjected to cube-root, eighth-root and logarithmic compression. The distributions are for the phones /ow/, /eh/, /n/, /r/, /s/, and /k/. Ranges and densities are scaled individually for comparison.	69
4.2	Skewness and Kurtosis statistics of the critical-band output centered at 570 Hz, and subjected to cube root, eighth root, and logarithm for the phones /ow/, /eh/, /n/, /r/, /s/, and /k/.	70
4.3	The delta calculation for PLP is replaced by temporal filters derived from LDA	75
4.4	Histogram distributions of the first, fourth, and seventh PLP cepstral coefficient. The distributions are for the phones /ow/, /eh/, /n/, /r/, /s/, and /k/. Ranges and densities are scaled individually for comparison.	76
4.5	The lowpass and bandpass filters in MSG are replaced by filters derived using LDA.	77
4.6	The fundamental frequency of the input remains after application of a non-linearity, but with added harmonics.	78
4.7	Difference between the frame accuracy of individual phones for MSG with and without LDA filters. Positive bars indicate MSG-LDA had higher frame accuracy.	82
5.1	Comparison of RASTA-PLP with LDA-RASTA-PLP using average and log-average posterior combination. Significant improvement is marked with an arrow.	99
5.2	Frame accuracy and WER for a range of artificial reverberant conditions using a weighted log-average between two LDA-RASTA-PLP streams trained on <i>clean</i> and <i>heavy</i> reverberation data. Tests performed on room impulses with DTR = -8 dB.	105

5.3	Frame accuracy and WER for a range of artificial reverberant conditions using a weighted log-average between two LDA-RASTA-PLP streams trained on <i>clean</i> and <i>heavy</i> reverberation data. Tests performed on room impulses with $T60 = 2$ sec.	106
5.4	Frame accuracy and WER for a range of artificial reverberant conditions using a weighted log-average between PLP and MSG streams trained on <i>clean</i> and <i>heavy</i> reverberation data respectively. Tests performed on room impulses with $DTR = -8$ dB.	107
5.5	Frame accuracy and WER for a range of artificial reverberant conditions using a weighted log-average between PLP and MSG streams trained on <i>clean</i> and <i>heavy</i> reverberation data respectively. Tests performed on room impulses with $T60 = 2$ sec.	107
B.1	Impulse and frequency responses for first three LDA filters derived with <i>clean</i> data.	129
B.2	Impulse and frequency responses for first three LDA filters derived with <i>heavy</i> reverberated data.	130
B.3	Impulse and frequency responses for first three LDA filters derived with <i>factory</i> noise data at 10 dB SNR.	131
C.1	First three LDA filters derived with syllable targets on <i>clean</i> data.	133
C.2	Comparison of averaged filters using syllable targets in different noise conditions.	134
D.1	First three LDA filters derived from PLP cepstra on <i>clean</i> data.	136
E.1	Histogram of WER for 500 recognition runs. In each run random incorrect frames were corrected to yield a frame accuracy of 70%.	139
E.2	WER for one recognition run of randomly chosen corrected frames where the value of the posterior placed corrected frames was varied.	140
E.3	WER for 20 recognition runs with a varying proportion of corrected silence frames.	141
E.4	WER for 20 recognition runs with a varying proportion of vowel frames corrected.	143
E.5	WER for 20 recognition runs with a varying proportion of vowel frames corrected. All silence frames were corrected independently.	143
E.6	WER for 20 recognition runs with a varying proportion of vowel frames corrected. All incorrect silence frames were left uncorrected.	144
E.7	WER for 20 recognition runs with a varying proportion of the corrected frames that bordered phone transitions in the hand transcription of the NUMBERS corpus.	145
E.8	WER for 20 recognition runs with a varying proportion of the corrected frames that were within 2 frames from phone transitions in the hand transcription of the NUMBERS corpus.	146

List of Tables

2.1	Description of noise conditions.	38
3.1	Frame accuracy results using RASTA-PLP, preliminary tests.	54
3.2	Word recognition results using RASTA-PLP, preliminary tests.	54
3.3	Frame accuracy results using LDA-RASTA-PLP, preliminary tests. The +(-) annotations mark significantly better(worse) performance than RASTA-PLP without LDA in Table 3.1.	55
3.4	Word recognition results using LDA-RASTA-PLP, preliminary tests. The +(-) annotations mark significantly better(worse) performance than RASTA-PLP without LDA in Table 3.2.	55
3.5	Frame accuracy results using RASTA-PLP, with per-utterance normalization.	59
3.6	Word recognition results using RASTA-PLP, with per-utterance normaliza- tion.	59
3.7	Frame accuracy results using LDA-RASTA-PLP, with per-utterance nor- malization. The +(-) annotations mark significantly better (worse) per- formance than RASTA-PLP without LDA in Table 3.5.	60
3.8	Word recognition results using LDA-RASTA-PLP, with per-utterance nor- malization. The +(-) annotations mark significantly better (worse) per- formance than RASTA-PLP without LDA in Table 3.6.	60
3.9	Frame accuracy using LDA filters derived from reverberant data and an MLP with a single frame of input features. The +(-) annotations mark where results using the <i>light</i> and <i>heavy</i> filters are significantly better (worse) than when using the <i>clean</i> filter.	63
3.10	WER using LDA filters derived from reverberant data and an MLP with a single frame of input features. The +(-) annotations mark where results using the <i>light</i> and <i>heavy</i> filters are significantly better (worse) than when using the <i>clean</i> filter.	63
3.11	Frame accuracy using LDA filters derived with reverberant data and MLP context window of 9 frames.	65
3.12	WER using LDA filters derived with reverberant data and MLP context window of 9 frames.	65

4.1	Frame accuracy results using PLP with per-utterance normalization. The +(-) annotations mark where the performance is significantly better(worse) than the RASTA-PLP with per-utterance normalization in Table 3.5. . . .	72
4.2	Word recognition results using PLP with per-utterance normalization. The +(-) annotations mark where the performance is significantly better(worse) than the RASTA-PLP with per-utterance normalization in Table 3.6. . . .	72
4.3	Comparison of PLP with delta features and PLP with LDA filters. MLP was trained with single frame context of acoustic features. The +(-) annotations mark where PLP with the LDA is significantly better(worse) than PLP with Δ s.	74
4.4	Comparison of original MSG and MSG with LDA-derived filters. MLP trained on acoustic context of 9 frames. The +(-) annotations mark where the MSG with LDA filters is significantly better(worse) than the original MSG.	80
4.5	Frame accuracy and WER with corrected silence phones for MSG and MSG-LDA.	83
5.1	Results when combining two trained MLPs at the frame level. One MLP is trained with <i>clean</i> data and the other with <i>heavy</i> reverberation data. RASTA-PLP features were used for both conditions. The “+” annotations mark where the combinations in the unseen <i>light</i> reverberation testing case are significantly better than both of the singly trained MLPs.	91
5.2	Word error results with a single MLP with twice the number of parameters trained with <i>clean</i> data, <i>heavy</i> reverberation data, and both.	92
5.3	WER Results from a frame-level combination of LDA-RASTA-PLP with LDA filters derived under <i>clean</i> and <i>heavy</i> reverberation conditions. The MLP probability estimator was trained with <i>clean</i> data and a single frame of acoustic features. The “+” annotations mark where the combinations are better than the single streams.	95
5.4	WER Results from a frame-level combination of LDA-RASTA-PLP with LDA filters derived under <i>clean</i> and <i>heavy</i> reverberation conditions. The MLP probability estimator was trained with <i>light reverberation</i> data and a single frame of acoustic features. The “+” annotations mark where the combinations are better than the single streams.	95
5.5	WER Results from a frame-level combination of LDA-RASTA-PLP with LDA filters derived under <i>clean</i> and <i>heavy</i> heavy reverberation conditions. The MLP probability estimator was trained with <i>heavy reverberation</i> data and a single frame of acoustic features. The “+” annotations mark where the combinations are better than the single streams.	95
5.6	WER Results from a frame-level combination of LDA-RASTA-PLP with LDA filters derived under <i>clean</i> and <i>heavy</i> reverberation conditions. The MLP probability estimator was trained with <i>clean</i> data and a context window of 9 frames. The “+” annotations mark where the combinations are better than the single streams.	97

5.7	WER Results from a frame-level combination of LDA-RASTA-PLP with LDA filters derived under <i>clean</i> and <i>heavy</i> reverberation conditions. The MLP probability estimator was trained with light reverberation data and a context window of 9 frames. The “+” annotations mark where the combinations are better than the single streams.	97
5.8	WER Results from a frame-level combination of LDA-RASTA-PLP with LDA filters derived under <i>clean</i> and <i>heavy</i> reverberation conditions. The MLP probability estimator was trained with heavy reverberation data and a context window of 9 frames. The “+” annotations mark where the combinations are better than the single streams.	97
5.9	Results from a frame-level combination of LDA-RASTA-PLP with LDA filters and an MLP trained under <i>clean</i> and <i>heavy</i> reverberation. The MLP had a single frame of acoustic features as input. The “+” annotation marks where the combination is significantly better than the single streams in the <i>light</i> reverberation test.	98
5.10	Results from a frame-level combination of LDA-RASTA-PLP with LDA filters and an MLP trained under <i>clean</i> and <i>heavy</i> reverberation. The MLP had an acoustic context of 9 frames. The “+” annotation marks where the combination is significantly better than the single streams in the <i>light</i> reverberation test.	98
5.11	WER Results from a frame-level combination of PLP and MSG with MLP probability estimators trained with clean data. The “+” annotation marks where the combination is significantly better than the single streams.	101
5.12	WER Results from a frame-level combination of PLP and MSG with MLP probability estimators trained with light reverberation data. The “+” annotation marks where the combination is significantly better than the single streams.	101
5.13	WER Results from a frame-level combination of PLP and MSG with MLP probability estimators trained with heavy reverberation data. The “+” annotation marks where the combination is significantly better than the single streams.	101
5.14	WER Results from a frame-level combination of PLP with its MLP trained on clean data and MSG with its MLP probability estimators trained with heavy reverberation data. The “+” annotation marks where the combination is significantly better than the single streams in the <i>light</i> reverberation test.	102
5.15	WER Results from a frame-level combination of PLP-LDA with its LDA filters and MLP trained on clean data and MSG-LDA with its LDA filters and MLP probability estimators trained with heavy reverberation data. The “+” annotation marks where the combination is significantly better than the single streams in the <i>light</i> reverberation test.	102
5.16	Comparison of frame accuracies for PLP with MSG combinations with and without LDA. The “+” annotation marks where the frame accuracy using LDA augmentation is significantly better than the original.	103

5.17	Four stream combination: PLP and MSG using both <i>clean</i> and <i>heavy</i> reverberation trained MLPs. The “+” annotation marks where the combination is significantly better than the single streams in the <i>light</i> reverberation test.	103
5.18	WER Results from a frame-level weighted log-average combination of LDA-RASTA-PLP with <i>clean</i> and <i>heavy</i> trained MLP and LDA filters using confidence based weighting. MLPs were trained with a single input frame of features. The “+” and “-” annotations mark two cases where the weighting produced WER that was respectively significantly better and worse than the equal weighting.	111
5.19	Final tests using four PLP and MSG streams trained in <i>clean</i> and <i>heavy</i> reverberation. Combination using log-average posteriors with equal weighting. The +(-) annotations mark where the log-average posterior merging produced WER that was significantly better (worse) than the single streams.	112
5.20	Combination of four PLP and MSG streams trained in <i>clean</i> and <i>heavy</i> reverberation with unequal weighting. Two <i>clean</i> streams weighted at 0.1 and <i>heavy</i> reverberation streams weighted at 0.4. The “+” annotations mark where the log-average posterior merging produced WER that was significantly lower than the single streams.	113
5.21	Final tests using four PLP and MSG streams trained in <i>clean</i> and the <i>moderately heavy</i> reverberation room impulse from the last row. Combinations used log-average posteriors with specified weighting. The + annotations mark where the log-average posterior merging produced WER that was significantly lower than the single streams.	114
A.1	Words contained in the subset of the OGI NUMBERS corpus used for word recognition experiments.	126
A.2	Set of phone classes used in ICSI recognition system.	127

Acknowledgments

This dissertation encompasses work from the final years of my graduate studies and was principally funded by the International Computer Science Institute (ICSI) and NSF Grant IRI-9712579. It would not have been possible were it not for many relationships with colleagues and friends that I developed and for which I am deeply grateful.

I am very much indebted to my advisor Nelson Morgan for his continual patronage, support and guidance over the span of my stay at U.C. Berkeley and ICSI. I consider myself extremely fortunate to have had an advisor who is approachable and always with practical advice, and who has been a reliable advocate for his students.

I would like to thank Steven Greenberg. I am continually impressed by his scholarship and extensive knowledge of literature regarding many aspects of audition and speech. His keen insights and attention to detail have constantly provided a sanity check for my work.

I would like to express my gratitude to Hynek Hermansky for his contagious enthusiasm and for the advisorial role he undertook while I conducted this research. Much of this dissertation owes to the excellent research by him and his students at the Oregon Graduate Institute (OGI). I would like to also acknowledge Narenderath Malayath, Sachin Kajarekar, Sangita Sharma, Sarel van Vuuren, and Carlos Avendaño from OGI for their helpful discussions.

I would like to thank David Wessel and Jitendra Malik for pleasantly serving on my thesis committee. I would also like to thank Jitendra Malik, Robert Brodersen, and Charles Stone for serving on my qualifying exam committee.

I conducted this research as a member of the ICSI Realization Group. ICSI provided a wonderful and rewarding environment for research. I am blessed to have been able to work alongside many gifted and supportive colleagues. I would like to acknowledge and thank the many members, past and present, who have all directly and indirectly contributed to my work in countless ways. Thanks go to Krste Asanovic, Jim Beck, Hervé Boulard, Michael Berthold, Shawn Chang, David Gelbart, Dan Gildea, Ben Gold, Andy Hatch, Joy Hollenback, Adam Janin, Dan Jurafsky, Yochai Konig, Kristine Ma, Nikki Mirghafori, Liz Schriberg, Rosaria Silipo, Andreas Stolcke, Gary Tajchman, Grace Tong, Warner Warren, Chuck Wooters, and Geoff Zweig. I'd like to give additional thanks to Brian Kingsbury, who provided me with reverberation material for my thesis; to Su-Lin

Wu, who provided the focus application for my early work with syllable-onset detection; to Barry Chen, my faithful Paduan learner and office mate, who helped me with many recent projects; to Eric Fosler-Lussier, the quintessential UNIX guru who kindly tolerated even my most inane system questions; and to Dan Ellis and Jeff Bilmes, brilliant, pleasant and prolific researchers and coders whose contributions to the ICSI speech software greatly facilitated my experiments. I have also benefited from help and interactions with Markham Dickey, Jane Edwards, Lila Finhill, David Johnson, Diane Pokorny, Maria Quintana the rest of the ICSI administrative staff.

As ICSI is an international research facility, I have had the privilege of meeting many international visitors. I would like to acknowledge Toshihiko Abe, Carmen Benitez, Stephane DuPont, Philipp Faerber, Javier Ferreiros Lopez, Jean Hennebert, Katrin Kirchhoff, Rainer Klisch, Hiroaki Ogawa, Florian Schiel, and Mirjam Wester for their friendly discussions. I'd like to give special thanks to Dominique Genoud and his family for their friendship and excellent wine. I also wish to express special appreciation to Takayuki Arai for his hospitality during my visits to his lab at Sophia University and to the members of his lab, especially Yuji Murahara and Akiko Kusumoto. I was also very fortunate to have spent several months on loan to Siemens ZT, AG in Munich and wish to thank my colleagues there, especially Josef Bauer, Joachim Köhler and Alfred Hauenstein.

I would lastly like to express my appreciation to my other friends and colleagues outside my field of specialization. Among my friends in the EECS department, special thanks go to Ron Galicia, Lillian Chu, Bill Chen, Tim Calahan, Nimish Shah, and Ruth Gjerd (the amiable interface between grad student and department). My community awareness and grad-school experience were significantly enhanced while I was a member and later principal coordinator of PANGIT and I am grateful to its former members. I am especially grateful to John Scott, the nuclear engineering bartender; Irene Soriano, always concerned with my social welfare; Jody and Marivi Blanco, with whom conversation was inexorably interesting; and Anatalio Ubalde, the consummate politician. Thanks also go to Maria Bates, Amanda Camposagrado, Glen Fajardo, Evelyn Rodriguez, and Erlene Scharff. My graduate school experience would have been neither enjoyable nor endurable were it not for these and other many friendships that I developed while at Berkeley.

Finally, I'd like to give my thanks to my many friends in San Diego and my love and thanks to my mother, father, sister, and brother who have all waited patiently for my life to begin.

Chapter 1

Introduction

For the past several decades, researchers have sought ways to automatically recognize and transcribe speech by machine. Continually improving techniques have raised the state of the art to achieving low error rates on a variety of tasks. Despite many advances, automatic speech recognition (ASR) still falls far short of the capability of humans [72]. This is often attributed to mismatches between the test material and the data used to train the recognizer. The mismatches are generally attributed to causes such as different environmental conditions and differing speaker characteristics. Because human recognition is typically much better in a wide range of acoustic environmental conditions, some of the problems may lie with how speech is analyzed and represented.

The typical ASR system proceeds along a single acoustic stream approach shown in Figure 1.1¹. First, a signal processing module extracts features from the speech. In Hidden Markov Model (HMM) systems or hybrid Artificial Neural Network - Hidden Markov Model (ANN-HMM) based systems, probabilities that a given set of generated features correspond to particular sub-word units are estimated and fed into the decoder. In Gaussian mixture model (GMM) systems the likelihood that the features are generated by a particular sub-word unit is estimated and used by the decoder². The feature extraction and probability estimation are commonly referred to as the *front-end* and *acoustic modeling* components of the ASR system. The decoder applies word models and grammar

¹This figure is an abstraction only; many systems have integrated some of these components and parameters. However, the principle is the same.

²Actually, scaled probabilities (whether posteriors from ANNs or likelihoods from GMMs) are commonly used in the decoding.

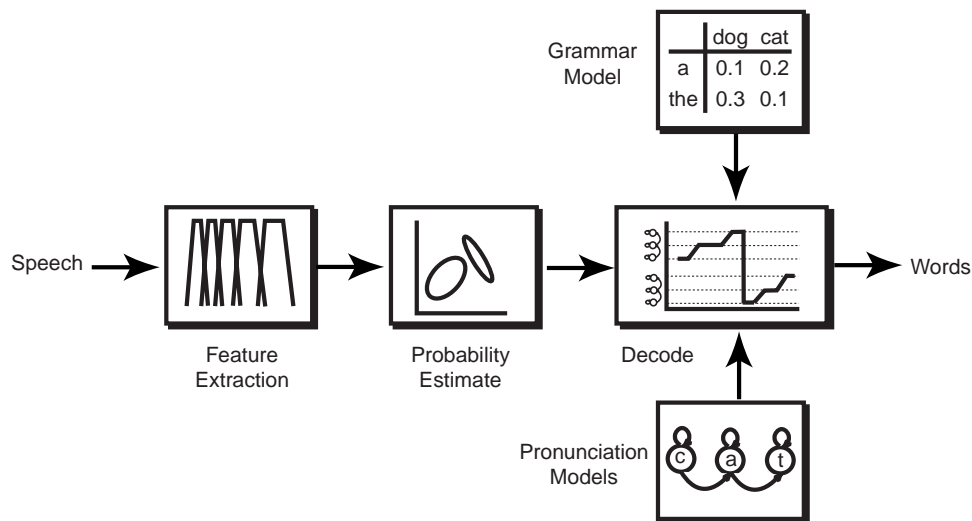


Figure 1.1: The typical ASR system relies on a single stream of probability estimates based on a fixed preprocessing.

constraints to the probability estimates to produce the most likely sequence of words. To handle differences between the training and testing data, researchers have experimented with modifications to each of the stages of the ASR system.

An inherent weakness in the typical system is that it relies on a single stream of acoustic information that is often insufficient to robustly handle all of the acoustic degradations encountered and completely characterize the words of the spoken utterance. A number of advances have been made in improving the robustness of the feature extraction algorithm and adapting the probability estimation. However, constructing a front-end algorithm that is robust to all unseen acoustic conditions is a daunting task. An alternate approach explored in this work is to use several front-end stages simultaneously. Each preprocessing stage would be designed or selected to maintain or improve recognition performance in a particular type of acoustic environment. Such a system falls within the realm of multi-stream ASR depicted in Figure 1.2. Though the number of acoustic environments is limitless, many of them degrade speech in systematic ways. Examples include additive noise and convolutional noise. Additive noise refers to the presence of sound from other sources that appear to the receiver in addition to the desired speech signal. Convolutional noise refers to the distortion of the speech signal caused by the transmission channel or transmission environment. A sampling of different styles of acoustic degradation may at the least increase the range over which the ASR system maintains performance. Unfor-

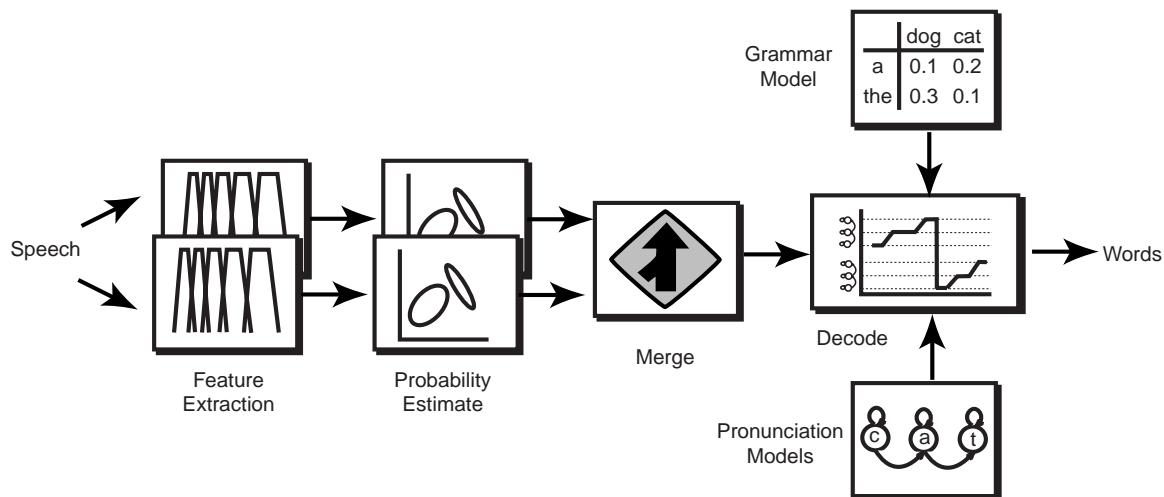


Figure 1.2: New ASR systems will incorporate a variety of knowledge sources to aid in speech recognition. This system has multiple front-end acoustic modeling stages.

Unfortunately, designing or selecting a preprocessing strategy that is robust to even a single acoustic condition remains a research issue. Rather than attempting to construct new feature-extractor stages we select, analyze, and adapt previous algorithms to specific conditions. In conjunction with this we tune the trainable parameters of the system to the specific acoustic condition.

1.1 Multi-Stream ASR

In recent years a number of researchers have independently investigated different approaches to incorporating additional knowledge sources and speech representations in to the ASR framework. Collectively, they suggest the utility of a parallelizable multi-stream approach to the recognition problem. Similar multi-stream and multi-classifier approaches have been explored extensively in other pattern recognition fields such as handwriting recognition [66, 86, 1, 73]. This section outlines some motivation for the multi-stream approach as well as related work.

Redundant Representations in the Human Auditory System

Just as speech is highly redundant, there is evidence to suggest that the human auditory system is also highly redundant [85, 37]. Numerous perceptual experiments have been conducted which systematically degrade speech in a variety of ways but where intelligibility was not significantly impaired. Such experiments include extreme low- and high-pass filtering of the speech signal [33, 2], filtering modulation energies [26, 5, 4], desynchronizing speech energy channels [44, 105], and minimizing spectral cues [40, 97, 72]. These experiments and many others suggest a redundancy in acoustic representation within the human auditory system such that when one or more representations are corrupted, enough additional representations remain robust enough to successfully decode the speech. Various physiological evidence suggests that the primary auditory cortex contains an elegant collection of repeated representations of the acoustic spectro-temporal information at various scales [112, 96, 39]. This redundancy of multi-scale representations is a key component in the ability of humans to recognize spoken utterances in acoustically adverse environments. For ASR systems to attain such robustness, it will probably be necessary to incorporate this style of multiple representations within the ASR framework.

Multiple Knowledge Sources

In terms of an engineering solution to the ASR problem, many researchers have already investigated incorporating additional knowledge sources into recognition systems. For example:

- Combined auditory and visual systems have been proposed for ASR improvement [77, 22, 16, 15]. Bregler and associates have used visual features from a lip-reading system to improve performance on a letter recognition task [14, 13].
- Segmental information derived from the speech has been successfully used as an additional knowledge source [120, 53].
- Wu and associates have successfully experimented with the incorporation of syllabic units in addition to phonetic units within the ASR framework [118, 117].

Combinations of Specialized Preprocessing

The feature extraction process has been continually refined over the years resulting in preprocessing systems that include perceptually inspired analysis and noise robustness (J-RASTA-PLP³ for example [67]). However, some have developed other preprocessing strategies based on alternate criteria. For instance, modulation spectral features that analyze longer time windows and display some invariance to reverberant conditions were developed by Kingsbury and Greenberg [62, 43]. Bilmes developed modulation correlation based features that capture some of the joint spectro-temporal distribution information [7]. Others have investigated the use of wavelet based features which provide some multi-resolution analysis of the speech, for example [112, 96]. Alone, these techniques provide encouraging recognition results. However, when some are combined with the more traditional feature extraction approaches such as Mel Cepstra and PLP, results improve even further, particularly when testing under conditions other than those originally trained on [7, 61]. This suggests that the alternate preprocessing strategies, though containing much overlapping information with the “standard” approaches, also contain information about speech cues that are not contained in the standard preprocessing or that may be more robust to a different set of adverse conditions.

Ensemble of Classifiers

In addition to supporting separate feature extraction procedures, researchers have frequently found advantages to supporting multiple classifiers. The multiple classifiers can operate on either identical, disjoint, or distinct but overlapping sets of classes and features. Some previous work involving multiple classifiers includes the following.

- Multiple classifiers have been used in speaker verification [100]. In speaker recognition task, arrays of binary classifiers have been used to distinguish hierarchically among speakers, for example in [18, 88].
- In multi-band analysis, the frequency space is partitioned into separate ranges and a separate classifier operates on each range to produce multiple probability estimates. This has been shown to reduce performance loss due to frequency localized noise

³RelAtive SpecTrAl - Perceptual Linear Prediction

[52, 107, 10, 11, 79].

- Multiple classifiers have been used to operate on separate sets of classes. For example, some have experimented combining classifiers trained to distinguish broad phonetic classes and articulatory features [64, 3]. Separate classifiers have also been used to separately classify transitional and non-transitional features for Chinese syllable recognition [123].
- Separate classifiers have been trained on separate data sets based on such criteria as gender and speaking rate to improve probability estimation [80]. Overall, recognition improved through a combination of the probability streams.
- Similar data space splitting has been done using an automatic hierarchical mixture of experts formulation [34] and using a boosting strategy with an ensemble of classifiers [114].

A common theme and motivation for choosing an array or committee of classifiers is that the inability of any single classifier to make the correct decision may be compensated for by another classifier. To illustrate, narrow-band noise in the features for a full-band classifier will affect the results for all of the classes. In the multi-band scenario, only one of the several classifiers will have results that are affected and overall performance of the ASR system will not degrade as rapidly. The machine-learning community has shown a growing interest in this mixture of experts philosophy.

Parallel Computation

Though increasing the number of preprocessing units, probability estimation units, and information sources will add to the computational load of the ASR system considerably, the parallel nature of the increase can be exploited accordingly. Most of the added processing is independent of others in the same stage and can be computed concurrently on additional computational hardware. The separate streams can be computed without an unreasonable increase in computation time. Furthermore, the nature of some of the processing is vectorizable and implementable over a networked facility or on vector hardware such as the SPERT [55], thereby offsetting some further increases in computation time.

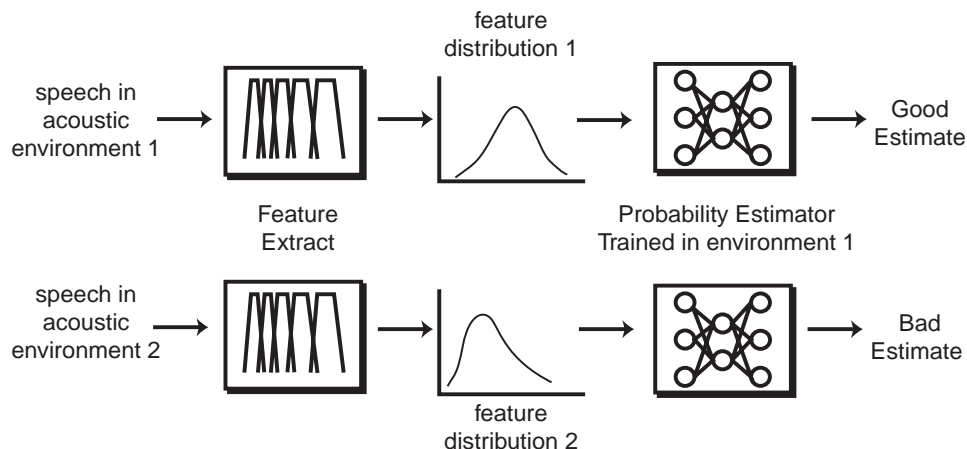


Figure 1.3: Speech features from different acoustic environments can exhibit different feature distributions.

1.2 Acoustic Environments

The acoustic realization of any given utterance suffers from many sources of variability. The number of potential sources are numerous but include variability due to the source of the speech (inter- and intra-speaker variability) and due to the environment in which the utterance is spoken (transmission channel, background noise, room acoustics). With so many affecting sources, no two realizations of a single utterance will ever be identical. Speaker-independent ASR attempts to model the linguistic information while removing or ignoring the information that is speaker-dependent. This, in itself, is challenging though numerous systems achieve usable levels of accuracy on a large number of tasks. Variability caused by a change in acoustic environment adds further challenge to the task.

A common observation among researchers is that the performance of ASR systems degrades, often drastically, when presented with speech in an alternate acoustic environment than that used during training. The alternate acoustic environment changes the realization of the received speech signal and therefore the distribution of the speech features (Figure 1.3). For example, the presence of background noise causes noise energy to be added to the signal. Room reverberation results in the addition of time-translated signal energy to itself. Modern feature extraction algorithms are considered ill-equipped at maintaining invariance to changes in acoustic conditions, though much progress has been made. Often environmental conditions can obfuscate the linguistic information in the

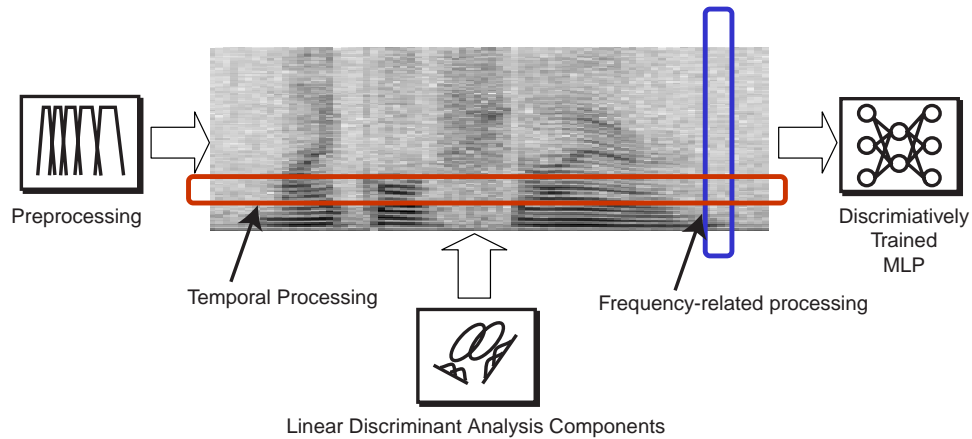


Figure 1.4: In addition to the non-linear discrimination used in the MLP along the frequency-related dimension, we apply discriminant training along the time dimension.

speech signal so that an ASR system may perform much worse even when it is trained in such an environment.

The experiments in this thesis focus on room reverberation with some additional work on added background noise. To counter the effects of acoustic degradation on recognition we adopt a strategy of improving the recognition accuracy in particular example environments. A combination of these tuned systems may then exhibit some robustness when presented with noise of a similar type. Since both background noise and room reverberation environments modify the speech signal in different ways, we also examine whether tuning the ASR system to an example of the noise will also demonstrate some robustness in other similar noise examples. In our approach we use multiple front-end acoustic modeling stages, each of which is trained on different acoustic conditions.

We attempt to improve performance in a particular condition by using discriminative training. Our system uses a discriminatively trained Multi-Layer Perceptron (MLP)⁴ that performs discrimination principally along the frequency dimension. We then include some further discriminative training along the temporal dimension to span the spectro-temporal space (Figure 1.4). We then combine the probability estimates from separate streams and examine the performance robustness. Optimal ways of combining these estimates remains a topic for further research. We experiment with a number of strategies found in the literature.

⁴An MLP is one type of artificial neural network having a feed-forward connectionist architecture.

1.3 Overview

The goal of this work is to demonstrate that robustness to unseen acoustic environment data can be achieved using the multi-stream approach. Many have experimented with the multi-stream paradigm in ASR and some have explicitly tested the robustness to noise conditions. It is common practice by researchers to conduct tests where the system was trained in a single acoustic condition (usually with clean data) and tested with noisy data. We deviate from this practice by adopting a strategy of a multi-stream system where the components are expressly designed for or trained in separate acoustic conditions. The course of this work proceeds in two stages. The first stage attempts to improve the front-end acoustic modeling portion of the ASR system for specific acoustic environments. This is accomplished through discriminative training of both the temporal filtering in the feature extraction routines and the probability-estimation components. With an appropriate set of front-end components the second stage tests the performance of their combination with special attention paid to the results using alternate, unseen acoustic conditions. Some of the results in this document have been reported in [102, 103, 104]⁵.

This thesis proceeds as follows. Background information on ASR is described in Chapter 2 with special attention paid to the front-end components. The use of an artificial neural network as a discriminatively trained probability estimator is described, as are typical signal-processing strategies used in feature extraction. Also included are descriptions of complete feature-extraction algorithms and the acoustic environments used in most of the experiments. Finally, a description of the experimental setup is included with further notes on the ASR system used. Chapter 3 describes the process of deriving temporal filters using Linear Discriminant Analysis. Observations and trends of how the discriminant filters vary with acoustic condition are demonstrated. Recognition experiments using RASTA-PLP with these filters in matched and mismatched training and testing conditions are described. In Chapter 4, we discuss the additional use of LDA for temporal processing using alternate feature-extraction strategies. PLP and MSG⁶ are used as the base feature-extraction algorithms that are augmented with LDA basis functions. Chapter 5 describes experiments using multiple front-end acoustic modeling stages. Front-

⁵Some reported experimental results are different due to changes in the ASR system setup.

⁶Modulation-filtered Spectrogram, a recent preprocessing algorithm developed by Kingsbury and Greenberg [62].

ends using the augmented feature-extraction routines from previous sections are combined and tested in unseen acoustic conditions. The tests comprise different combinations of feature extraction and probability estimation components, each of which is trained and tested under separate acoustic conditions. A number of encouraging results using simple combination strategies are examined and final tests with novel reverberation room impulses are described. The final chapter summarizes the informative trends that can be observed from the experiments. It also suggests avenues of further study and the promise of future improvement using multiple front-end components in ASR. Several appendices are included that contain information related to this work.

Chapter 2

Automatic Speech Recognition

The task of automatic speech recognition systems involves determining a sequence of words from the speech signal. Modern ASR systems use statistical pattern recognition in a probabilistic framework. The typical system proceeds as illustrated in Figure 2.1. First, features are computed from the acoustic speech signal. These are designed to preserve and enhance the linguistic information present in the speech signal while attempting to reduce the non-linguistic variability. Additionally, the features are usually transformed to a domain better suited for classification. Probability estimates are then computed from the acoustic features. The decoding stage takes the acoustic probability estimates together with pre-computed or *a priori* language information to produce a recognized sequence of words.

The basic goal of statistical ASR can be stated as follows: Find the most probable sequence of words given acoustic features and linguistic constraints. Such constraints can include vocabulary, grammar, pronunciation and phonotactics. Let $X = (x_1, x_2, \dots, x_n)$ represent a sequence of acoustic vectors, $M = (m_1, m_2, \dots, m_k)$ represent a sequence of word models, and \mathcal{L} as the universe of all possible model sequences. The overall goal is to find the word sequence M^* that maximizes the joint probability of the word sequence and the sequence of acoustic-feature vectors.

$$M^* = \operatorname{argmax}_{M \in \mathcal{L}} P(M, X) \quad (2.1)$$

$$= \operatorname{argmax}_{M \in \mathcal{L}} P(M|X)P(X) \quad (2.2)$$

$$= \operatorname{argmax}_{M \in \mathcal{L}} P(X|M)P(M) \quad (2.3)$$

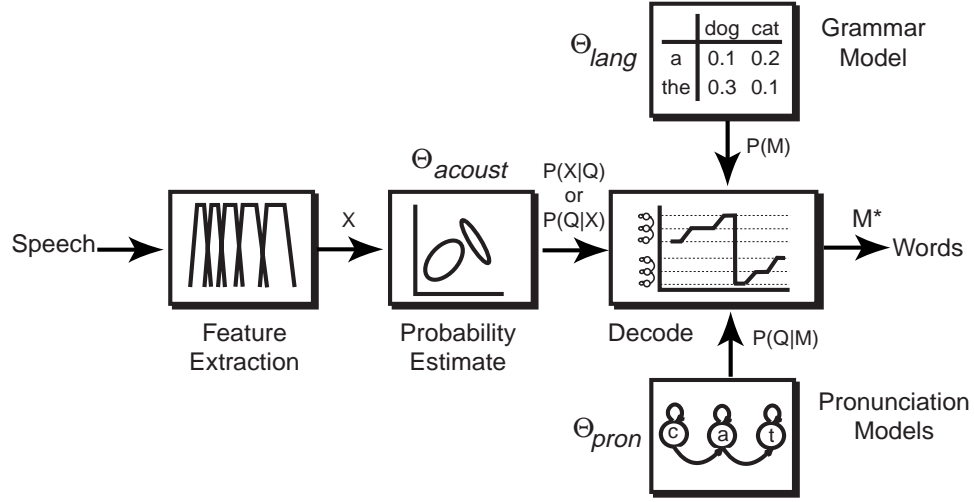


Figure 2.1: Abstract depiction of a typical ASR system.

Implicit in this formulation are the added constraints. Modeling the acoustic features from all possible word sequences, $P(X|M)$, becomes intractable for all but the smallest isolated word tasks. In practice, the words in M are subdivided into a sequence of states $Q = (q_1, q_2, \dots, q_m)$ where each state q corresponds to a sub-word unit.

$$M^* = \operatorname{argmax}_{M \in \mathcal{L}} \sum_Q P(X|Q, M)P(Q, M) \quad (2.4)$$

$$= \operatorname{argmax}_{M \in \mathcal{L}} \sum_Q P(X|Q, M)P(Q|M)P(M) \quad (2.5)$$

$$\approx \operatorname{argmax}_{M \in \mathcal{L}} \sum_Q P(X|Q)P(Q|M)P(M) \quad (2.6)$$

In equation 2.6 we introduce the assumption that the acoustic features are independent of the word sequence, given the word model sequence. In order to reduce the computation involved in searching through sequences of states, a Viterbi approximation is introduced; the sum over all possible state sequences is replaced by the most probable sequence. The Viterbi algorithm is a computationally efficient means of determining this path.

$$M^* \approx \operatorname{argmax}_{M \in \mathcal{L}} \max_Q P(X|Q)P(Q|M)P(M) \quad (2.7)$$

The probability $P(M)$ is the prior probability of the word sequences. In practice we construct a *language model* that describes to some degree the dependence of words on previous words. The most common means of doing this is the n -gram language model. The

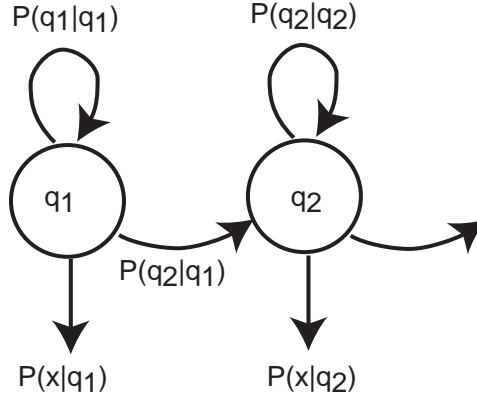


Figure 2.2: Hidden Markov Model.

probability of a given word in the sequence is dependent on only the previous $n - 1$ words.

$$P(M) = P(m_1, m_2, \dots, m_k) \quad (2.8)$$

$$= P(m_1) \prod_{i=2}^k P(m_i | m_1, \dots, m_{i-1}) \quad (2.9)$$

$$= P(m_1) P(m_2 | m_1) \dots \prod_{i=n}^k P(m_i | m_{i-(n-1)}, \dots, m_{i-1}) \quad (2.10)$$

The probability $P(m_1)$ is the unigram prior probability of the first word.

The probability $P(Q|M)$ is determined by using *pronunciation models*. Each word is modeled by a stochastic finite-state automaton as shown in Figure 2.2. Models include a first-order Markov assumption.

$$P(q_{t+1} | q_t, q_{t-1}, \dots) = P(q_{t+1} | q_t) \quad (2.11)$$

A dictionary file can be stored that contains all of the allowable words together with the state sequences of each word and the associated transition probabilities. Often an intermediate collection of base-form sequences is introduced for convenience in large vocabulary tasks.

$$P(Q|M) = P(Q|B)P(B|M) \quad (2.12)$$

The B sequences often model complete phones including a distribution for phone duration determined by the number of states and the transition probabilities. The word models can be expressed as a concatenation of constituent phonemes. The phones usually are modeled independently of the word sequence, though they need not be. Phones are, however,

sometimes modeled with a dependence on contextual phones. This is done to handle the effects of variability due to coarticulation. This work uses context-independent phonemes with states that correspond to phonetic classes. Many researchers have opted to subdivide phone segments further (for example into tri-state phone models). Tri-state models typically include states for the beginning, middle and ending of the phone.

The probability $P(X|Q)$ is the *acoustic likelihood* probability. In the HMM framework each acoustic feature x_t is considered to be a random variable emitted from a single state q_t that is independent of other states and independent of other features given the state.

$$P(X|Q) = P(x_1, x_2, \dots, x_N|Q) \quad (2.13)$$

$$= \prod_{t=1}^N P(x_t|q_1, q_2, \dots, q_N) \quad (2.14)$$

$$= \prod_{t=1}^N P(x_t|q_t) \quad (2.15)$$

Equation 2.14 arises from the assumed conditional independence of the features given the states. Equation 2.15 arises from the Markov assumption of the conditional independence of states.

Complete ASR systems have many parameters that are trained to a given recognition task. Some parameters are used for the acoustic probability estimation while others are associated with the pronunciation models, language models and search. We treat these parameters as separable and independently trainable.

$$M^* \approx \operatorname{argmax}_{M \in \mathcal{L}} \max_Q P(X|Q, \Theta_{acoust})P(Q|M, \Theta_{pron})P(M|\Theta_{lang}) \quad (2.16)$$

Θ_{lang} can include, for example, the unigram priors and the n -gram probabilities that are estimated *a priori* from a speech corpus. Θ_{pron} can include the state description and transition probabilities for the sub-word models. These can also be estimated statically and *a priori* from a speech corpus. There are also other system parameters that are manually tuned. Some of these parameters are, for example, associated with the decoding stage, such as adjusting the amount of search space that is pruned and the relative weighting of the acoustic- and language-model scores. The experiments in this thesis concern the use of the acoustic probabilities $P(X|Q)$. These and their trained parameters, Θ_{acoust} are discussed

further in the following section. The other components of the system are kept static and not explored in this work.

2.1 Probability Estimation

The HMM emission probability distributions $P(X|Q, \Theta_{acoust})$ are most commonly estimated from training data using Gaussian mixture models (GMMs) [87]. The distribution is characterized by a weighted sum of Gaussian density functions. The parameters Θ_{acoust} are the collection of means μ_k and covariances Σ_k of the Gaussians and relative weightings α_k .

$$P(x|q) = \sum_k \frac{\alpha_k}{(\sqrt{2\pi}|\Sigma_k^{-1}|)^N} e^{-(x-\mu_k)\Sigma_k^{-1}(x-\mu_k)^T} \quad (2.17)$$

$$\sum_k \alpha_k = 1 \quad (2.18)$$

where N is the number of components in feature vector x . The parameters are estimated from a training data set using, for example, the Expectation-Maximization (EM) algorithm [25].

An alternative method for acoustic probability estimation is used in hybrid Artificial Neural Network (ANN) - HMM systems. In these systems, discriminatively trained ANNs directly estimate the acoustic posterior $P(q|x)$ instead of the likelihood $P(x|q)$. As before, these quantities are related by Bayes rule, though the method of estimation is quite different. This work uses a feed-forward ANN also called a multi-layer perceptron (MLP). The architecture of this network is shown in Figure 2.3 for the three layer network that is principally used. The trained parameters Θ_{acoust} for this method are the collection of weight $\{\omega\}$ and bias $\{\beta\}$ values associated with each of the connections and nodes of the hidden and output layers.

The input feature vector x_t and optionally a number of contextual previous and following frames to $x_{t\pm c}$ are input into the MLP. The outputs of the perceptron nodes in the middle hidden layer are non-linear sigmoid functions applied to an affine combination of the nodes inputs with weight vector ω and bias β .

$$y(x) = \frac{1}{1 + e^{-\omega^T x + \beta}} \quad (2.19)$$

The output layer consists of the individual state acoustic posterior probabilities $P(q^i|x)$.

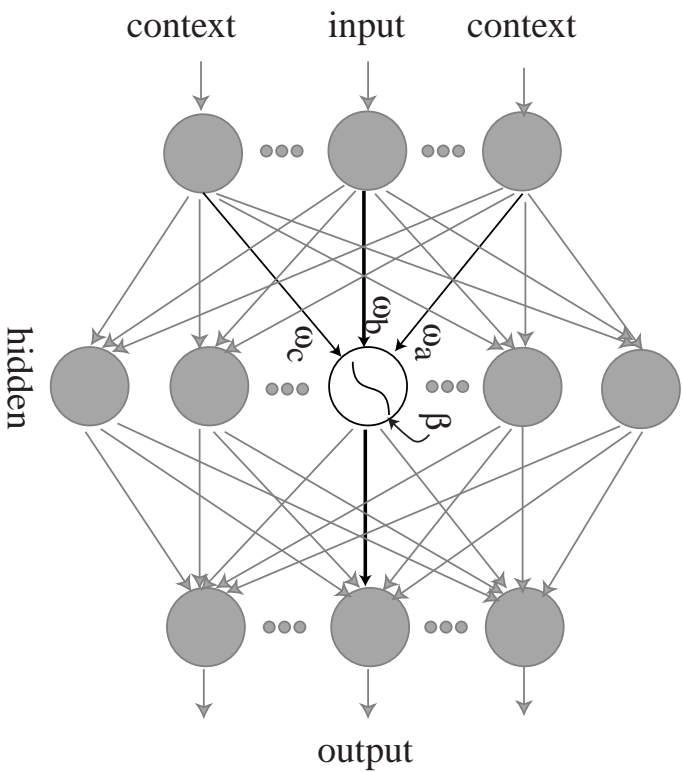


Figure 2.3: Fully connected multi-layer perceptron.

The perceptron nodes consist of soft-max functions according to

$$p(q^i|x) = \frac{e^{\omega_i^T x + \beta_j}}{\sum_j e^{\omega_j^T x + \beta_j}} \quad (2.20)$$

and is normalized to 1 over all states q^i to preserve a probabilistic interpretation [17]. The network is fully connected; all outputs of one layer appear as inputs to all of the nodes of the following layer. The parameters of the network are determined from stored input and output training examples using a relative entropy criterion

$$\Theta_{acoust}^* = \underset{\Theta_{acoust}}{\operatorname{argmin}} P(q|x) \log \frac{P(q|x)}{P(d|x)} \quad (2.21)$$

where $P(q|x)$ is the MLP output vector and $P(d|x)$ is a one-hot distribution that is near 1 at the i th position for the corresponding correct state q^i . In practice the weight and bias values are determined using error back-propagation (EBP) and an on-line stochastic gradient descent procedure. An overview of the use of MLPs to train posterior estimates in ASR is described in [12].

For practical reasons, the input features are commonly normalized to have zero mean and unit variance prior to use by the MLP. Doing so aids in MLP training by ft-

ting the feature values to a known range coinciding with the “active” region of the sigmoid function. This allows for selecting reasonable initial weights and has some numerical advantage. The input normalization parameters are computed over the training set, though they can also be determined from each testing utterance or using an online estimate.

2.2 Speech Feature Extraction

A number of speech feature extraction algorithms exist; some are used for speaker verification as well as for speech recognition. Among the most common are Mel-Frequency Cepstral Coefficients (MFCC) [24] and Relative SpecTrAl - Perceptual Linear Prediction (RASTA-PLP) [48, 50]. A number of variations exist but most contain common elements. In particular, speech feature extraction involves a decomposition of the speech signal into a time-frequency matrix to which further processing is applied. Such processing includes frequency smoothing and temporal filtering. Typically, transformations are applied to aid in pattern recognition. Many of the processing steps applied to the time-frequency matrix are inspired by human perception as well as by mathematical convenience. Other processing steps are set through empirical experimentation or by experimenter intuition. Some of the modifications have been designed to either reduce the effect of noise, model a specific perceptual phenomenon or aid in probability estimation. This section briefly describes some of the elements common to feature extraction routines that are used in practice. In particular, elements of RASTA-PLP, which serves as a base extraction routine, are described. Additionally, Modulation-filtered Spectrogram (MSG), which is a relatively recent algorithm developed at ICSI, is described [60, 62].

Analysis proceeds by first sampling the speech waveform with an analog-to-digital conversion module. Since most of the speech information is carried in frequencies up to 3300 Hz and because the collection of utterances used for experimentation were recorded over a band-limited telephone channel, the processing in this work assumes a sampling rate of 8 kHz. The speech samples are stored for repeated analysis and all further processing is carried out in the discrete domain.

2.2.1 Time-Frequency Analysis

Feature extraction techniques trace their origins to early synthesis and analysis devices such as the Voder and Vocoder [29, 32]. Researchers noticed that phonetic segments in speech appear as energy fluctuations over time in different frequency bands. This may be observed by processing the speech signal through a bank of narrow-band filters spanning frequencies up to 4 kHz and examining the power present in each band over time. A convenient alternative is to compute the magnitude squared of the Short-Term Fourier Transform (STFT): The Discrete Fourier Transform (DFT) computed over a finite window of samples. The magnitude of the STFT is an estimate of the power spectral density, under the assumption that the speech signal is locally stationary. This is not strictly correct, though it is a common and useful assumption since speech can exhibit a quasi-stationary behavior over a narrow segment of time. By computing the local power spectra over adjacent windows of speech we obtain an estimate of the time evolution of the spectral energy. The STFT is written as

$$X(m, k) = \sum_{n=0}^{N-1} x(pm + n)w(n)e^{-j2\pi kn/N} \quad (2.22)$$

where $w(n)$ is a finite window frame that is “slid” over the speech waveform, N is the length of the window, and p is the number of samples to step ahead. m represents the current frame of speech and k represents the discrete frequency at frame m . A number of different window functions are used in practice. A common one that is used in this work is the Hamming window:

$$w(n) = \begin{cases} \alpha - (1 - \alpha) \cos\left(\frac{w\pi n}{N-1}\right) & : 0 \leq n \leq N - 1 \\ 0 & : \text{otherwise} \end{cases} \quad (2.23)$$

with $\alpha = 0.54$. The windowing function reduces the effect of the discontinuity at the endpoints since the DFT coefficients assume a periodic signal. Multiplication in the discrete time domain implies circular convolution in the discrete frequency domain. The window therefore also smoothes the computed frequency values.

The magnitude square ($|X(m, k)|^2$) completes the computation of the local power spectral estimate. Effectively, the phase information from the short-term spectral analysis, which is largely considered unimportant for speech intelligibility, is discarded. Further, since the speech signal is real, this quantity is symmetric and only half of the values

are kept for further analysis. Experiments reported in this work compute power spectral estimates over 25-ms frames of speech stepped uniformly at 10-ms intervals.

Critical Bands

Frequency analysis in ASR often includes a number of approximations made from observations by scientists studying auditory physiology and human auditory perception. One such observation concerns the frequency resolution of the auditory periphery and, in particular, the cochlea. The tonotopic organization of the cochlea itself suggests that the human auditory system performs some kind of frequency analysis [38, 85]. Numerous perceptual experiments have tested the detection of controlled signals, often in the presence of masking noise. A commonly observed result pertains to the notion of the “critical-band” first described by Fletcher in his masked sinusoid experiments [33, 2]. The phenomena in general refers to the frequency-local processing and integration that occurs within the human auditory system. From numerous perceptual experiments, interference signals (such as masking noise) outside of this critical bandwidth does not significantly alter the detection threshold of signals within the frequency range. This bandwidth is nonlinearly dependent on frequency and sound pressure level. A number of functions approximating the frequency dependence of the bandwidth were constructed as the result of specific experiments. For example, the Bark scale, describes the frequency dependent bandwidth of a masking signal over a sinusoidal signal [33, 124, 93]; the Mel scale approximates the frequency dependence from experiments in pitch perception [106]; while a scale developed by Greenwood corresponds to the frequency bandwidth for equal spacing along the cochlea [45]. The different experiments and scales have the commonality of being approximately logarithmic above 1 kHz. Below 1 kHz, the spacing is not logarithmic and sometimes modeled as nearly linear. An alternative scaling with some of these properties is the *constant-Q* filter-bank with spacings ranging between one-third and one-fourth of an octave.

The critical-band scale is used in speech feature extraction for the spacing and bandwidths of the filter-bank. That is, filters at higher frequencies have wider bandwidths than at lower frequencies. RASTA-PLP, the primary base feature extraction method employed in this thesis, uses the Bark scale in its frequency analysis. The filter-bank is approximated by integrating discrete frequencies from an STFT along one-Bark intervals with trapezoidal functions. The Bark intervals are determined from the following frequency

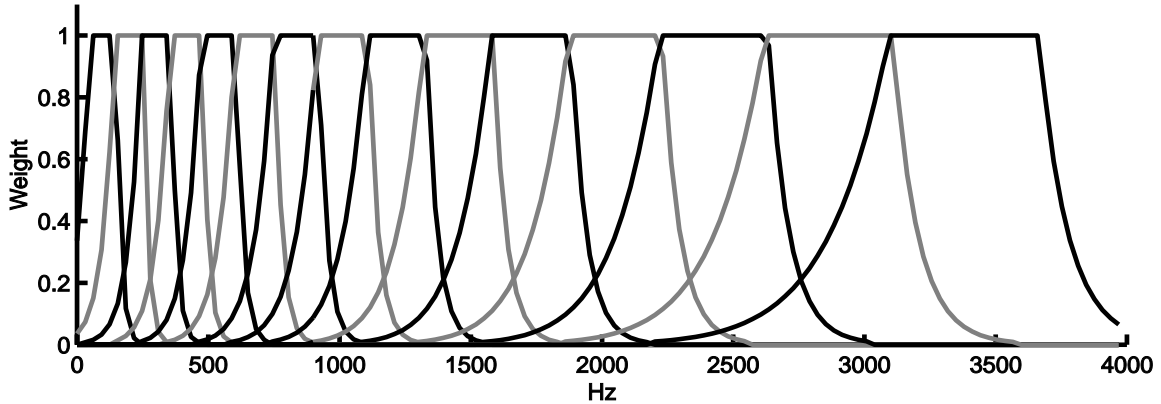


Figure 2.4: Integration windows of critical-band-like ranges spaced at 1 Bark intervals.

warping function originally proposed by Schroeder [93, 48]:

$$\Omega(\omega) = 6 \log \left\{ \frac{\omega}{1200\pi} + \left[\left(\frac{\omega}{1200\pi} \right)^2 + 1 \right]^{\frac{1}{2}} \right\} \quad (2.24)$$

Ω is measured in Barks while ω is in radians per second. An example of the critical-band integration weights is shown in Figure 2.4. 17 Barks span the frequency range between about 50 and 4 kHz, though the lowest and highest critical-bands are often discarded; the lowest contains little speech information while the highest is often of marginal value when used with telephone signals.

Human Auditory Scaling

In addition to critical-band spacing, other approximations based upon perceptual data can be included in feature extraction algorithms. For example, in PLP, approximations to loudness functions in human hearing are applied to the spectral values prior to further modeling. Loudness is a perceptual phenomenon related to sound pressure level (SPL). The perceived loudness varies with frequency for a given SPL. For example, a lower frequency signal would require a higher SPL for the same perceived loudness than in the mid-to-high frequency ranges. This too is dependent on the actual signal strength, though a fixed weighting approximation is used for convenience. A cube root is used to approximate the power law of loudness. This reflects a compression due to perceived differences in intensity.

2.2.2 Feature Orthogonalization

Though spectral values convey much of the desired linguistic information they are highly correlated. Adjacent frequency channels tend to rise and fall in synchrony and therefore carry redundant information. In statistical pattern recognition tasks, it is often helpful for modeling purposes to have feature components that are orthogonal. When using Gaussian densities or mixtures of Gaussian densities, a considerable number of parameters can be eliminated by using diagonal covariance matrices. Gaussian models can therefore more accurately describe feature vectors with uncorrelated components.

Cepstra

The cepstrum (sometimes called the real cepstrum) is computed as the inverse Fourier transform of the log magnitude of the Fourier transform of the signal portion of interest.

$$c(m, n) = \frac{1}{2\pi} \sum_{k=0}^{N-1} \log |X(m, k)| e^{j2\pi kn/N} \quad (2.25)$$

Here $X(m, k)$ is the estimated power spectral values for the m th frame. Since the power spectra are, by definition, real and symmetric this computation is equivalent to a Discrete Cosine Transform. Restated, the log power spectral estimates are projected onto an orthogonal set of cosine basis functions. The off-diagonal elements of the covariance matrix of the coefficients $c(m, n)$ (computed over n) are very small, though they can be significant near the diagonal.

Cepstral processing is a subset of homomorphic processing techniques first studied in depth by Bogert et. al.[9] and Oppenheim [84, 83]. A property of cepstral processing is the separation of the signal into components that vary over time at different rates. When applied to speech along the time axis, it has demonstrated some utility in separating the glottal source and vocal tract transfer function and has been used in pitch estimation [83]. In ASR, cepstra are commonly used for its quasi-orthogonalizing properties.

Linear Discriminant Analysis

Feature vectors can also be orthogonalized directly and completely over a given data set, in contrast to the approximate decorrelation in cepstral processing. Two re-

lated methods used in statistics and pattern recognition are Principal Component Analysis (PCA) and Linear Discriminant Analysis (LDA). LDA figures prominently in this work, though PCA is also described for comparison. In each, a set of orthonormal basis functions ϕ_j that span the feature space are computed from statistics estimated from a training data set. Further, these basis functions can be ranked by order of importance according to a specific criterion. Let x represent the feature vector with D components and Φ a matrix where each column is one of J basis vectors ϕ_j and $J \leq D$. The basis decomposition and recombination can be written as:

$$y_j = \phi_j^T x \quad (2.26)$$

$$y = \Phi^T x \quad (2.27)$$

$$\hat{x} = \Phi y \quad (2.28)$$

$$\Phi^T \Phi = I \quad (2.29)$$

Where y is a new feature vector, possibly of smaller dimension. PCA basis vectors are obtained from minimizing the mean square error between the reconstructed and original set of data vectors.

$$\Phi_{PCA} = \underset{\Phi}{\operatorname{argmin}} \sum_x \|\hat{x} - x\|^2 \quad (2.30)$$

$$= \underset{\Phi}{\operatorname{argmin}} \sum_x \|\Phi \Phi^T x - x\|^2 \quad (2.31)$$

It can be shown that the general solution satisfies the eigenvalue problem [35].

$$S\phi_j = \lambda_j \phi_j \quad (2.32)$$

Where $S = \operatorname{cov}(x, x)$, the sample autocovariance matrix of x . The basis functions are determined as the eigenvectors of the covariance matrix, $\Phi_{PCA} = \operatorname{eig}\{S\}$. The new set of basis functions amount to a rotation and alignment of the features according to dimensions of maximum variance. This is also known as the discrete version of the Karhunen-Loève transform. The basis functions can be ranked in descending order of corresponding eigenvalues, corresponding to dimensions of decreasing amounts of variance. PCA guarantees minimum reconstruction error when successive basis functions, corresponding to the smallest eigenvalues, are eliminated. Interestingly, an informative result by Malayath [75] is that the basis functions derived from PCA bear striking similarity to the cosine basis functions from the DCT when applied to log spectral values. This result provides additional support

for using cepstra in pattern recognition tasks. The DCT has the added advantage of being a simple and general decorrelation scheme, while the PCA basis vectors must be derived from a given data set.

LDA basis functions are computed in a similar manner but through a different criterion.

$$\Phi_{LDA} = \operatorname{argmax}_{\Phi} \frac{|\Phi^T S_B \Phi|}{|\Phi^T S_W \Phi|} \quad (2.33)$$

The quantities S_W and S_B are the within-class and between-class covariances matrices respectively. Taking X as a matrix, where each column corresponds to a feature vector, and X_c as a matrix of feature vectors corresponding to class $c \in \mathcal{C}$, these quantities are computed as

$$S_B = \sum_{c \in \mathcal{C}} N_c (X_c - \bar{X})(X_c - \bar{X})^T \quad (2.34)$$

$$S_W = \sum_{c \in \mathcal{C}} (X - X_c)(X - X_c)^T \quad (2.35)$$

$$\bar{X}_c = \frac{1}{N_c} \sum_{x \in X_c} x \quad (2.36)$$

$$\bar{X} = \frac{1}{N} \sum_{x \in X} x \quad (2.37)$$

N is the number of example feature vectors and N_c is the number of example vectors in class c . The basis functions that satisfy equation 2.33 are the solution to the general eigenvalue problem [35].

$$S_B \phi_j = \lambda_j S_W \phi_j \quad (2.38)$$

The basis functions are determined as the eigenvectors of the between-to-within covariance ratio, $\Phi_{PCA} = \operatorname{eig}\{S_W^{-1} S_B\}$. The resulting rotation aligns the features to dimensions of maximum linear separability among defined classes instead of among dimensions of maximum variation. The LDA basis functions again can be ranked in order of principle dimensions of linear separability according to the magnitude of the associated eigenvalues. A related measure of class separability is the Fisher ratio [28, 76], which has several similar definitions, but for our purposes is $\operatorname{trace}(S_W^{-1} S_B)$. Intuitively, this is the ratio of the variance between classes to the average variance within classes. Separability increases as the class means are spread further apart and the spread of each class becomes more confined.

While PCA computes the principle dimensions of variability, it is not necessarily optimally suited to tasks of class discrimination. Figure 2.5 is an illustrative example of

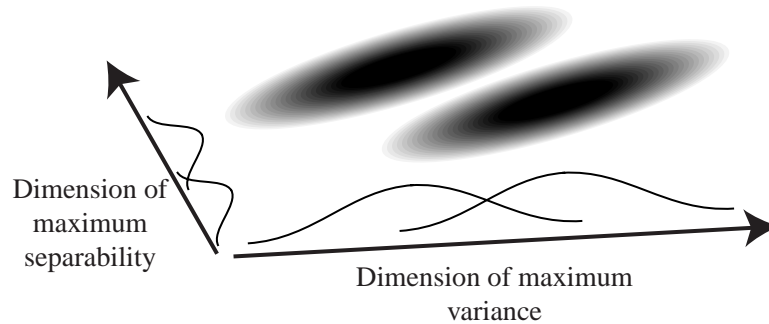


Figure 2.5: Dimensions of maximum variance and linear separability may not coincide.

this with two classes. The dimension of maximum variance obtained by PCA does not coincide with the principle dimension of maximum discriminability obtained from LDA. Unfortunately, LDA only provides optimally linear separation under homoskedastic-normal assumptions; the class covariances must be Gaussian with equal covariance matrices. This is usually not the case for many defined classes such as phones. Saon et. al. have recently introduced Heteroskedastic Discriminant Analysis (HDA) using a modification of the objective criterion to remove the equal class covariance requirement [91]. Nevertheless, though technically suboptimal, LDA has been used with success as a decorrelation method that preserves discriminability.

The work presented in this thesis does not apply LDA in the frequency dimension. The reasons are twofold: Cepstral computation is a simple and general decorrelation scheme and our probability estimator consists of a discriminatively trained artificial neural network. For the latter, the discriminant linear separability can be considered redundant to the non-linear discriminant analysis implicit in the neural network training. Yet, this work does make heavy use of LDA as a technique applied to the temporal trajectories of critical-band energy. This application of LDA was pioneered by researchers at the Oregon Graduate Institute [6, 110, 109]. The direct application will be described in further detail in Chapter 3.

2.2.3 Frequency Smoothing

The shape of the local speech spectrum reflects the state of the vocal tract cavity and source excitation. This shape in turn reflects the current phone being uttered. The

pattern of resonances, known as formants, can be observed from the spectral envelope and must usually be inferred from the fine structure pattern of the harmonics. It can be distorted by noise and the frequency characteristics of a microphone or transmission channel. The formant patterns also vary with the speaker. Many techniques exist to enhance and preserve the formant information. Common ones for ASR systems involve types of frequency smoothing and are described here.

Dimensionality Reduction

One technique that has the added benefit of reducing computation is dimensionality reduction of orthogonalized feature vectors. As noted in the previous section, the linear basis functions for each of the new features can be ranked in order of variability or class separability. Truncating those feature coefficients that correspond to the basis functions that explain the least amount of variability removes a source of less useful variation in the speech spectrum. These basis functions typically correspond to more rapidly changing fine structure in the speech spectrum. Eliminating these components effectively smoothes the shape of the spectrum.

Similarly, smoothing can be done by truncating the number of cepstral coefficients. This can also be interpreted as a multiplication of the cepstra by a rectangular window. After an inverse DCT, this is equivalent to convolution of the log speech spectrum by the window's response. The rectangular window frequency response is well known to be a sinc function which has a lowpass characteristic. In effect, the log spectrum is smoothed.

Linear Prediction

A more direct approach is linear prediction. Linear prediction has been used by speech researchers since the 1960's as a tool for modeling the formant patterns directly with an auto-regressive (AR) all-pole model

$$H(z) = \frac{1}{1 - \sum_{j=1}^p a_j z^{-j}} \quad (2.39)$$

where p is the order of the model. The coefficients a_j are determined from minimizing the error between the predicted model and the signal. This can be computed using algorithms to solve the appropriate normal equations [74]. By using higher-order models, the

prediction error can be made arbitrarily small, though in this specific application it is not desirable to model the spectrum with ultimate precision.

Intuitively, the model places poles (determined from the a_j coefficients) where the peaks of the spectrum reside. This “peak-hugging” property is desirable as it emphasizes the resonances of the vocal tract. It is often considered that these formant peaks are more linguistically important than the spectral valleys. The AR model provides a good match as it models the peaks more accurately than the valleys. Reducing the order of the model reduces the number of poles for peak modeling and therefore results in a smoother function. Restated, N values can be modeled exactly (to within a scaling factor) by an order $p = N$ AR model. By setting $p < N$, the model provides the best smoothed fit by pole placement, in the mean-squared-error sense, between the autocorrelation functions.

2.2.4 Temporal Processing

In addition to frequency smoothing, pattern recognition has been aided by temporally processing the sequence of spectral or spectrally related values. The most common techniques include the use of delta features, Cepstral Mean Subtraction, and RASTA filtering, each of which is briefly described here.

Delta Features

Delta cepstral features, introduced by Furui [36], provide a mechanism to capture some of the dynamics of the speech in ASR. The cepstral features are appended with an estimate of the first and sometimes second derivatives. The estimates are commonly performed as a finite difference, often of a smoothed time series

$$\Delta c(m, k) = c(m, k) - c(m - 1, k) \quad (2.40)$$

or as a regression,

$$\Delta c(m, k) = \frac{\sum_{i=-T}^T r_i c(m + i, k)}{\sum_{i=-T}^T r_i^2} \quad (2.41)$$

The second form is used primarily in this work.

ASR systems have consistently benefited from the addition of delta features though it does increase the amount of computation required for probability estimation.

One of the effects of the delta computation is the removal of the DC component of the cepstral trajectories. This is done directly in the Cepstral Mean Subtraction method.

Cepstral Mean Subtraction

In Cepstral Mean Subtraction (CMS), a time average of the cepstral values (the DC value) is subtracted from the values at each frame.

$$c_{new}(m, k) = c(m, k) - \bar{c}(k) \quad (2.42)$$

$$\bar{c}(k) = \frac{1}{T} \sum_{m=1}^T c(m, k) \quad (2.43)$$

This is usually computed over the length T of a complete utterance as a way of normalizing for channel effects and adjusting for spectral slope. Normalizing over the utterance length introduces some latency in the processing, though it is a simple and effective technique. Alternatively, online techniques such as highpass filtering or normalization over a moving window can also be applied instead. Related to CMS is RASTA filtering.

RASTA Filtering

RASTA (RelAtive SpecTral Analysis) filtering in general refers to filtering of the temporal trajectories of some function of each of the spectral values. The filter is usually applied to power spectra to which a compressive nonlinearity is applied, such as a root power or logarithm. Typically the filtering is done in the log-spectral domain as in CMS. In contrast to CMS, the RASTA filter is applied to the individual compressed spectral bands instead of the linear combination of the compressed bands. Further, the RASTA filter is often a bandpass filter rather than a strict mean removal filter, as occurs in CMS. The filtering of individual bands allows for further operations such as additional frequency smoothing and modeling.

The original RASTA filter proposed by Hermansky and Morgan [50] is a finite differentiator followed by a leaky single-pole integrator.

$$H(z) = \frac{.25z^2 + .125z^1 - .125z^{-1} - .25z^{-2}}{1 - \alpha z^{-1}} \quad (2.44)$$

The pole $\alpha = 0.94$, determined from numerous recognition experiments, is commonly used. The impulse and frequency response of this filter are displayed in Figure 2.6. We refer to

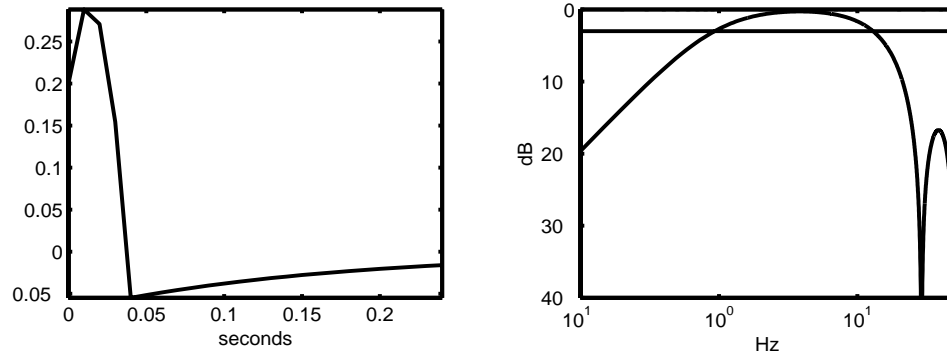


Figure 2.6: Impulse and frequency response for standard RASTA filter.

this filter as the *standard* RASTA filter.

Intuitively, the RASTA filter was constructed to improve robustness to slowly varying channels. Consider an original speech signal time-frequency response $S(k, n)$ and channel response $H(k, n)$. Modeling the channel as a convolution in the time domain of the speech with the channel response, the frequency-domain response is a multiplication of the responses

$$X(k, n) = S(k, n)H(k, n). \quad (2.45)$$

Taking the logarithm, the multiplication becomes addition

$$\log X(k, n) = \log S(k, n) + \log H(k, n). \quad (2.46)$$

If the rates at which the two right terms vary are significantly different, the channel response term may be eliminated through application of a linear filter. In particular, if the channel varies very slowly, it may be eliminated by filtering out the extremely low frequencies around DC. This is similar to what is achieved with CMS. An assumption here is that the channel response is short relative to the analysis window for processing.

Removal of the low-frequency components in the log-spectral domain can also be interpreted as a kind of automatic gain control (AGC). Subtracting the mean from the signal in the logarithmic domain is equivalent to dividing by the exponential of the mean of the logarithm of the signal. That is, mean removal in the logarithmic domain is equivalent to normalizing the signal by its geometric mean. For non-ideal highpass filters or for bandpass filters, the log-domain filtering is equivalent to normalizing by a weighted geometric mean.

The RASTA filter was also intuitively realized to emphasize the regions of spectral change. Many of the perceptual senses of biological organisms are organized to detect areas of contrast. This is considered the case, for example, in the human visual system as well as in the auditory system. In practice, the bandpass filtering preserves the signal fluctuations that modulate within the range of about 1 to 12 Hz, commensurate with the range of modulation rates of speech.

2.2.5 Complete Algorithms

This section describes the complete feature extraction algorithms used in the remainder of this work. The experiments began with replacement of the RASTA filter in RASTA-PLP with filters derived using LDA. Additionally, experiments using PLP without critical-band RASTA processing and the recent Modulation-filtered Spectrogram (MSG) method, were conducted. Many of the feature extraction processing techniques previously described are combined to form these algorithms. Other similar algorithms such as MFCC also include many of the components, though they are not described in detail.

RASTA-PLP

The basic processing steps for RASTA-PLP are showed in Figure 2.7. The shaded boxes consist of RASTA processing steps that were not included in the original PLP algorithm.

Frequency analysis. The speech signal is grouped into overlapping frames to which a windowing is applied. The magnitude squared of the DFT gives an estimate of the local power spectra for each frame.

Critical band integration The power spectra values are integrated using the trapezoidal windows spaced at one Bark intervals.

RASTA processing. When applied, a compressive memoryless nonlinearity is applied to power spectral values. The RASTA bandpass filters are applied to these values along the time dimension. A matching inverse non-linearity (expansive) is applied to return the values to the original power spectral domain.

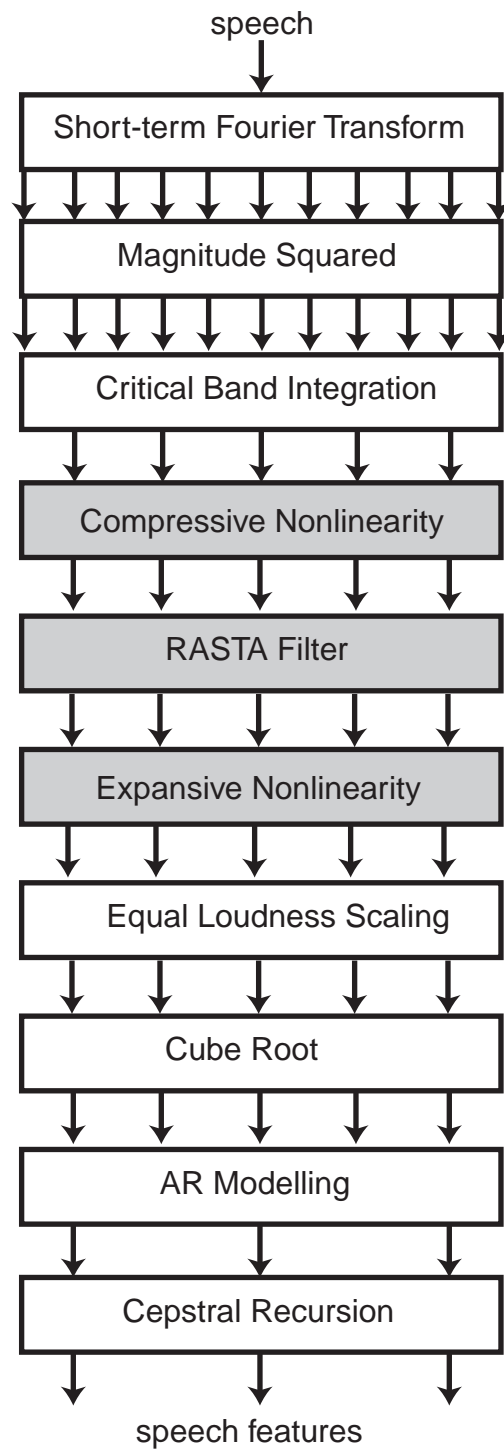


Figure 2.7: Processing steps for RASTA-PLP.

Loudness equalization and cube root. An approximation to the equal loudness curve is applied to the spectral values, followed by a cube root.

AR modeling. Coefficients for an auto-regressive model are computed by solving the appropriate normal equations.

Cepstral transformation. The AR coefficients are transformed using cepstral recursion into cepstral coefficients.

The feature extraction algorithm carries a number of specifiable parameters, some of which were mentioned in previous sections. All of the speech data used for training and testing was sampled at 8 kHz. The experiments in this work used a Hamming analysis window of 25 ms stepped in 10-ms increments. The critical-bands were stepped at single Bark intervals yielding 17 critical-band values per frame, and the lowest and highest were discarded. Log-RASTA was applied for many of the experiments; a logarithm and exponential were used as the compressive and expansive non-linearities respectively. 8 coefficients were selected for the AR model order along with a gain feature. The 8 AR coefficients were transformed into 8 cepstral coefficients with the energy feature preserved. Delta and double-delta coefficients were often computed for all of the features in baseline tests. The energy feature was nominally discarded, while the delta and double-delta energies were preserved, yielding 26 features when delta and double-delta features were appended.

Modulation-Filtered Spectrogram

The Modulation-filtered Spectrogram (MSG) is a recent feature extraction algorithm using perceptually inspired signal-processing strategies. The basic processing steps are shown in Figure 2.8 while a more comprehensive description can be found in [62]. There are several versions of the processing algorithm. One used in this work proceeds as follows.

Bark-scale filterbank Speech is analyzed into critical-band power spectral values in a manner similar to that in RASTA-PLP. 13 bands spanning the 230 Hz to 3000 Hz are retained.

Square root A square root places the power spectra into an amplitude spectral domain.

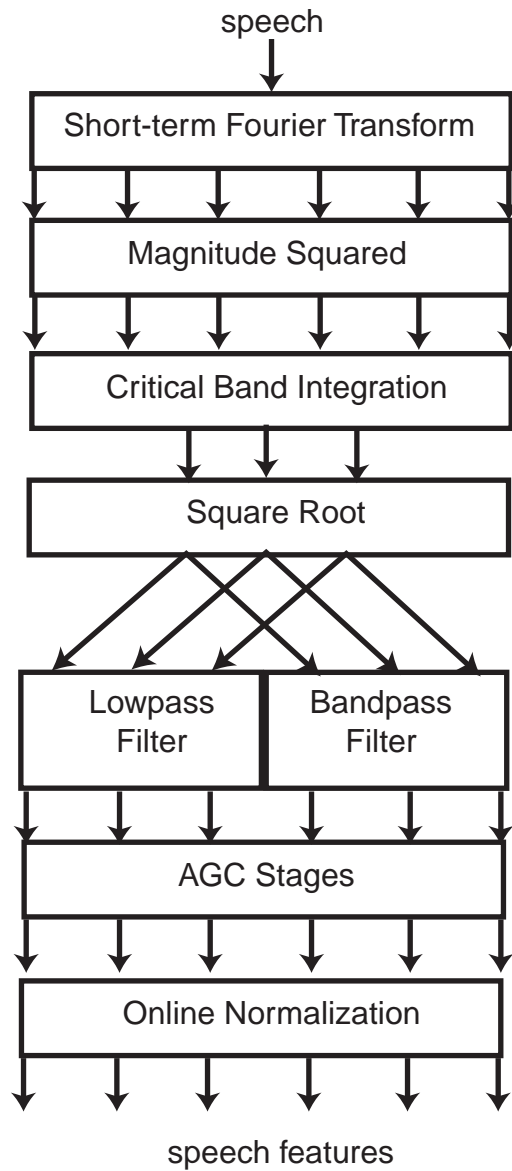


Figure 2.8: Processing steps for the MSG features.

Envelope filters Filters are applied temporally to the energy trajectories. Two sets of filters are applied. The first set consists of cascaded, lowpass, second-order IIR filters with a cutoff at 8 Hz. The second set consists of cascaded, bandpass, second-order IIR filters with a passband between 8 and 16 Hz. The end result is the creation of two sets of critical-band energies.

AGC Feedback automatic gain control stages are applied to individual bands. The first stage had a time constant of 160 ms, while the second had a longer time constant of 320 ms.

Online normalization The features are locally normalized to have zero mean and unit variance.

The latter processing stages are novel to this algorithm, although they are conceptually similar to previous techniques and require some further explanation. As with other algorithms, such as RASTA-PLP, processing begins by analyzing the speech signal into critical-bands. In lieu of a logarithm as in RASTA-PLP, a square root serves as the compressive non-linearity. The lowpass and bandpass filters then serve as the temporal filters. The range of these filters are consistent with the range of the RASTA filter, though they separate it into two mostly non-overlapping ranges.

Instead of an implicit log-RASTA style of AGC (normalization by a weighted geometric mean), AGC stages are explicitly included. Further stages of spectral smoothing, whether by AR modeling, cepstral truncation, or other means, are absent as is a final orthogonalization step. The resulting lowpass and bandpass features are therefore correlated. The use of the MLP as a general non-linear probability estimator can be assumed to reconcile this. For Gaussian-mixture estimators, either a full covariance model must be implemented or an additional post-processing step for orthogonalization can be added when using diagonal covariance models.

The final stage of online normalization aids in placing the features within a reasonable range for use by the MLP probability estimator. It consists of subtracting an estimate of the local mean of each feature and subsequently dividing the result by a local estimate of the standard deviation. In MSG both the local mean and standard deviation are computed using single-pole IIR filters with time constants of approximately 2 seconds applied to each feature and the square of each feature, as shown in Figure 2.9. An offset,

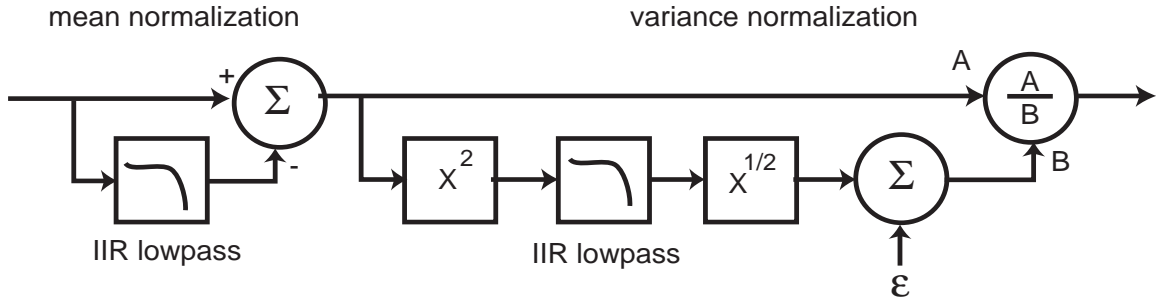


Figure 2.9: Processing diagram for online normalization.

ε , prevents numerical problems when the standard deviation estimate becomes small. The online nature of subtracting the mean can be considered similar to CMS, though with different properties since there is no logarithm inherent in the processing. The local scaling to unit variance adds another useful property and will be discussed further in Section 3.3.2. The online normalization stage can be applied or approximated conveniently in other feature extraction algorithms as a post process.

The AGC consists principally of locally scaling a signal by a lowpass version of itself. That is, a value is scaled by a weighted sum of locally surrounding values. Figure 2.10 shows the feedback architecture used in this rendition of MSG. The single pole lowpass filter is given as

$$H(z) = \frac{1 - a}{1 - az^{-1}} \quad (2.47)$$

where a is related to the time constant τ by a frame stepping-rate factor. When incorporated, the AGC behaves as a square-root compressor with a variable gain that is a function of the dynamics of the input.

2.3 Acoustic Environments

This work investigates ASR performance in reverberant environments with some additional work with additive noise. For experimental purposes, examples of each are artificially applied to test data. This allows us to use identical speech data throughout the recognition experiments and judge the effects on recognition by the speech environment discounting the differences that would be inherent between different speech corpora. Arguably, modifying speech in this manner does not accurately reflect spoken utterances in

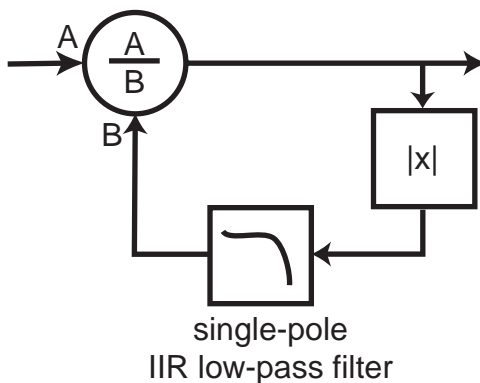


Figure 2.10: Processing schematic for AGC.

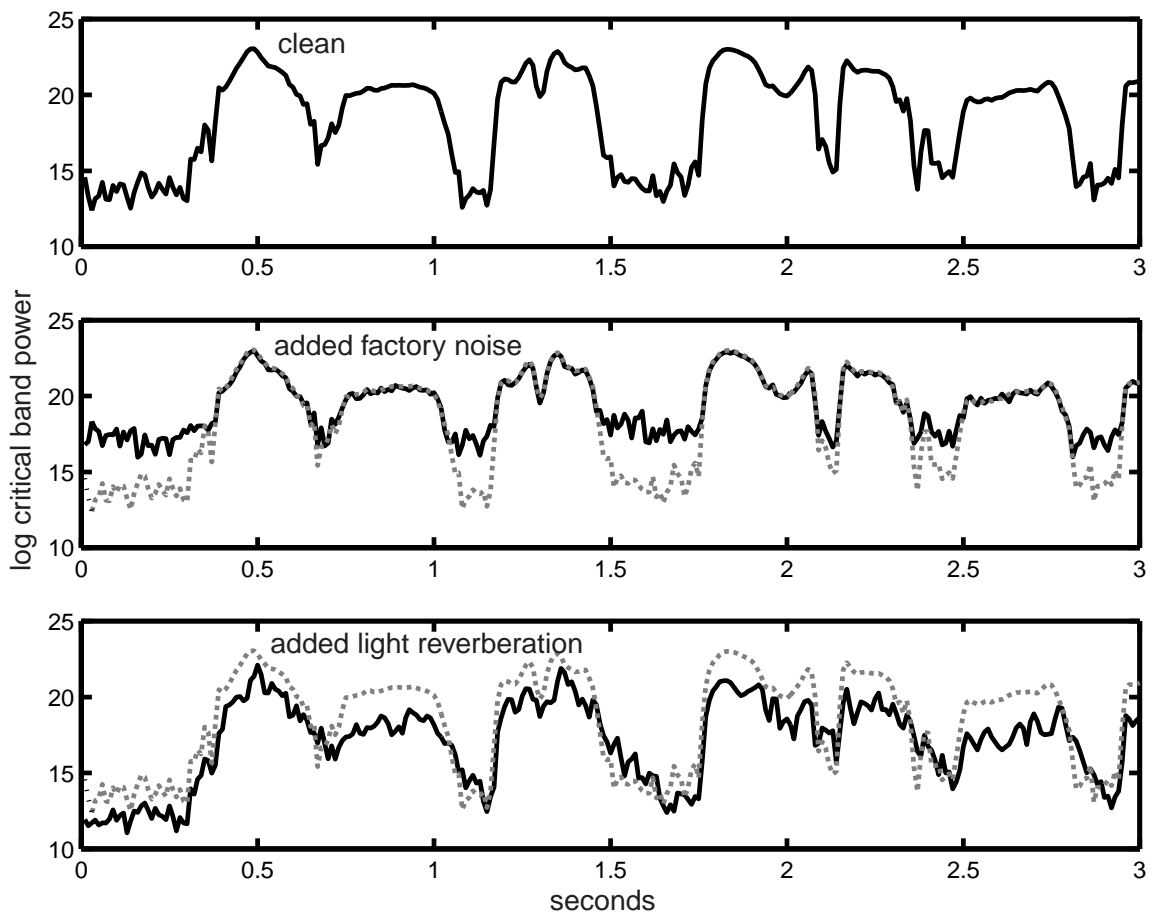


Figure 2.11: Log-power trajectory of 3 seconds of the same utterance under the original *clean* condition, with added *factory* noise at 10 dB SNR, and lightly reverberated with a characteristic reverberation time of 0.5 seconds. The utterance is of a male speaker saying “Well, uh, maybe I should tell ya about how...”

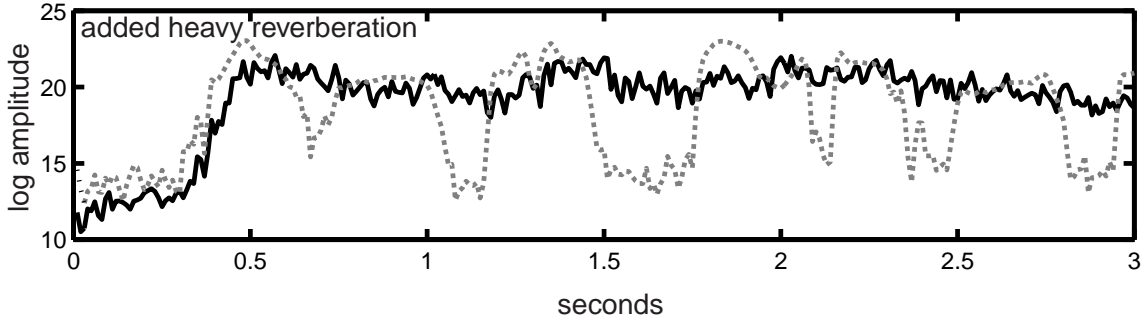


Figure 2.12: Log-power trajectory of same utterance as in Figure 2.11 under severely reverberated condition (characteristic reverberation time of 2.5 seconds).

a naturally noisy environment; the presence of noise typically causes a speaker to increase vocal effort and modify the durations of the words spoken. This modification is called the Lombard effect or Lombard reflex and presents an additional challenge in ASR [57, 46, 47]. However, simulating a noisy environment in an artificial manner seems sufficient and desirable for algorithm development purposes.

For additive noise, we simply add scaled samples of recorded noise to the speech data. For a speech signal $s(n)$ and noise signal $v(n)$, the resulting signal $x(n)$ is $x(n) = s(n) + v(n)$. The relative scaling between the two is specified to a desired signal-to-noise ratio (SNR), defined as the ratio in dB of the variance in the signal to the variance in the noise. The noise term shows up in power spectral computation as an offset term and an interaction term. Examining one frame in our spectral estimation step we have:

$$x(n) = s(n) + v(n) \quad (2.48)$$

$$|S_x(k)|^2 = |S_s(k) + S_v(k)|^2 \quad (2.49)$$

$$= |S_s(k)|^2 + |S_v(k)|^2 + 2\text{Re}\{S_s(k)S_v^*(k)\} \quad (2.50)$$

The signal and noise can be assumed independent and uncorrelated, causing the cross power term to be absent in equation 2.49. The first two plots in Figure 2.11 show examples of a logarithm of the critical-band power trajectory, for the band centered at 570 Hz, in the *clean* condition and with *factory* noise added at 10 dB SNR. The principal observation from these plots is a raising of the noise floor. The distance between the peaks and the valleys of the plot is smaller with the added noise than in the original *clean* condition case.

Reverberation is artificially added to the speech via convolution with a room

impulse response, $h(n)$. Reverberation is affected by the volume and shape of the room, the reflective properties of the surfaces, the relative location and orientation of the microphone and source within the room, and the absorption properties of the air. Two parameters that are often used to describe the rooms reverberation characteristics are the direct-to-reverberant ratio (DTR) and the reverberation time, T60. DTR is the ratio of the power in the direct impulse to the power in the remaining tail, expressed in dB:

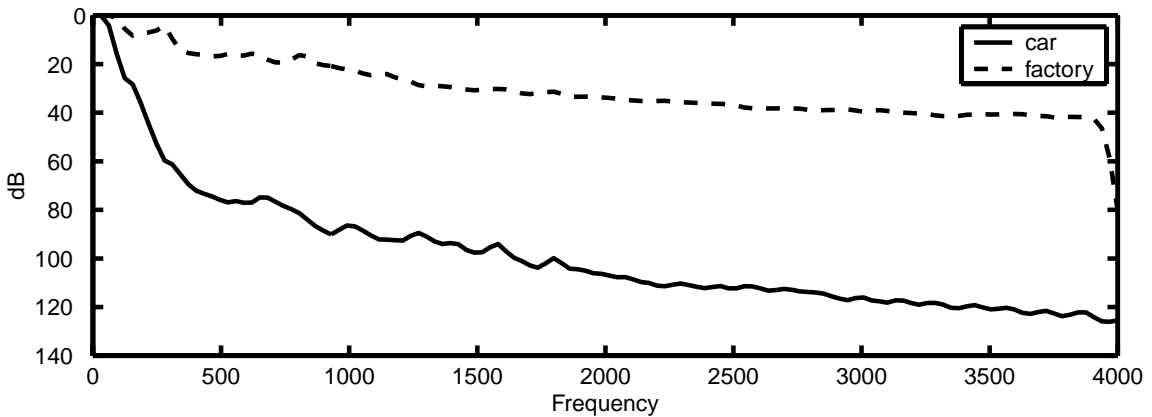
$$\text{DTR} = \frac{h^2(0)}{\sum_{n=1}^N h^2(n)} \quad (2.51)$$

The reverberation time, T60, is the time from the impulse to where the energy decays by 60 dB. The reverberation decays in an approximately exponential manner with higher frequencies often decaying more quickly than lower frequencies. Common reverberation times are below 0.5 seconds for a typical small office but can be 2 or more seconds for larger or more reflective rooms. With a decay on the order of a second, the effects of reverberation greatly exceed the analysis window used for feature extraction. Since the reverberation impulse is causal, speech energy is smeared forward in time, with energy in one analysis frame appearing fractionally in many ensuing frames. Some of this can be witnessed in the last plot of Figure 2.11 which shows the log critical-band trajectory affected by a room with DTR of -2 dB and T60 of approximately 0.5 seconds. We can observe speech energy “bleeding” forward in time. A more extreme example is shown in Figure 2.12 where the envelope of the speech energy is severely obfuscated. Amazingly, the utterances remain largely intelligible to human listeners owing to the robustness of the human speech perception, though high-level contextual knowledge also plays an integral part.

We were interested in the effects of various noise conditions on the data-driven discriminant filter design and on the acoustic modeling. For this purpose we modified the raw speech with examples of additive and reverberant noise, as listed in Table 2.1. For the additive-noise experiments we artificially added noise recorded from a car (Volvo) driving at 55 miles per hour with closed windows. This recording was taken from the NOISEX database [111] and added to the speech at 0 dB SNR. We separately added *factory* noise also from the NOISEX database at 10 dB SNR. The normalized average spectral power of both noise conditions is shown in Figure 2.13. The energy from the *car* noise is largely concentrated in the low frequencies while the *factory* noise is more distributed. This causes

Noise Name	Description
<i>clean</i>	Unaltered speech
<i>car</i>	Added Volvo noise from the NOISEX database at 0 dB SNR
<i>factory</i>	Added <i>factory</i> noise from the NOISEX database at 10 dB SNR
<i>light</i>	Room reverberation measured from a varechoic chamber. T60 = 0.5 sec, DTR = -2 dB
<i>heavy</i>	Room reverberation measured from a concrete basement hall at ICSI. T60 = 2.5 sec, DTR = -8 dB

Table 2.1: Description of noise conditions.

Figure 2.13: Average spectral power for *car* and *factory* noise.

the *factory* noise conditions to sound perceptually noisier than the car noise even though it possessed less overall power.¹

Two examples of reverberation were added for the reverberation experiments. The impulse response of one example was constructed based on speech recordings in a 6.1m × 2.4 m × 1.7 m basement hallway at ICSI by Brian Kingsbury. Reverberation times were estimated in different frequency bands by correlating simultaneous recordings from a head-mounted microphone and an omni-directional microphone positioned 2.5 meters from the talker. The impulse response was manufactured using decaying white Gaussian noise samples that were filtered and shaped to match the decay characteristics in each of the

¹Another descriptive specification would be to use an A weighted measurement, which applies a loudness correction. This is useful for estimating perceived loudness by humans though it can be misleading in machine-based recognition conditions.

frequency bands. Early reflections were added using estimates from a time-domain image expansion simulation. The resulting impulse had a T60 of approximately 2.5 seconds and a DTR ratio of -8 dB. This is referred to as the *heavy* or *heavy reverberation* condition in this document. The impulse response of the other example was one of twelve recorded in the Bell Labs Varechoic [113] chamber. This chamber is a 6.71 m \times 5.94 m \times 2.74 m room composed of 368 panels that can be individually placed in an open or closed state. In the closed state, the panel is highly reflective while in the open state highly absorbent material is exposed. Measurements were recorded by four microphones placed 2 m, 2.35 m, 2.7 m, and 3.05 m from the source with the room configured in three states: All panels closed, 43% of the panels open, and all panels open. The room impulses were estimated using a chirp-excited system identification method. The impulse used in most of the experiments in this thesis was from the 2 m microphone with 43% of the panels open. It has a T60 of 0.5 seconds and a DTR of -2 dB and is referred to as the *light* or *light reverberation* condition. The remaining room impulses were reserved for concluding tests.²

2.4 Experimental Setup

The research and experiments in this work were conducted at the International Computer Science Institute (ICSI). The ASR system is a hybrid ANN-HMM system. Many of the parameter choices for the recognition experiments, such as frame analysis windows, stepping time, and number of feature coefficients were described in previous sections. Only the front-end components of the system were varied for these experiments; decoding algorithms, speech corpora, and model parameters available in the ICSI research environment were kept fixed during the experiments.

The ICSI system uses 56 mono-phone classes that are listed in Appendix A. HMM states correspond to single phone classes. Most of the experiments listed here used the CHRONOS speech decoder written by Tony Robinson at SoftSound, Cambridge, England [89]. It is a stack-based decoder designed for large vocabulary tasks. Most of the manually adjustable decoder parameters were kept at default values. However, the language model scaling factor was set to yield the lowest word error rate on the small set of CV utterances. The system uses context-independent phone models; phone models are independent of the

²Much appreciation goes to Brian Kingsbury and Carlos Avendaño for providing me with these room impulse responses and measurements.

constituent words. Static phone models consisted of one or two phone states with fixed transition probabilities computed *a priori* from a training set. Word models were constructed by a concatenation of the constituent phone models. A multiple-pronunciation dictionary was constructed that covered 90% of pronunciation variations in the NUMBERS corpus (described below) by Dan Gildea at ICSI. The MLPs were trained using the QUICKNET libraries and programs principally written by David Johnson and contributors at ICSI. MLPs were trained on SPERT fixed-point vector processors [55] to reduce training time.

2.4.1 Speech Corpora

The experiments in this document involve two training corpora, which were quite distinct from one another, to promote generality. The principal corpus used for recognition training and testing is a subset of the Oregon Graduate Institute (OGI) NUMBERS corpus [19]. This corpus consists of naturally spoken connected numbers such as “thirty-nine fifty” and “seven seven oh four five.” Utterances from numerous speakers were recorded over the telephone and hand-labeled with phonetic transcriptions by trained phoneticians. With a small vocabulary size of 32 words (see Appendix A), recognition rates above 90% can be achieved. This is useful for studying the detrimental effects of adverse acoustic environments and observing performance changes when experimenting with new ASR techniques. This corpus was further divided into three independent subsets: a training set, a development test set, and a final test set. The training set consists of 3590 utterances comprising approximately 3 hours of speech data and is used for training the front-end MLP probability estimator. 10% of the training set is set aside as a cross-validation (CV) set. The CV set was used in the stopping criterion for the MLP training and was also used for parameter tuning for the speech decoder. Most of the recognition scores were generated using the development test set. It consists of 1206 utterances comprising approximately 1 hour of speech. A final test set consisting of 1.5 hours of speech was also to a slight degree used and kept for concluding results since repeated experimentation with the development set can lead to training on that set.

The second corpus used is the English portion of the OGI multi-lingual database [20], often referred to as the STORIES corpus. This collection is of many speakers who were instructed to speak for approximately one minute about any topic of their choice. There were 210 of these naturally spoken minute-long utterances recorded over a telephone

and hand-labeled and segmented into phonetic units by trained phoneticians. This corpus is used solely as the data set for deriving discriminative temporal filters. The procedure involves analyzing relatively long time windows of speech. The length of the utterances facilitated this longer temporal analysis; the utterances in the numbers corpus were on the order of seconds in length instead of a minute. Further, the stories corpus has a much larger vocabulary and a correspondingly larger number of phone examples. In contrast, the NUMBERS corpus, with its limited vocabulary, contains examples for only 32 of the 56 possible phonetic classes listed in Appendix A. Finally, the independence of the two corpora allows for testing the generality of the discriminatively trained filters.

Chapter 3

LDA Temporal Filters for RASTA-PLP

This chapter describes efforts to improve word recognition in adverse acoustic environments through discriminant training of the front-end acoustic modeling stages. In our hybrid ANN-HMM system an MLP was discriminatively trained to classify phonetic class targets. This MLP operated on features primarily along the frequency dimension. To further improve classification, discriminant training was added along the temporal dimension. Linear Discriminant Analysis was the tool that was used to derive discriminatively trained temporal filters. The experiments examined the filter characteristics and word-recognition performance in the presence of acoustic degradation using these temporal filters with RASTA-PLP preprocessing.

3.1 Temporal Filter Design with Linear Discriminant Analysis

Linear Discriminant Analysis (LDA) has been used in speech feature extraction for integrating adjacent feature frames, for feature selection and as an alternative to cepstral analysis. Both LDA and cepstral techniques orthogonalize the feature-vector components (the cepstra approximately so). LDA additionally arranges the feature components in dimensional order of linear separability. This procedure was often applied to one or more

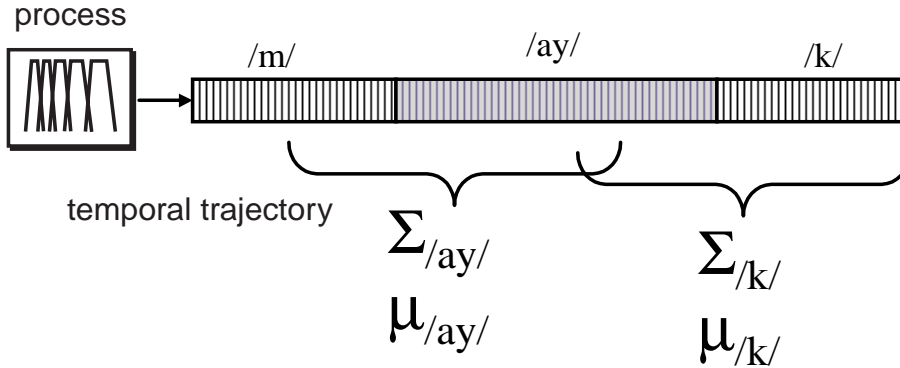


Figure 3.1: LDA is applied to the temporal trajectories of the log-critical-band energy. Linguistic classes are assigned to the center of relatively long time spanning windows of trajectories. Means μ and covariances Σ are collected for each class.

frames of speech features, but principally spanned the frequency dimension. In work by van Vuuren and Hermansky, the LDA technique was applied along the temporal dimension instead of the frequency dimension. In applying LDA to sub-band log-energy envelopes, they were able to construct linear filters in an automatic fashion from data [110, 6, 109]. Their method provided insights concerning the temporal properties that are useful for discrimination. Results from their work showed similarities to the RASTA bandpass filter and its first and second derivative [49]. The bandpass properties were consistently seen across a number of speech corpora. Additionally, they showed how the filters were modified when artificial channel noise was added, the principle effect being DC suppression. In this work we extended these experiments to derive discriminant filters for other corrupting conditions including added *car* noise, added *factory* noise and two examples of room reverberation.

The data-driven filter design procedure involves analyzing relatively long time windows of log critical-band trajectories (Figure 3.1). The speech is analyzed into critical-band power spectra (energy computed from a bark-scale spaced filter bank) followed by a logarithm, as is done in the first few processing steps of RASTA-PLP. LDA follows by capturing approximately 1 second's worth of frames separately for each critical-band and subsequently assigning to it the linguistic unit that corresponds on the center of this segment. From these class bins of trajectory segments two quantities are computed, the within-class covariance, S_W , and the between-class covariance, S_B . The principal discriminant basis functions are then taken as the eigenvectors of $S_W^{-1}S_B$ that have the largest associated eigenvalues [28]. Again, S_W is the average within-class covariance and S_B is the

covariance between the means of each class. As these eigenvectors are applied to temporal sequences, they are effectively FIR filters. That is, the output of FIR filtering can be interpreted as the inner product between the FIR filter coefficients and a sliding window of the signal input.

Design of the RASTA-style filters was based on the STORIES labeled corpus. Then the full speech recognition system was trained and tested on the NUMBERS corpus, using filters from the STORIES corpus in the feature extraction.

3.2 Temporal LDA Filters in Varying Acoustic Conditions

Environmental conditions often have a pronounced detrimental effect on automatic speech recognition. One effect of the environmental condition is an altering of the distribution of the feature vectors, thereby creating a mismatch between training and testing conditions. As mentioned in Section 2.2.2, an effect of additive noise is an offset in of the power spectra while the principal effect of reverberation is smearing of the spectral energy forward in time. We were interested in the effect of various noise conditions on the data-driven discriminant filter design. For this purpose we modified the raw speech with examples of reverberation and additive noise.

3.2.1 Clean Speech Data

Figure 3.2 shows the impulse and frequency responses for the three principal discriminant basis filters. The impulse responses exhibited a “Mexican hat” shape with frequency responses that were band-pass in nature. The first discriminant filter in particular exhibited a frequency response that is similar to the IIR RASTA filter (Figure 2.6). The filter passed the modulation frequencies between about 1 and 13 Hz. The second and third filters resembled first and second derivatives of the first filter. The filters were approximately symmetric and had linear phase characteristics allowing the phase of the modulations to pass relatively unaffected. Although the speech corpora for the filter design was described as *clean*, it was in fact recorded over the telephone and some channel variability, as well as speaker variability, was present. Since RASTA filtering was designed to reduce the effects of channel variability, it is encouraging to see that filters designed directly from a discriminant criteria exhibited some of the same properties. In all cases involving

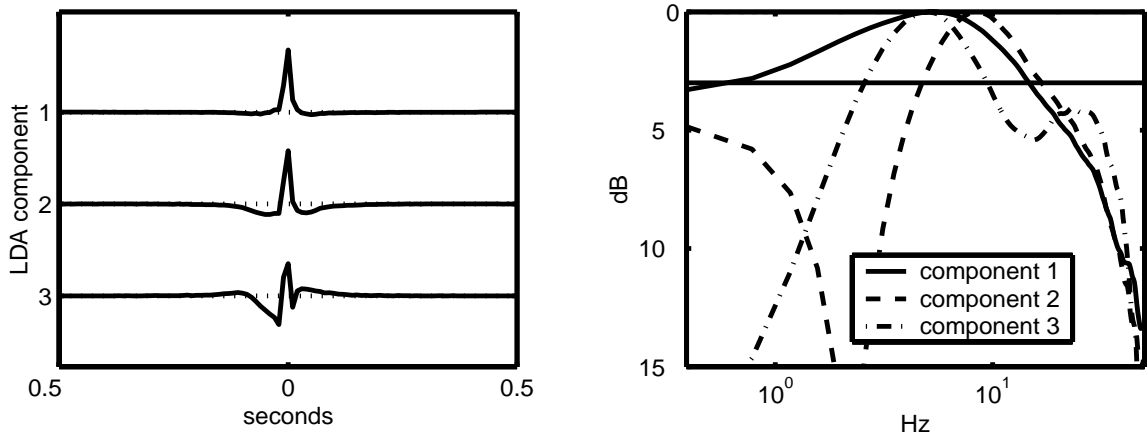


Figure 3.2: Averaged impulse and frequency responses for LDA filters derived with *clean* data.

a number of different acoustic environments, the first three discriminant filters accounted for about 95% of the variance in the data. The first component typically accounted for between 75% and 80% while the second explained an additional 10% to 15%.

The LDA technique was applied to trajectories for each of the critical-band filterbanks spanning the range of 15 Bark. All of the derived filters were similar in shape and frequency response except for possibly the lowest and highest bands, due to telephone bandwidth limitations. Filters in Figure 3.2 represent an average of the individual responses excluding the lowest and highest bands. Appendix B contains more detailed plots of individual critical-band filters. The responses of the lower bands sometimes appeared to have slightly broader impulses with narrower frequency bandpass ranges. Vocalic phones, which often constitute syllable nuclei, tend to dominate the lower frequencies. Thus modulations at this frequency range can vary closer to a syllabic rate. The difference between filters for different frequency bands increased in the presence of added noise or reverberation.

3.2.2 Reverberated Speech Data

Figure 3.3 shows averaged LDA filter responses when the speech data was convolved with the *light* and *heavy* room impulse responses described in Section 2.3. The *clean* responses are shown for comparison. Again, the filters represent an average over all of the individual critical-bands (except the lowest and highest) and some individual responses are

located in Appendix B. When comparing among the *clean*, *light*, and *heavy* reverberation cases the impulse responses became broader. With the heavier reverberation, the principal response lost some of its symmetry, commensurate with the causal nature of reverberation.

In the principal component, the upper cutoff frequency decreased from 13 Hz for the *clean* case to about 8 Hz for the *light* reverberation case and about 5 Hz for the *heavy* reverberation case. The second and third component also shifted towards the lower modulation frequencies. This indicated that the useful discriminant information in the presence of reverberation was better preserved in the low modulation frequencies corresponding to syllabic rates. It lends credence to the notions of stability of syllables and syllabic rates to this type of acoustic corruption [43, 39]. From a signal standpoint, the modulation frequency response of the room impulse began to cut into the modulation frequency response of speech, which peaks between 4 and 5 Hz [94]. Further, the reverberation response often affected the different frequency ranges unequally, with longer reverberation tails in the lower frequencies than in the higher. This caused some difference between the filters of individual bands.

3.2.3 Speech Data With Added Noise

Figure 3.4 shows LDA filter responses when the training speech data was subjected to added 0 dB SNR *car* noise and 10 dB SNR *factory* noise. We again observed a little bandwidth narrowing in the presence of noise, though not as severe as with reverberation. Not much change was apparent in the shape of the impulse responses. The color of the added noise caused some frequency ranges to be affected more than others. This caused some additional differences between the filter response of individual bands. Some individual bands are plotted for illustration in Appendix B.

3.2.4 Varying Noise SNR and Reverberation Parameters

The experiments here attempted to expose in more detail the effects of varying environmental noise parameters on the resultant LDA filters. First, increasing amounts of *car* noise were added to the speech prior to LDA computation. The noise SNR ranged from 20 dB to -20 dB SNR in 5 dB increments. The impulse and frequency responses of the first principal LDA component for the critical band centered at 500 Hz is displayed in the first

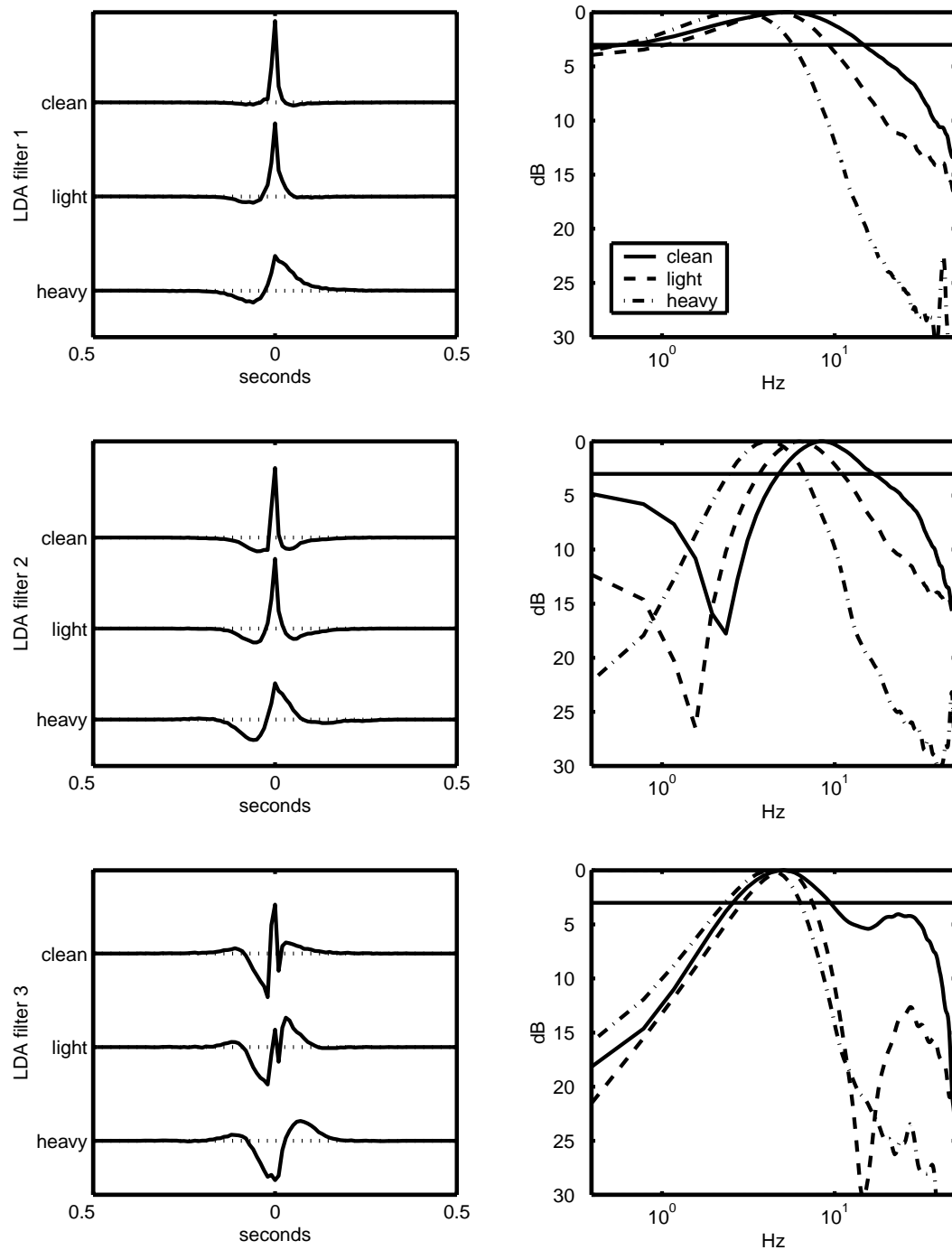


Figure 3.3: Impulse and frequency responses for averaged LDA filters derived with reverberated data.

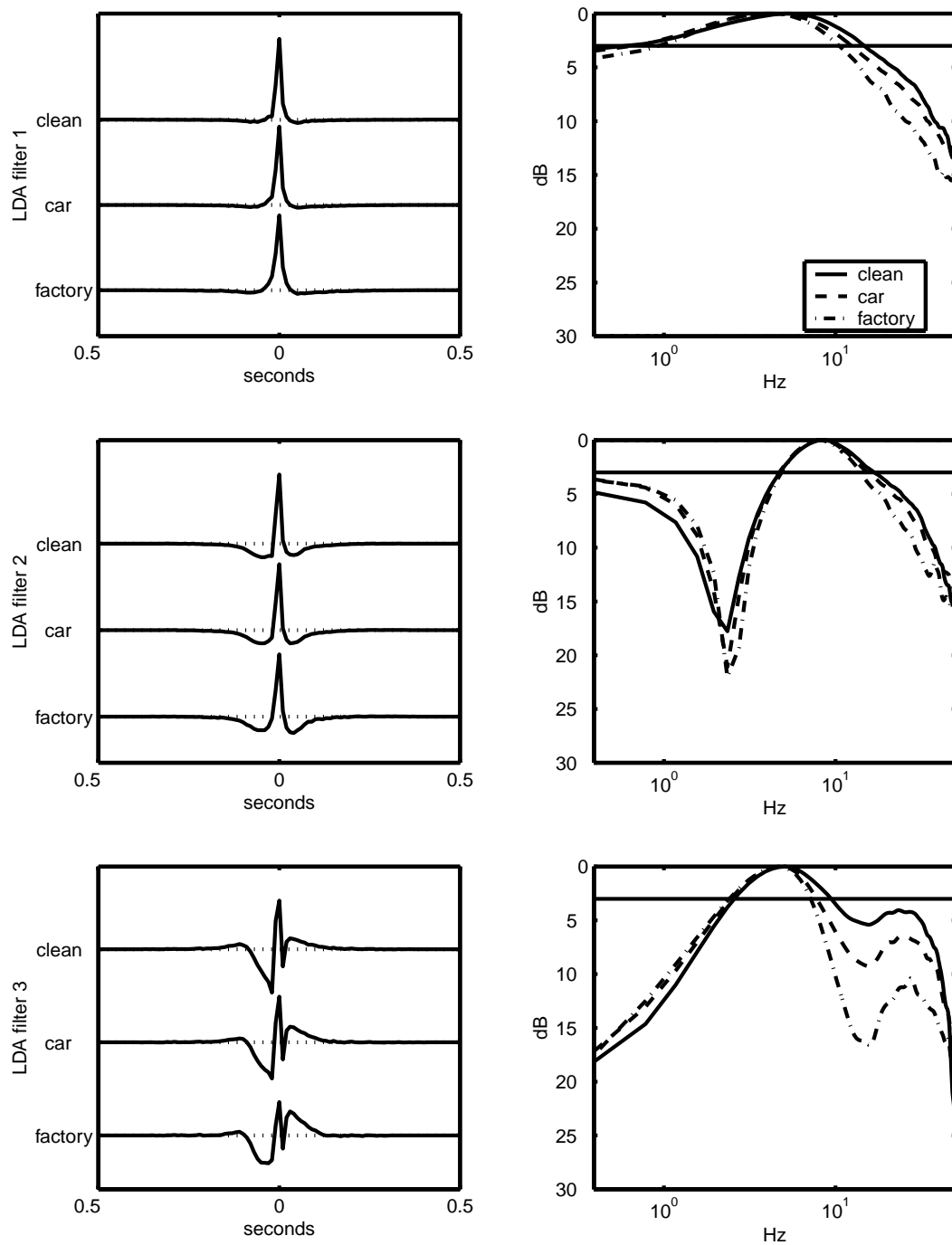


Figure 3.4: Impulse and frequency responses for filters derived from speech data with added noise.

row of Figure 3.5. The basic shape of the filter remained the same though increasing the amount of noise caused a narrowing of the bandpass from 13 Hz down to 8 Hz.

Next, two characteristic parameters of room reverberation were artificially adjusted and applied to the speech prior to filter derivation. The two parameters adjusted were the T60 reverberation time and the DTR. Room impulses with these characteristics were created artificially by modifying the room impulse response that corresponded to *heavy* reverberation. The DTR was adjusted by scaling the direct impulse with respect to the energy in the reverberation tail. T60 was adjusted by applying an exponential decay $10^{-\alpha}$ to the reverberation tail with α selected to yield a specific reverberation time. Adjusting these parameters can be considered as an approximation to adjusting the distance from the microphone to the impulse source and modifying the room characteristics (volume, shape, and surface reflection) in a systematic fashion. Admittedly, when applied to speech, the reverberation effect had an artificial quality. Further, this method of adjusting T60 adjusted the reverberation time equally at all frequencies. Though room changes alter the higher frequencies differently than the low frequencies, it was a useful and convenient approximation.

The second row of Figure 3.5 shows the resultant principal LDA filter for the 500 Hz band when the T60 was varied from 0.25 seconds to 2.5 seconds in 0.25 second increments. The DTR for this plot was fixed at -8 dB. When the reverberation time increased, the preferred frequency range decreased. The smaller reverberation time resembled the response for the *light* reverberation condition described earlier with a high cutoff at approximately 9 Hz. The longest reverberation time, resembling the unaltered *heavy* condition, had a cutoff at around 5 Hz.

Results from adjusting the DTR between -8 dB and 2 dB in 1 dB increments while keeping the T60 fixed at 2.0 seconds did not show as dramatic an effect on the LDA filters as shown in the third row of Figure 3.5. When the DTR was adjusted with a smaller reverberation time (not shown), there was some decrease, but again not as dramatic as modification of the reverberation time itself. The last row shows results when both the DTR and reverberation time varied simultaneously with increasing DTR and decreasing T60. The responses resemble that of the second row in which only the reverberation time alone was varied. The principal observation we gathered was that when there was significant energy in the reverberation tail with respect to the direct impulse, the reverberation time

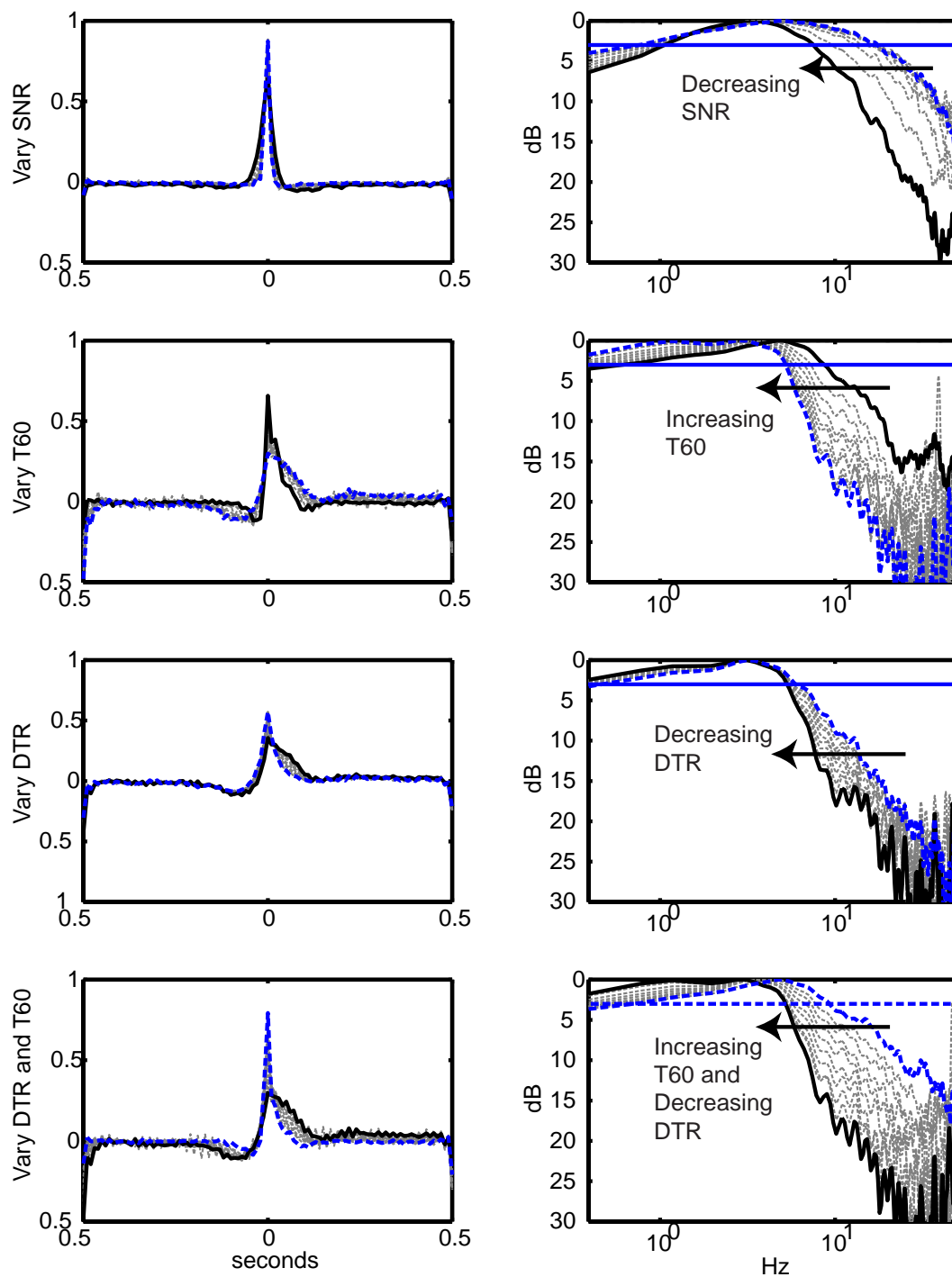


Figure 3.5: Impulse and frequency responses for filters derived with varying *car* noise SNR, reverberation T60, reverberation DTR, and reverberation T60 and DTR.

dominated the changes in the LDA filter’s preferred frequency range.

Experiments were also conducted where the filters were derived using both *clean* and *heavy* reverberation data together. Figure 3.6 shows LDA filter responses when varying the proportion of *clean* and *heavy* training data. The proportion ranged from equal parts of each to purely *heavy* reverberation training data. With equal proportions, the filter resembled that of the pure *clean* case. This was because the covariances for the *clean* conditions were larger than their heavily reverberated counterpart. One can recall for example in Figure 2.12 that the “smearing” effect of the *heavy* reverberation leads to a flatter critical-band trajectory than the *clean* example. This flatter trajectory leads to a smaller variance range and the *clean* case would then dominate the LDA computation. However, when the proportion of *heavy* reverberation data became significant, the response “morphed” smoothly between the two extremes. At some point in the transition the filter resembled that derived in the *light* reverberation case.

3.3 Recognition Results

This section reports recognition results using the LDA-derived filters as a replacement for the standard single-pole RASTA filter (Figure 3.7). Since we were interested in recognition performance in a variety of acoustic environments the tabulated results include mismatched tests (i.e. tests using speech in conditions other than the one that the front-end acoustic modeling was trained). In the tabulated scores the elements along the diagonal correspond to matched training and testing conditions.

3.3.1 Initial Experiments

Tables 3.1 and 3.2 contain the frame accuracy and recognition results respectively using the original RASTA filter. Frame accuracy is determined by declaring a hard classification on each frame based upon the maximum posterior estimate¹. For each frame the phone with the highest posterior probability estimate is declared as the recognized class and is registered as a correct classification if it corresponds to the reference phonetic transcription. Word error rate (WER) consists of the ratio of the number of mis-recognized

¹Classification based upon maximum *a posteriori* probabilities is often referred to as Bayesian classification.

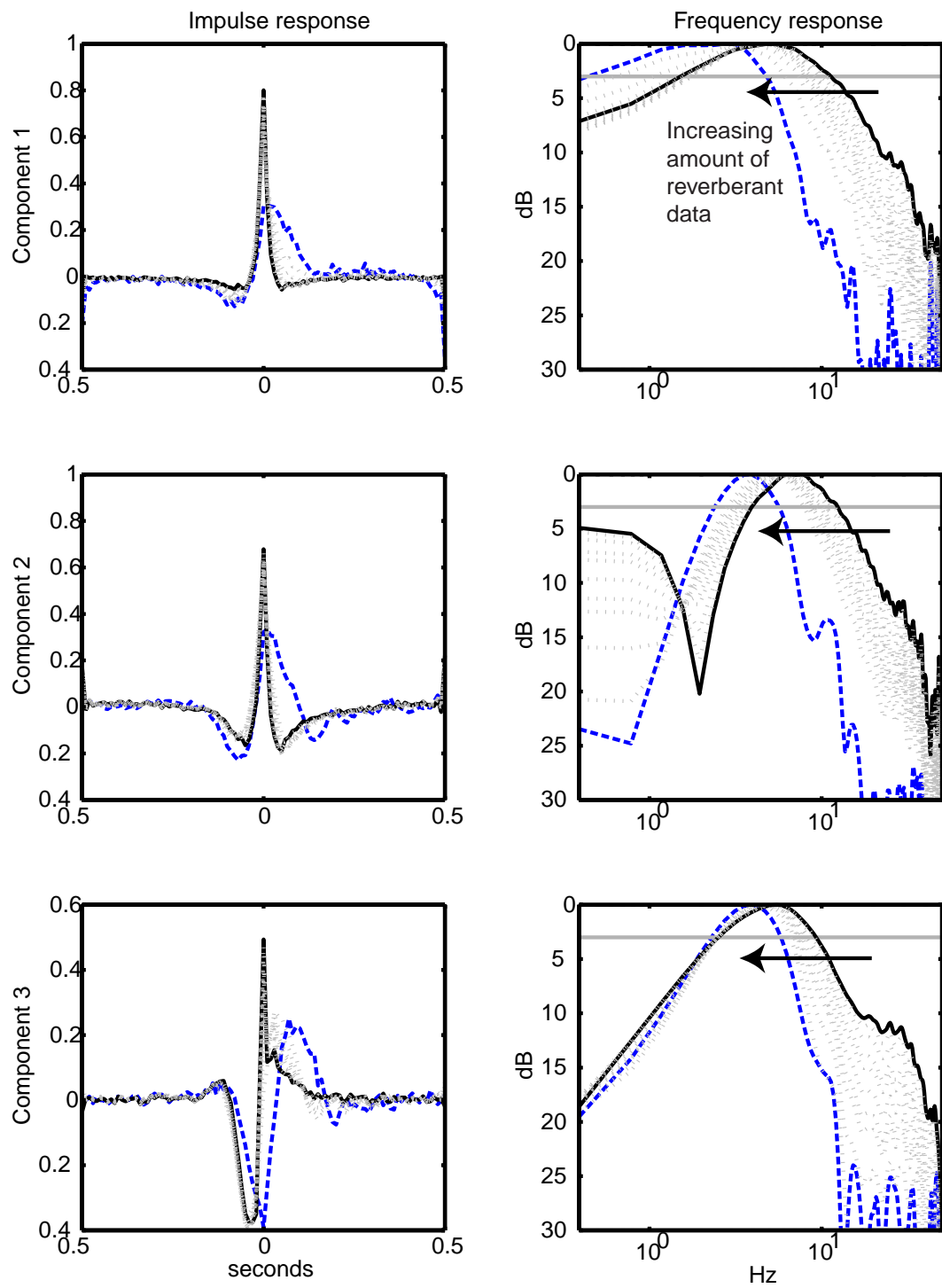


Figure 3.6: Impulse and frequency responses when varying the proportion of *clean* and *heavy* reverberated training data.

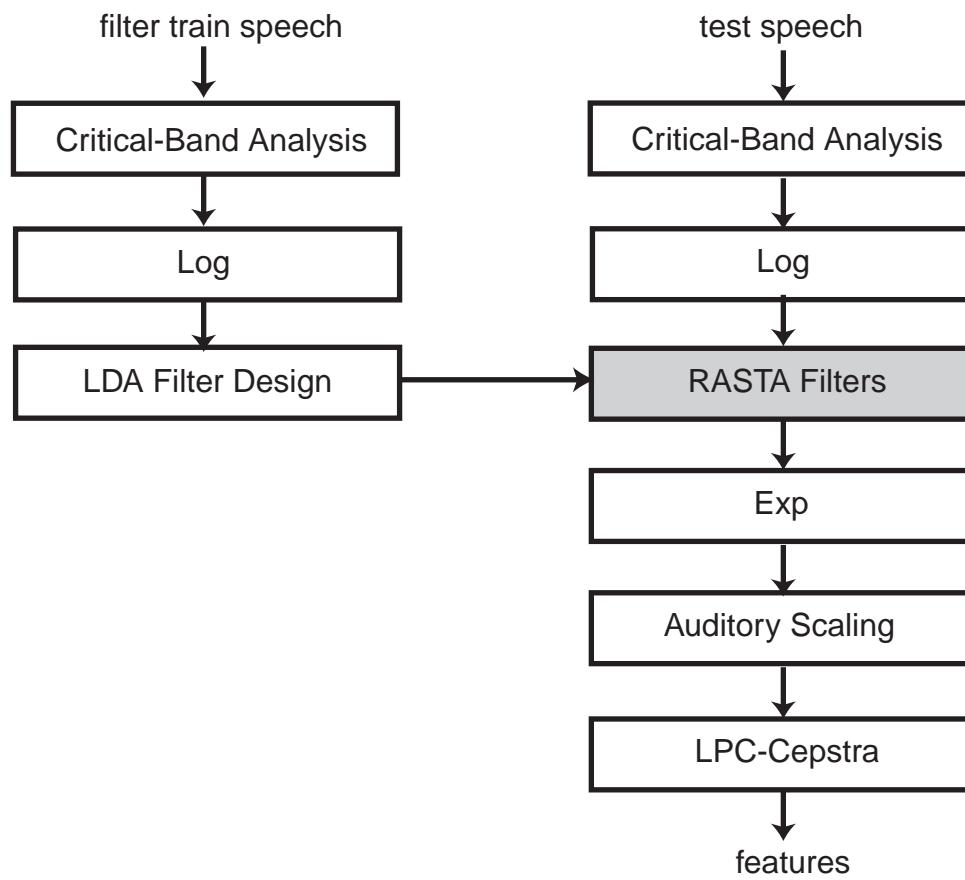


Figure 3.7: The RASTA filter is replaced by filters derived from LDA based on the Stories corpus. Recognition tests used the NUMBERS corpus.

MLP train	Tests Frame Accuracy (%)				
	<i>clean</i>	<i>light</i>	<i>heavy</i>	<i>car</i>	<i>factory</i>
<i>clean</i>	77.49	53.93	33.96	71.32	62.98
<i>light</i>	59.23	70.65	37.77	57.18	60.81
<i>heavy</i>	40.40	43.38	53.63	42.42	40.46
<i>car</i>	62.67	45.01	31.79	78.24	64.20
<i>factory</i>	61.92	50.42	33.48	71.65	73.08

Table 3.1: Frame accuracy results using RASTA-PLP, preliminary tests.

MLP train	Tests WER (%)				
	<i>clean</i>	<i>light</i>	<i>heavy</i>	<i>car</i>	<i>factory</i>
<i>clean</i>	5.80	28.40	70.60	10.80	15.70
<i>light</i>	22.30	11.70	64.20	31.80	20.00
<i>heavy</i>	67.00	50.30	34.90	61.20	59.60
<i>car</i>	23.30	44.90	74.50	6.20	14.70
<i>factory</i>	21.30	35.90	72.20	10.80	8.60

Table 3.2: Word recognition results using RASTA-PLP, preliminary tests.

word hypotheses to the total number of reference words in the test set. Mis-recognized words can appear as substitutions (where erroneous words are substituted for the correct ones), deletions (where correct words are absent from the recognized strings) and insertions (where recognized words appear where there were originally none in the utterance strings). Varying the decoder parameters affects the relative occurrence of these errors. We adjusted the parameters to yield the lowest overall WER. The utterance decoder contains a number of tunable parameters that alter the recognition performance. The parameters yielding the optimal performance vary as a function of recognition testing environment. Consequently, parameters were adjusted in each test to minimize the WER on the independent cross-validation (CV) subset prior to processing the development test set. In doing so we obtained a sample of the best parameters for recognition when using a specific training and testing set.

A trend that was obvious and commonly seen in recognition tests was that recognition scores were best when the testing environment matched the training environment. When testing in a different environment recognition performance sometimes became

MLP,LDA train	Tests Frame Accuracy (%)				
	<i>clean</i>	<i>light</i>	<i>heavy</i>	<i>car</i>	<i>factory</i>
<i>clean</i>	80.85 +	55.56 +	31.28 -	73.07 +	58.93 -
<i>light</i>	64.35 +	75.57 +	35.64 -	46.42 -	45.12 -
<i>heavy</i>	44.19 +	47.21 +	60.79 +	38.96 -	36.38 -
<i>car</i>	53.21 -	23.63 -	22.52 -	80.40 +	55.01 -
<i>factory</i>	67.46 +	43.93 -	29.64 -	67.67 -	75.84 +

Table 3.3: Frame accuracy results using LDA-RASTA-PLP, preliminary tests. The +(-) annotations mark significantly better(worse) performance than RASTA-PLP without LDA in Table 3.1.

MLP,LDA train	Tests WER (%)				
	<i>clean</i>	<i>light</i>	<i>heavy</i>	<i>car</i>	<i>factory</i>
<i>clean</i>	6.30	36.40 -	74.00 -	10.90	31.50 -
<i>light</i>	21.60	10.80	68.20 -	53.90 -	59.30 -
<i>heavy</i>	35.50 +	30.90 +	29.80 +	45.20 +	47.50 +
<i>car</i>	52.30 -	82.40 -	81.20 -	6.30	34.20 -
<i>factory</i>	18.00 +	58.20 -	78.20 -	14.70 -	10.00 -

Table 3.4: Word recognition results using LDA-RASTA-PLP, preliminary tests. The +(-) annotations mark significantly better(worse) performance than RASTA-PLP without LDA in Table 3.2.

abysmal. For example, the ASR system trained with *clean* data degraded from 5.8% error to 70.6% error on the same speech degraded by *heavy* reverberation. When training on the *heavy* reverberation data, the performance improved to 34.90% but dramatically increased the WER for the *clean* data (67%).

In classic form of RASTA-PLP the same filter is applied to all critical band power spectra. From the previous sections, we noted that there was a slight difference between the LDA filters of the individual bands. Experiments here include individual LDA filters for each band. Tables 3.3 and 3.4 show a number of recognition tests using the matrix of filters in lieu of the single-pole RASTA filter. In the tables the training condition corresponded to the condition from which both the MLP and the LDA filters were derived. Matched training and testing conditions are highlighted in bold type. Decoding parameters were adjusted for each recognition experiment.

The plus and minus symbols adjacent to each score denote where LDA-RASTA-

PLP performed significantly better or worse than RASTA-PLP. Where there is no symbol, the score differences were not statistically significant ($p=0.05$, 4763 words). Adding the discriminatively trained filters improved the frame accuracy in all matched training and test conditions (diagonal elements). This result was expected as the filters were designed to discriminate among phonetic classes at the frame level. These improvements in frame accuracy, however, did not necessarily translate into improvements in word recognition; three of the matched testing conditions were not significantly different than RASTA. Most cross-condition tests fared worse than RASTA. One possible explanation is that there may be some degree of over-specificity of the derived filters. The only consistent improvements appeared to be in the case of the *heavy* reverberation training condition. In that instance all cross-recognition tests with reverberant training yielded significantly better results than RASTA. In particular, when training on *heavy* reverberation and testing on *clean* data, the word error rate was 35.50% while using RASTA resulted in a WER of 67%. Recall that the difference between the processing was that the LDA derived filter in this training case had a preferred frequency range commensurate with syllabic rates up to 5 Hz while the original RASTA filter had a 12-Hz range. Processing that preserved these syllabic rates demonstrated some stability in the recognition results across these tests.

3.3.2 Recognition with Local Normalization

In the cross-condition tests the trained MLP was presented with speech in a different acoustic environment. Different environments create changes to the feature distribution. The MLP, being trained on a particular feature distribution, then degrades in performance when presented with a changed distribution. In the initial experiments of the previous section, there was no processing to account for the change in feature distribution other than what was inherent in the feature extraction. Recall in Section 2.1 that the training features are normalized across the entire set to have zero mean and unit variance to aid in MLP training. These scaling parameters are also applied to the test speech as part of the feed-forward process into the MLP. In a different acoustic environment the normalization parameters are no longer a good match. One solution is to measure normalization parameters of the test data prior to recognition. This would move the test-feature distribution to a range similar to that trained. Though this can be done with collected testing data it is not as suitable for real-time deployment.

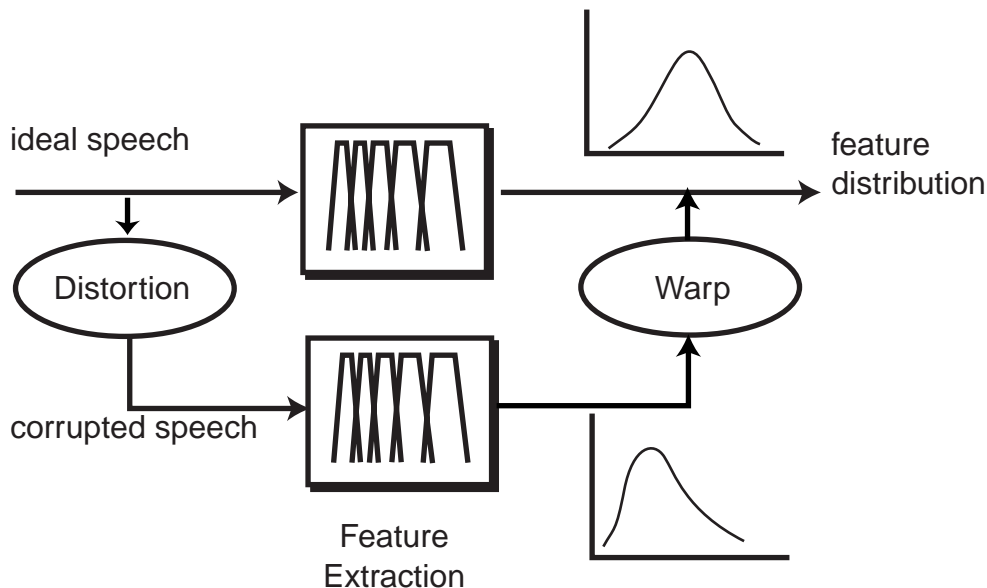


Figure 3.8: Feature distributions from speech distorted by environmental conditions can be warped to match an undistorted distribution.

An attractive alternative is to compute normalization parameters in a local manner instead of over a complete collection of utterances. Such normalization parameters would change over time and hence provides a form of adaptation. Features for individual utterances would be guaranteed to fit into a dynamic range that the MLP expects and hence would also help correct for differences in the speech energy that can be apparent between separate utterances of the same data collection. Ideally, a distribution-correction procedure would warp the feature distribution from acoustically corrupted speech into one matching an ideal distribution, as depicted in Figure 3.8. An easily implementable approximation is to adapt the means and variances of the corrupted distribution to match the ideal condition. Alternatively, as ideal conditions may not be available, the distributions of the features of different conditions can be offset and scaled to specified values (in this instance zero mean and unit variance). Local normalization can be performed in an online manner similar to that described in Section 2.2.5 or on a per-utterance basis if the utterances are relatively short (as they are in the NUMBERS corpus). Such local normalization has useful properties that in some ways have been implemented by other means in the front-end; normalizing to a zero mean is equivalent to CMS when the normalization is applied to cepstra. Normalizing locally to unit variance is similar to application of automatic gain control

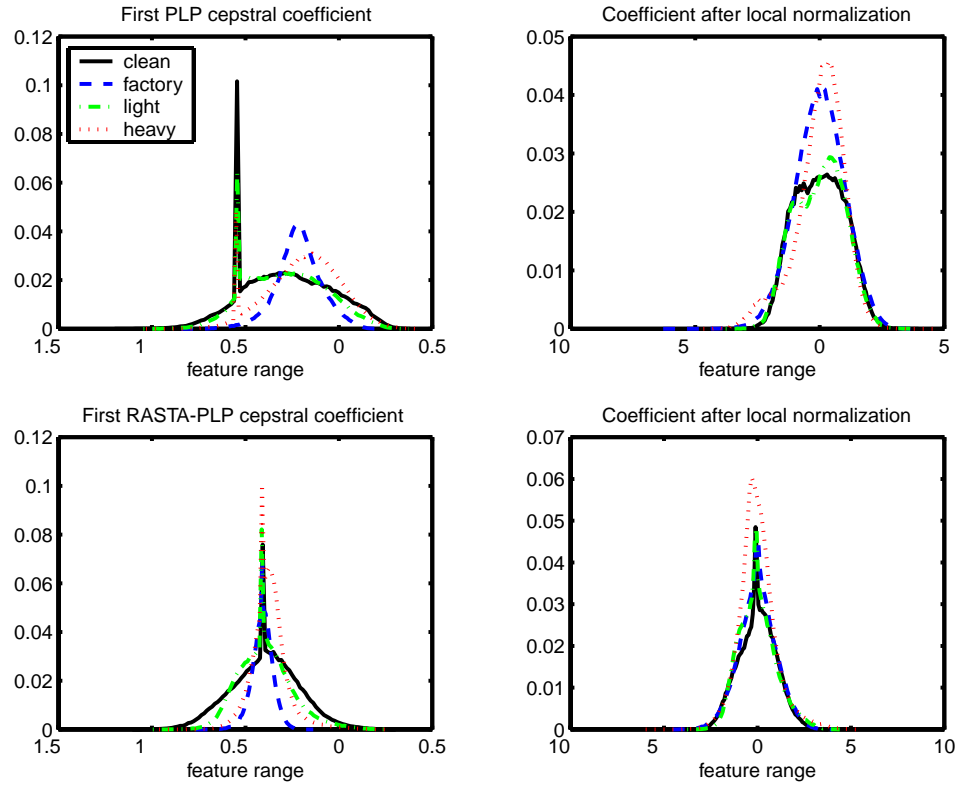


Figure 3.9: Examples of the histogram distribution of first cepstral coefficient for PLP and RASTA-PLP before and after per-utterance local normalization.

where the time constant is on the order of a few seconds. Figure 3.9 contains example histogram distributions of the first cepstral feature component of PLP and RASTA-PLP. The pooled distributions are of data in different acoustic environments.² In the un-normalized distributions in the left plots one can witness the distributional changes that result from different acoustic environments. The short-term adaptation due to RASTA processing can also be observed as the feature distributions in the different environments become centered with respect to one another. After per-utterance local normalization the distributions in all of the environments are similar having the same mean and variance.

In the following, the experiments of the previous section were repeated with the added local (per-utterance) normalization step. The features of each utterance of the training and test corpora are normalized to have zero mean and unit variance. Tables

²The conspicuous spike in the clean and reverberant distributions in the left column is an artifact from zero-padding each of the utterances.

MLP train	Tests Frame Accuracy (%)				
	<i>clean</i>	<i>light</i>	<i>heavy</i>	<i>car</i>	<i>factory</i>
<i>clean</i>	77.39	54.78	32.53	70.82	65.11
<i>light</i>	64.89	69.59	34.52	57.88	59.21
<i>heavy</i>	45.14	48.80	51.95	48.65	45.49
<i>car</i>	62.78	42.81	30.10	77.82	64.84
<i>factory</i>	67.63	50.58	31.98	73.85	72.74

Table 3.5: Frame accuracy results using RASTA-PLP, with per-utterance normalization.

MLP train	Tests WER (%)				
	<i>clean</i>	<i>light</i>	<i>heavy</i>	<i>car</i>	<i>factory</i>
<i>clean</i>	6.40	27.00	68.50	11.50	13.40
<i>light</i>	16.50	12.40	64.60	31.40	21.10
<i>heavy</i>	49.00	37.10	38.00	39.90	46.90
<i>car</i>	19.00	51.60	79.00	6.20	15.60
<i>factory</i>	13.80	37.60	75.60	8.20	8.90

Table 3.6: Word recognition results using RASTA-PLP, with per-utterance normalization.

3.5 and 3.6 show results for RASTA-PLP with per-utterance local normalization. These results served as a baseline of comparison to the modified feature processing.

We expected local normalization to offer some advantage when training and testing on different acoustic environments. Comparing tables 3.6 with 3.2, we see many significant changes in the word error with the local normalization. Many improvements occurred in cross condition tests. There was consistent improvement when training on *heavy* reverberation and testing on many conditions, and when training on other conditions and testing on *clean* data. For example, the *heavy*-trained and *clean*-tested WER improved by 18% absolute. There was, however, some reduction in performance in the matched conditions and on some of the cross conditions. A problem with local normalization is that the normalization parameters are not an accurate sampling of the feature distribution; the phonetic composition of the utterance is different across utterances and the shortness of the utterances can make the estimate very poor or inaccurate. Local normalization may not be ideal in all situations. However, the improvements tended to be much greater than the penalty among tests.

Replacement of the RASTA filters with those obtained through LDA revealed

MLP,LDA train	Tests Frame Accuracy (%)				
	<i>clean</i>	<i>light</i>	<i>heavy</i>	<i>car</i>	<i>factory</i>
<i>clean</i>	81.18 +	60.99 +	33.15 +	75.66 +	65.14
<i>light</i>	71.04 +	75.53 +	39.75 +	60.49 +	58.45 -
<i>heavy</i>	43.21 -	49.94 +	60.21 +	38.54 -	38.38 -
<i>car</i>	71.86 +	48.41 +	30.34 +	80.40 +	66.99 +
<i>factory</i>	71.17 +	51.97 +	31.69 -	74.50 +	75.79 +

Table 3.7: Frame accuracy results using LDA-RASTA-PLP, with per-utterance normalization. The +(-) annotations mark significantly better (worse) performance than RASTA-PLP without LDA in Table 3.5.

MLP,LDA train	Tests WER (%)				
	<i>clean</i>	<i>light</i>	<i>heavy</i>	<i>car</i>	<i>factory</i>
<i>clean</i>	5.20 +	27.20	75.10 -	9.10 +	19.20 -
<i>light</i>	11.50 +	10.70 +	57.80 +	24.70 +	25.50 -
<i>heavy</i>	37.00 +	31.10 +	30.30 +	43.50 -	51.80 -
<i>car</i>	9.50 +	45.30 +	77.90	5.90	17.50 -
<i>factory</i>	11.60 +	34.50 +	73.50 +	11.00 -	9.20

Table 3.8: Word recognition results using LDA-RASTA-PLP, with per-utterance normalization. The +(-) annotations mark significantly better (worse) performance than RASTA-PLP without LDA in Table 3.6.

a consistent improvement over standard RASTA. The results of using LDA-RASTA-PLP are shown in Tables 3.7 and 3.8. Matched-condition WER scores with the LDA basis functions were consistently better with the reverberation cases. There was also a consistent improvement in the mismatched reverberation testing conditions. Penalties when using the LDA filters occurred principally in cases where training was based on reverberation data and testing was performed on additive-noise data, such as *factory* noise. The frame accuracy also revealed an overall improvement in most cases when using the LDA filters.

3.3.3 Performance of Individual LDA Filters

So far our tests had been conducted by using MLP probability estimators and LDA filters trained under identical acoustic conditions. It was instructive to examine the performance of the MLPs when using LDA filters derived from a different condition. As we noted earlier the principal differences among the filters was in the pass-band frequency range. Since the filters from the different reverberation conditions produced the most dramatic changes in these ranges these tests only included the reverberation conditions together with the *clean* condition.

To better judge the effectiveness of the filters, we performed tests using MLPs with the input consisting of a single frame of feature vectors; no contextual frames were added to the MLP input. The MLPs used in this test therefore had many fewer parameters, having only 26 inputs and a reduced hidden layer of 400 nodes. Tables 3.9 and 3.10 show the frame accuracy and WER, respectively, using this configuration with LDA filters derived from different reverberation conditions. The +(-) postfixes indicate better (worse) performance than the tests using the LDA filter derived from *clean* data. Matched training, testing, and LDA filter conditions are shown in boldface. An initial observation was that the LDA filters provided the best WER scores when used in the matched training and testing environments. For example, the *heavy* reverberation filter provided the best score when the MLP was trained and tested on reverberation. This indicated that this method for deriving temporal filters provided an additional level of discriminative training for that environment. Additionally, there were other instances where using the reverberant LDA filters improved performance over the *clean* trained LDA filters. These occurred in cases where we tested on a reverberated environment.

From Table 3.9 we can see that each set of LDA filters provided similar phone classification accuracy rates. The accuracy using the *heavy* LDA filters, that preferred lower modulation frequency ranges, were consistently better. In fact, there were numerous instances where similar or slight improvements in the frame accuracy did not also improve the WER and in some cases produced the opposite effect. For example, when the MLP was trained and tested on *clean* data and the *heavy* LDA filter was used, the frame accuracy was higher than the *clean* LDA filter but the WER was significantly worse. In a complementary fashion, when training the MLP with *heavy* reverberation data and testing on *clean* data, the *heavy* LDA filter showed lower frame accuracy than the *clean* LDA filter, but the WER was significantly better. Although frame accuracy is generally correlated with WER, a positive or negative change in the frame accuracy does not guarantee a corresponding change in word recognition performance. This is not an uncommon observation among researchers.

Unfortunately, the different LDA filters did not exhibit as noticeable a positive effect when the MLP was allowed a context of several adjacent acoustic feature frames. Tables 3.11 and 3.12 show frame accuracy and WER results when using the LDA filters in the normal recognition setting. The MLP included 9 frames of acoustic features with 800 hidden units. Here, the different LDA filters did not exhibit much advantage. That is, the *clean* LDA filter performed about as well the other filters, often better in mismatched conditions. The difference with the *clean* LDA filter in matched training, testing, and LDA conditions (shown in bold) were not statistically significant.

The purpose of adding discriminatively trained filters was to add a discriminative component along the temporal dimension in addition to the frequency-related direction. With an acoustic context of 9 frames, the MLP had access to about 100 ms of acoustic information. The MLP, being non-linear and discriminatively trained, could therefore incorporate temporal processing and in some sense mimic certain properties of the temporal LDA filters. The reverberation-trained LDA filters were linear and more frequency restrictive and may have discarded information exploitable by the MLP. Further, the reverberation-derived filters exhibited a broader temporal response and may have brought in more acoustic context into the MLP than was necessary. Earlier experiments by ICSI researchers conducted by varying the input context of the MLP reveal that increasing the number of input feature frames from a single frame improves word recognition

Frame Accuracy (%)				
MLP env.		LDA training environment		
train	test	<i>clean</i>	<i>light</i>	<i>heavy</i>
<i>clean</i>	<i>clean</i>	73.55	73.53	74.27 +
<i>clean</i>	<i>light</i>	54.41	54.59	58.48 +
<i>clean</i>	<i>heavy</i>	31.83	29.20 -	32.36 +
<i>light</i>	<i>clean</i>	62.31	61.90 -	63.46 +
<i>light</i>	<i>light</i>	66.15	67.57 +	68.59 +
<i>light</i>	<i>heavy</i>	36.75	36.82	38.07 +
<i>heavy</i>	<i>clean</i>	45.79	43.86 -	42.57 -
<i>heavy</i>	<i>light</i>	48.20	48.33	47.13 -
<i>heavy</i>	<i>heavy</i>	50.44	51.68 +	54.64 +

Table 3.9: Frame accuracy using LDA filters derived from reverberant data and an MLP with a single frame of input features. The +(-) annotations mark where results using the *light* and *heavy* filters are significantly better (worse) than when using the *clean* filter.

WER (%)				
MLP env.		LDA training environment		
train	test	<i>clean</i>	<i>light</i>	<i>heavy</i>
<i>clean</i>	<i>clean</i>	9.10	9.00	12.00 -
<i>clean</i>	<i>light</i>	33.10	31.70	30.20 +
<i>clean</i>	<i>heavy</i>	72.50	73.00	73.40
<i>light</i>	<i>clean</i>	16.90	16.30	20.10 -
<i>light</i>	<i>light</i>	18.90	16.40 +	18.30
<i>light</i>	<i>heavy</i>	62.60	61.40	63.50
<i>heavy</i>	<i>clean</i>	47.00	45.50	43.20 +
<i>heavy</i>	<i>light</i>	42.70	36.80 +	37.80 +
<i>heavy</i>	<i>heavy</i>	45.50	42.10 +	38.90 +

Table 3.10: WER using LDA filters derived from reverberant data and an MLP with a single frame of input features. The +(-) annotations mark where results using the *light* and *heavy* filters are significantly better (worse) than when using the *clean* filter.

scores. However, the performance begins to degrade when the context becomes too wide [81, 116]. Previous tests have indicated that a context window of about 9 frames yields good classification results. This also covers the breadth of the active region of the impulse responses of the LDA filters.

3.4 Discussion

We see that a difference in the acoustic environment can have a highly detrimental effect on recognition performance. Merely training the probability estimator on the new condition will improve results dramatically. In addition to discriminative training of an MLP to produce posterior estimates, we also attempted to add another level of trained discriminability along the temporal dimension. LDA provides an interesting mechanism for determining the proper temporal filters in RASTA-PLP. Not only does it verify some of the intuition behind the design of the original RASTA filter but it adds a direct and “automatic” means of determining and analyzing the discriminant basis functions along the temporal dimension. Since these filters were determined from a collection of data there remains a danger that they may only be applicable to specific situations. This was one of the reasons for using a speech corpus for filter derivation different from the one used for word-recognition tests. However, another complication exists in that the units for deriving the discriminant filters may not be optimal for the overall task. The LDA filters were derived using phonetic labels from hand transcriptions. Therefore, the filters in some sense sought to improve phonetic classification of these labels on a frame by frame basis. This does not ensure that the overall word recognition will also be improved. It can be argued that a good frame accuracy of phone classes is necessary for good word recognition. However, an improvement in frame accuracy is not a sufficient condition for improved word recognition. A further discussion of this appears in Chapter 4 and Appendix E.

The principal difference between the filters derived from different conditions was in the width and range of the pass-band. For increasingly noisy environments there was a tendency for the filters to prefer the lower-modulation frequency range. Additive noise did not appear to exhibit as much of a change as the addition of reverberation. The reverberation-trained filters may therefore not be as helpful for additive-noise cases. Our results showed a consistent problem when training on the reverberation environment and

Frame Accuracy (%)				
MLP env.		LDA training environment		
train	test	<i>clean</i>	<i>light</i>	<i>heavy</i>
<i>clean</i>	<i>clean</i>	81.18	81.11	79.91 -
<i>clean</i>	<i>light</i>	60.99	61.03	61.03
<i>clean</i>	<i>heavy</i>	33.15	32.13 -	31.81 -
<i>light</i>	<i>clean</i>	71.80	71.04 -	68.89 -
<i>light</i>	<i>light</i>	75.44	75.53	74.18 -
<i>light</i>	<i>heavy</i>	38.77	39.75 +	39.46 +
<i>heavy</i>	<i>clean</i>	47.22	47.17	43.21 -
<i>heavy</i>	<i>light</i>	52.51	52.87 +	49.94 -
<i>heavy</i>	<i>heavy</i>	60.75	60.26 -	60.21 -

Table 3.11: Frame accuracy using LDA filters derived with reverberant data and MLP context window of 9 frames.

WER (%)				
MLP env.		LDA training environment		
train	test	<i>clean</i>	<i>light</i>	<i>heavy</i>
<i>clean</i>	<i>clean</i>	5.20	5.30	7.00 -
<i>clean</i>	<i>light</i>	27.20	25.20 +	25.80
<i>clean</i>	<i>heavy</i>	75.10	73.60 +	73.70
<i>light</i>	<i>clean</i>	10.80	11.50	14.00 -
<i>light</i>	<i>light</i>	11.10	10.70	12.40 -
<i>light</i>	<i>heavy</i>	59.00	57.80	60.20
<i>heavy</i>	<i>clean</i>	31.60	30.80	37.00 -
<i>heavy</i>	<i>light</i>	25.80	24.90	31.10 -
<i>heavy</i>	<i>heavy</i>	30.70	30.10	30.30

Table 3.12: WER using LDA filters derived with reverberant data and MLP context window of 9 frames.

testing on the added noise environment, and vice versa. Since the difference was rather pronounced, it may be necessary to retain multiple front-end and acoustic modeling stages for handling each environment until the differences can be reconciled by other means. A suitable combination of the acoustic processing stages may be employed when the target environment is unknown. One effect of the added environments is a change in the trajectory of the critical-band energy. As a result, the variance patterns of the trajectories are altered, typically reduced to some degree. Added noise and room reverberation change the distribution and the covariance in a different manner. Since the LDA calculation is based upon covariance calculations, we expect some modification of the basis functions if the environments affect the within- and between-class covariances to a different degree.

The *heavy* reverberation case caused a severe flattening of the critical-band trajectory and hence was associated with smaller variance. This case resulted in the most limiting frequency response, keeping frequencies between 1 and 5 Hz in the principal LDA component. Since this range was commensurate with syllabic rates we also conducted some tests where we derived LDA filters using syllable targets instead of phone targets. These are described in in Appendix C. One of the results of using syllables as targets was that the filter impulse responses were broader and also kept a pass-band of about 1 to 5 Hz and bore strong similarity to the filters derived in severe reverberation. Further, this rate appeared stable regardless of the acoustic environment added to the data. This appears to support the benefit of analyzing wider analysis windows using a more syllabic rate for perceptual stability. In noisy environments phonetic identity often becomes obscured. A back-off strategy to wider temporal integration and higher-level knowledge may be employed to aid in decoding the utterance. Further discussion and work on the use of syllable or syllable-like information for speech recognition can be found in [39, 117, 120, 101].

Since the responses of the LDA filters across all frequency bands were similar, with some differences among bands, we also experimented with applying a single filter to all of the frequency bands just as the standard RASTA-PLP does. This single filter was the averaged response of all of the individual responses. Pilot tests with these averaged filters yielded results that were consistent with the tests here, though with slightly worse performance. Subtle differences among the responses of the individual band filters account for this. However, different types of phone classes carry different temporal properties and occupy different frequency ranges. For example, vocalic phones principally occupy the lower

frequency bands and have some durational differences from other phones such as stops and plosives that have a shorter duration but span higher frequencies. Using a single bank of filters designed to discriminate among all phones may in the future be further augmented by filters designed to discriminate among certain classes of phones similar to the TRAPS filters derived by Sharma [99, 98, 51]. TRAPS filters are matched filters derived from averaging the temporal trajectories of phone classes and have been used successfully in an articulatory feature based system and in multi-stream systems. Many options for temporal filtering exist. LDA provides a relatively simple method of obtaining filters derived from a discriminative criterion. It further allows us to examine the trends in the modulation spectrum that carry phone discriminative information in the presence of signal degradation due to acoustic environments.

Chapter 4

LDA temporal filters with PLP and MSG

In the previous chapter, LDA was applied individually to the logarithm of the critical-band trajectories. In RASTA-PLP, filtering in the log-power spectral domain allowed for transforming convolutional noise into additive noise, to which a linear filter can be applied. Applying LDA in this domain produced basis filters with consistent properties. It was demonstrated that using discriminatively trained LDA filters could further improve classification and recognition performance. Since there are situations when different feature-extraction algorithms will perform better it was worthwhile to explore the potential enhancement of other algorithms with the temporal LDA technique. In this chapter we explore the application of LDA filter design to two other preprocessing configurations, PLP-cepstra and MSG.

4.1 Logarithm of the Power Spectra

First we must consider where application of LDA is suitable. RASTA-PLP applies temporal filtering to compressed power spectra. The compressing function is memoryless and is usually a logarithm, though other functions, such as a root power, can also be used. Other preprocessing strategies such as MSG use a root power in lieu of a logarithm applied to the power spectral estimates. The question arises as to which domain is best or whether the difference in domain is important. For the application of LDA we find that the domain

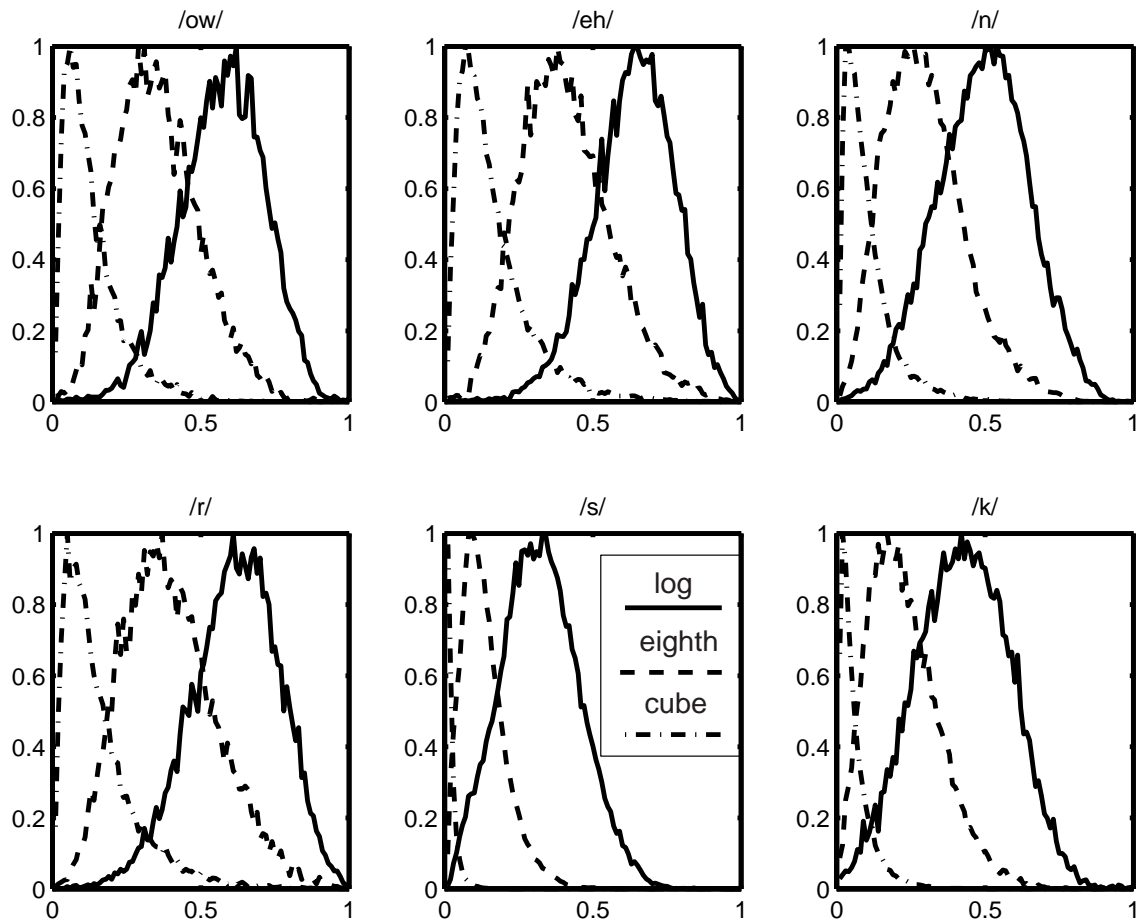


Figure 4.1: Histogram distributions of the critical-band output centered at 570 Hz, and subjected to cube-root, eighth-root and logarithmic compression. The distributions are for the phones /ow/, /eh/, /n/, /r/, /s/, and /k/. Ranges and densities are scaled individually for comparison.

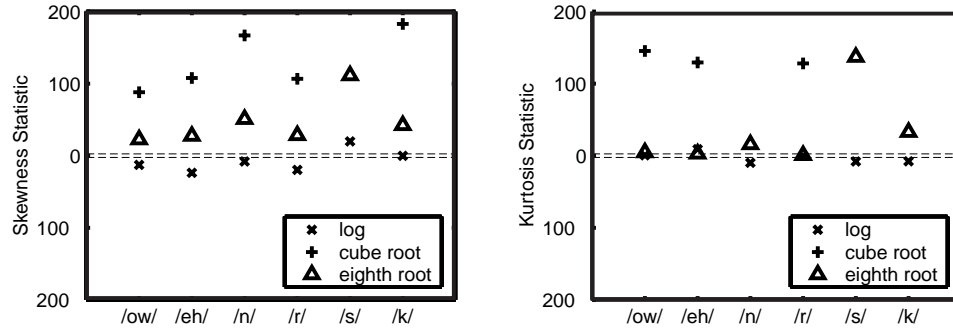


Figure 4.2: Skewness and Kurtosis statistics of the critical-band output centered at 570 Hz, and subjected to cube root, eighth root, and logarithm for the phones /ow/, /eh/, /n/, /r/, /s/, and /k/.

should be considered when performing analysis.

Recall that one of the criteria for optimal linear separability using LDA is that the underlying class distributions be Gaussian. With that in mind, the logarithm of the power spectra offers several advantages over certain other memoryless non-linearities such as a root-power. The resulting distribution when taking a logarithm of the critical-band trajectories is closer to a Gaussian distribution. Consider for example the histograms in Figure 4.1. Histograms for several phone classes are illustrated for conditions where the critical-band output is subjected to cube-root, eighth-root and logarithmic compression. The range and scale of each of the different distributions are independently scaled in order to compare the shapes on the same plot. The cube-root distribution is asymmetric with more values clustered at the lower end of the range of values. Taking smaller roots, such as an eighth-root, improves the symmetry, making the distribution closer to a Gaussian form¹. The logarithm of the critical-band power most closely approximates a Gaussian distribution compared to the other root powers based on quantile-quantile plots. In addition, the Fisher ratio, which is related to the separability of the classes, is highest for the logarithm form of compression.

Application of a logarithm is a common statistical technique for normalizing data. Unfortunately, the log-energy envelopes can be strongly non-Gaussian, as demonstrated by Yang and colleagues [122, 121]. Simple normality tests used skewness S and kurtosis K

¹The AGC stages in MSG have a square root steady state response, resulting in an eighth-root applied to the power spectral energy. This compression may contribute to the success of the MSG features.

statistics:

$$S = \frac{1}{\sqrt{6T}\hat{\sigma}^3} \sum_{t=1}^T (x_t - \hat{\mu})^3 \quad (4.1)$$

$$K = \frac{1}{\sqrt{24T}\hat{\sigma}^4} \sum_{t=1}^T (x_t - \hat{\mu})^4 - \sqrt{\frac{3T}{8}} \quad (4.2)$$

where $\hat{\mu}$ and $\hat{\sigma}$ are the sample mean and standard deviations of envelope x_t . S and K are standard normal under the null hypothesis. Whereas the total pooled distribution is strongly non-Gaussian, phonetic class subsets appear to be better behaved. Statistics for several phones, subjected to logarithm, cube-root, and eighth-root compression are shown in Figure 4.2. From this plot, the logarithmic data is closer to the critical significance range of ± 2.58 ($p=0.01$). The logarithm does not support the Gaussianity null hypothesis in many tests but is demonstrably superior to the cube- and eighth-root forms of compression. The logarithm also offers some mathematical advantages over the root powers. As mentioned in Section 2.2.4, the logarithm provides justification for transforming convolutional noise into additive noise. Log-domain filtering can be interpreted as short-term adaptation or as some form of automatic gain control. Additionally, the spectral distribution resulting from a logarithm is shape-invariant to both scaling and powers of the input, whereas the root power is only shape-invariant to scaling of the input. Scaling the input by a constant factor merely adjusts the span of the domain of the distribution for the root-powers and shifts the domain for the logarithm since $\log(aX) = \log(a) + \log(X)$. Observing the logarithmic property that $\log(X^p) = p \log(X)$, we also see that powers of the input also appear as a scaling constant and therefore only affect the span of the distribution; the shape of the distribution remains intact. To reiterate, a scale and power operation results in a shift and scale operation after a logarithm. When the resulting distribution is Gaussian, such a shift and scale amounts to adjusting the mean and the variance while preserving the Gaussian nature of the distribution.

4.2 Delta Calculation with Perceptual Linear Prediction

Numerous tests have revealed that RASTA processing aids in reducing the channel variability introduced by a change in microphone or telephone line [82, 50]. Since the typical response of these channels is short enough to be contained within a single analysis window, this form of convolutional noise can be dealt with using RASTA filtering in

MLP train	Tests Frame Accuracy (%)									
	<i>clean</i>		<i>light</i>		<i>heavy</i>		<i>car</i>		<i>factory</i>	
<i>clean</i>	78.70	+	56.50	+	27.06	-	72.51	+	65.56	+
<i>light</i>	68.39	+	71.61	+	32.53	-	57.07	-	58.06	-
<i>heavy</i>	45.10		48.66		54.06	+	44.61	-	37.66	-
<i>car</i>	62.71		39.56	-	22.59	-	78.82	+	63.45	-
<i>factory</i>	69.46	+	50.07	-	26.60	-	74.72	+	72.93	

Table 4.1: Frame accuracy results using PLP with per-utterance normalization. The +(-) annotations mark where the performance is significantly better(worse) than the RASTA-PLP with per-utterance normalization in Table 3.5.

MLP train	Tests WER (%)									
	<i>clean</i>		<i>light</i>		<i>heavy</i>		<i>car</i>		<i>factory</i>	
<i>clean</i>	5.10	+	24.90	+	77.60	-	8.30	+	11.50	+
<i>light</i>	12.00	+	10.90	+	58.80	+	27.60	+	20.80	
<i>heavy</i>	39.20	+	31.40	+	35.40	+	35.30	+	48.10	
<i>car</i>	17.00	+	50.70		83.50	-	5.90		17.20	-
<i>factory</i>	11.00	+	34.00	+	72.90	+	8.30		8.90	

Table 4.2: Word recognition results using PLP with per-utterance normalization. The +(-) annotations mark where the performance is significantly better(worse) than the RASTA-PLP with per-utterance normalization in Table 3.6.

the log-spectral domain. However, subsequent tests revealed that this processing is less effective with additive noise. This was one of the motivations behind the J-RASTA-PLP processing variation [67]. By applying a filter to $\log(1 + Jx)$ and adjusting the J parameter, the filtering can be effectively switched from the log domain to an approximately linear domain. Room reverberation presents an additional problem since the breadth of the impulse spans many analysis frames. Numerous tests have shown that PLP without the log-RASTA processing, but with local normalization, can be a more effective feature extraction algorithm in environments other than channel convolution.

For the acoustic environments used in this work, PLP with local normalization demonstrated consistent improvements over RASTA-PLP in this task. Frame accuracy and word recognition results are shown in Tables 4.1 and 4.2, respectively. The +(-) symbols signify where PLP did significantly better(worse) than RASTA-PLP. Most of the training and testing cases showed significant improvement on the order of 2% to 3% absolute and principally pertained to the clean and reverberation conditions. The final stage of PLP is the computation of cepstral coefficients from a scaled and smoothed auditory spectrum. Recall that cepstral coefficients are a linear transformation of the log of the spectrum. Cepstral-mean removal mimics the high-pass characteristic of the RASTA processing, eliminating some of the channel variability. Variance normalization is similar to the short-term adaptation and automatic gain control that is also part of RASTA processing.

From Section 4.1, we noted that the log-spectra is suitable for LDA computation. Observations from the cepstra output, being a linear transformation of this domain, indicate that it is also possible to apply LDA. A sample plot of class histograms is shown in Figure 4.4. In lieu of performing the analysis directly to the PLP cepstral coefficients we applied the LDA to the coefficients that had been normalized to zero mean and unit variance. Samples of the basis filters are shown in Appendix D. We again see that the discriminant information resided in the low modulation frequencies, with the basis filters passing frequencies around this range.

We applied the first three discriminant filters to the outputs of the cepstral coefficients, as depicted in Figure 4.3. When used in this fashion, the 2nd and 3rd discriminant filters can be considered as replacements of the delta and double-delta calculation steps normalized locally for posterior probability computation. For recognition tests, we trained

Environments		Frame Accuracy %			WER %		
train	test	PLP+ Δ_s	PLP-LDA		PLP+ Δ_s	PLP-LDA	
<i>clean</i>	<i>clean</i>	70.75	74.65	+	7.80	8.80	-
<i>clean</i>	<i>light</i>	49.83	55.08	+	28.90	30.10	
<i>clean</i>	<i>heavy</i>	24.66	29.99	+	77.40	73.40	+
<i>clean</i>	<i>car</i>	62.59	67.20	+	12.20	14.10	-
<i>clean</i>	<i>factory</i>	57.51	58.07	+	14.90	22.50	-
<i>light</i>	<i>clean</i>	59.98	60.71	+	16.60	18.60	-
<i>light</i>	<i>light</i>	62.05	67.74	+	16.20	17.60	-
<i>light</i>	<i>heavy</i>	28.66	37.07	+	62.00	59.40	+
<i>light</i>	<i>car</i>	44.77	50.52	+	37.60	32.60	+
<i>light</i>	<i>factory</i>	49.06	54.82	+	27.30	27.70	
<i>heavy</i>	<i>clean</i>	39.48	41.89	+	45.70	56.50	-
<i>heavy</i>	<i>light</i>	40.10	47.03	+	41.00	42.90	-
<i>heavy</i>	<i>heavy</i>	45.59	53.48	+	46.10	40.40	+
<i>heavy</i>	<i>car</i>	42.39	44.14	+	41.60	47.60	-
<i>heavy</i>	<i>factory</i>	32.96	41.81	+	55.10	54.40	
<i>car</i>	<i>clean</i>	50.66	62.57	+	32.00	16.10	+
<i>car</i>	<i>light</i>	30.99	40.99	+	63.90	52.80	+
<i>car</i>	<i>heavy</i>	18.79	26.37	+	85.90	77.80	+
<i>car</i>	<i>car</i>	71.05	75.00	+	7.50	8.20	
<i>car</i>	<i>factory</i>	54.02	58.90	+	23.60	22.50	
<i>factory</i>	<i>clean</i>	61.94	67.25	+	12.90	13.40	
<i>factory</i>	<i>light</i>	45.58	49.39	+	38.60	36.90	+
<i>factory</i>	<i>heavy</i>	23.72	31.58	+	76.20	70.00	+
<i>factory</i>	<i>car</i>	65.87	70.45	+	10.00	12.30	-
<i>factory</i>	<i>factory</i>	63.60	69.70	+	11.90	12.60	

Table 4.3: Comparison of PLP with delta features and PLP with LDA filters. MLP was trained with single frame context of acoustic features. The +(-) annotations mark where PLP with the LDA is significantly better(worse) than PLP with Δ_s .

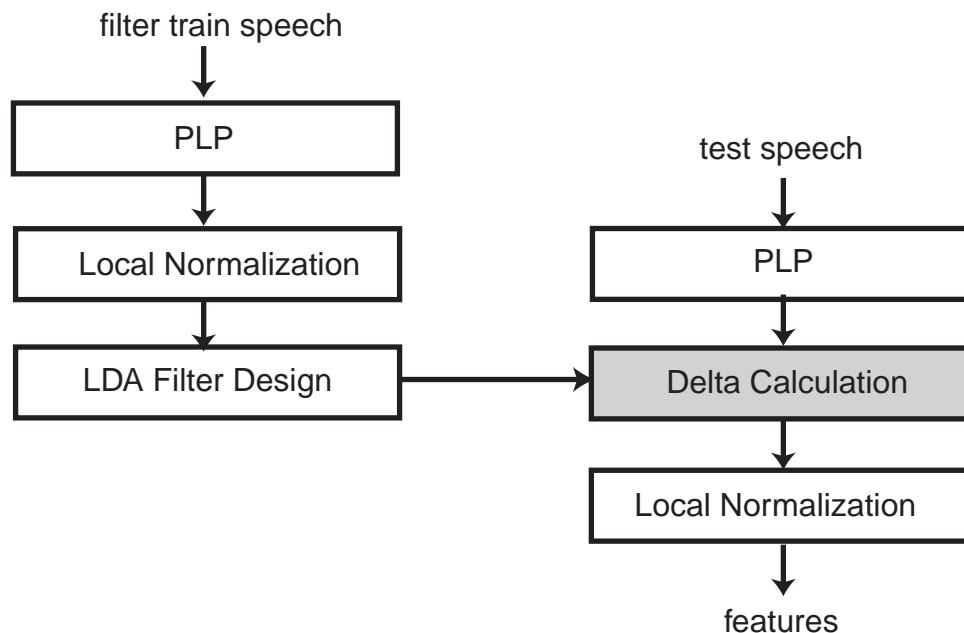


Figure 4.3: The delta calculation for PLP is replaced by temporal filters derived from LDA

the MLP with a single frame of 26 acoustic features² and with 800 hidden units. We removed the contextual frames to better gauge the usefulness of this style of temporal processing as was done in Section 3.3.3. Delta features were originally appended as a means of incorporating some of the speech dynamics into the ASR system. Allowing the MLP many contextual frames gives it access to these dynamics and may therefore obfuscate the effect of the delta features. On the other hand, using delta features has sometimes proven useful overall in hybrid ANN-HMM systems, even with contextual frames.

Table 4.3 compares PLP with the appended delta and double-delta coefficients as well as with PLP using the delta coefficients replaced by LDA components. Both the frame accuracy and the word error rate are shown over the span of training and testing conditions. All features were normalized on a per-utterance basis for these tests. The frame accuracy was uniformly better for all training and testing cases using the LDA components. Matched training and testing conditions yielded about 5% absolute phone classification improvement. However, we see again that this did not correlate well with word error. The instances where word error was penalized significantly were numerous

²Eight cepstral coefficients with first and second derivatives, and the first and second derivative of the log-energy.

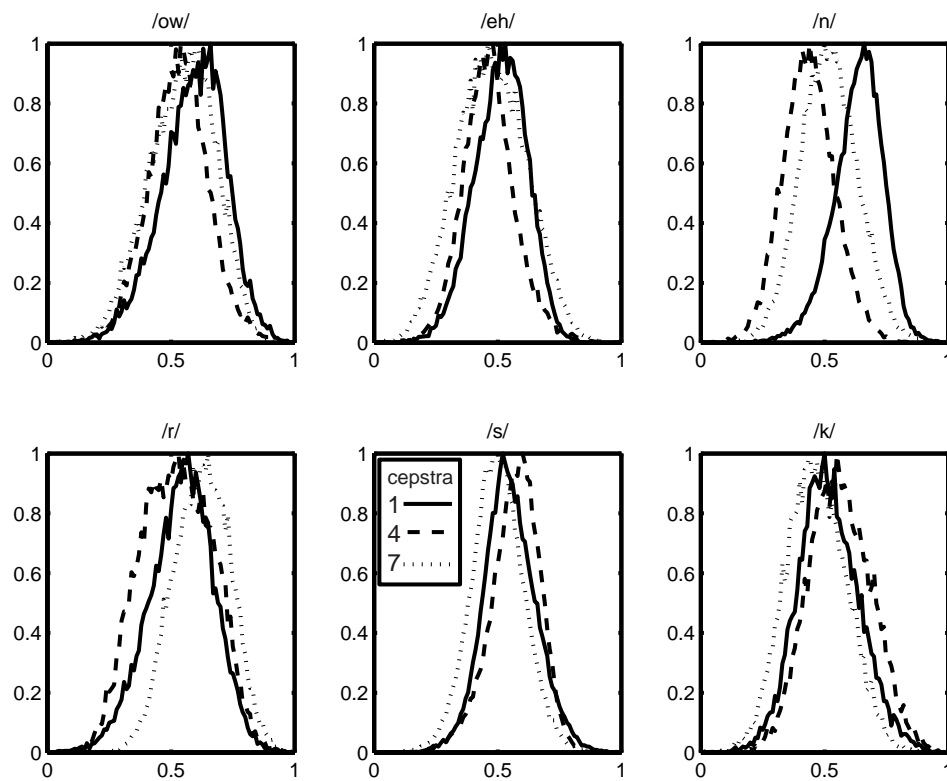


Figure 4.4: Histogram distributions of the first, fourth, and seventh PLP cepstral coefficient. The distributions are for the phones /ow/, /eh/, /n/, /r/, /s/, and /k/. Ranges and densities are scaled individually for comparison.

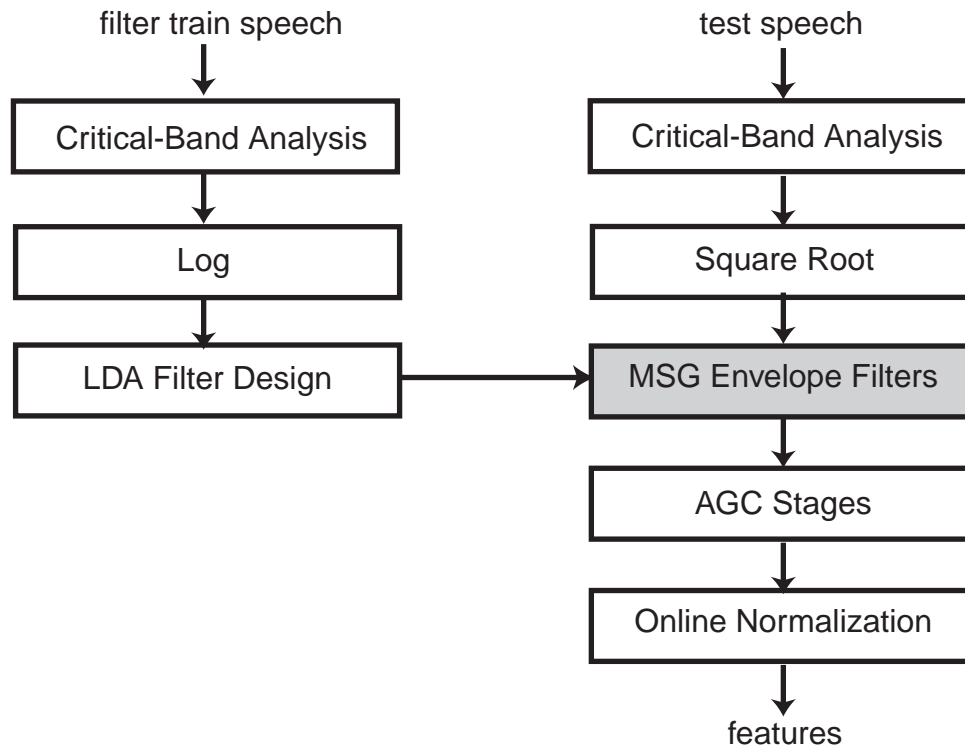


Figure 4.5: The lowpass and bandpass filters in MSG are replaced by filters derived using LDA.

and the only consistent improvements occurred with the *heavy* reverberation tests, where despite the improvement the errors remained too large to be considered useful. There appeared to be no apparent advantage for using LDA filters in place of delta calculations for word level ASR in our system.

4.3 Temporal Filtering with the Modulation-Filtered Spectrogram

A recent preprocessing strategy developed primarily from perceptual experiments is the Modulation-filtered Spectrogram (MSG) [62]. Experiments with this preprocessing have demonstrated some advantages when dealing with reverberant environments. A brief description of the algorithm was included in Section 2.2.5. To summarize, the speech signal is analyzed into critical-band amplitude modulation spectra. A pair of envelope filters are applied to the modulations, after which a few stages of automatic gain control are applied.

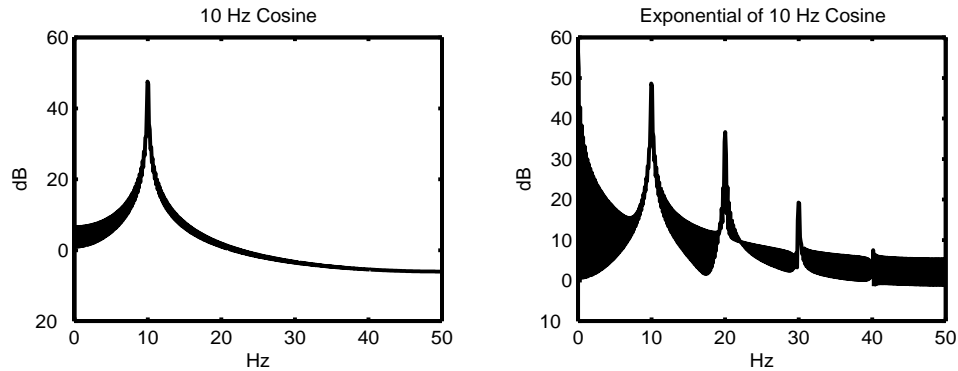


Figure 4.6: The fundamental frequency of the input remains after application of a nonlinearity, but with added harmonics.

The envelope filters were originally determined through several iterations of recognition experiments. These filters were constructed as IIR filters with specified frequency ranges. The two found to be helpful for this task had the range of DC to 8 Hz and 8 to 16 Hz. We attempted here to replace these envelope filters with filters derived directly using LDA, as depicted in Figure 4.5. The filter derivation stages analyzed log-critical-band spectra in a manner identical to that conducted with LDA-RASTA. The first two discriminant filters then substituted the envelope filters in MSG. For the *clean* condition case, the principal filters ranged between 1 and 13 Hz and between 4 to 15 Hz. In the reverberant cases the ranges were lower.

There are two apparent oddities in this setup that require some further explanation. The first concerns the reason we derive the filters in the log-spectral domain instead of the amplitude-spectrum domain. The second pertains to whether it is justifiable to use the filters derived from the log-spectral domain in settings of the amplitude-spectrum domain. For the former we determined that the amplitude spectrum is not a proper domain with which to apply LDA for reasons discussed in Section 4.1. When tapping the outputs of the square-root in the processing chain, a logarithm should be applied in order for linear separability assumptions to be better met. Since the square root only affects the scaling of the distribution in the logarithm domain, it is not necessary in the filter derivation step. However, we must then contend with using filters derived in one domain and applied to another. There are a number of ways to view the matter but a common one is from the perspective of harmonic energy. Imagine that the incoming data was originally formed in

the log-spectral domain to which an exponential was applied prior to filtering. In the frequency domain the effect of applying an exponential (and a large class of other memoryless non-linearities) is the introduction of harmonics. For example, Figure 4.6 shows the magnitude frequency response of a 10-Hz cosine along side the magnitude frequency response after the cosine is exponentiated. The non-linearity preserves the basic fluctuation of 10 Hz but additional harmonics are created at integer multiples of this frequency. Other than the DC component, the main harmonic at 20 Hz in this case is 10 dB below the 10-Hz fundamental. If the signal of interest is in a narrow enough frequency range, the original signal may be extracted through filtering. This frequency component will be affected by the presence of other frequencies however. The presence of another frequency component at 5 Hz would place a main harmonic at 10 Hz. Additionally, owing to the periodic nature of the discrete time domain, the presence of frequencies at 35 Hz and 45 Hz also place a harmonic at 10 Hz. Fortunately, the energy at these latter frequencies is small in the modulation spectrum of speech. More generally, the result of this nonlinearity would be a raising of the noise floor in a signal-dependent fashion.

From this perspective, the LDA filters in this case may be interpreted a little more generally in that they may be applied to modulation trajectories that are warped by a memoryless nonlinearity. The principal LDA filters preserved the lower modulation frequencies up to 16 Hz. This is commensurate with the modulation rates of speech. Experiments by Drullman et. al. [27], Arai et. al. [5] and Silipo et. al. [105] indicate that modulation frequencies in this range are crucial for the intelligibility of speech. What is important is the preservation of the rates with which speech modulates.

When we replaced the envelope filters in MSG with those derived directly from data, we obtained results that were similar to the effect when we replaced PLP delta coefficients with LDA-filtered coefficients. We obtained a consistent improvement in the frame accuracy in both matched and mismatched training and testing conditions. However, this consistent improvement in frame accuracy was again not reflected in the word-recognition error. There were many cases where an improvement in frame accuracy resulted in a corresponding penalty in word-recognition performance. These tests were conducted using the larger connected MLP with 9 frames of input context and 800 hidden units. Results were similar when using a single frame of acoustic features.

Environments		Frame Accuracy %			WER %		
train	test	MSG	MSG-LDA		MSG	MSG-LDA	
<i>clean</i>	<i>clean</i>	76.96	78.40	+	6.50	7.00	
<i>clean</i>	<i>light</i>	63.85	65.75	+	15.30	16.20	
<i>clean</i>	<i>heavy</i>	32.52	33.04	+	77.70	75.50	+
<i>clean</i>	<i>car</i>	73.12	69.75	-	8.10	12.20	-
<i>clean</i>	<i>factory</i>	62.40	63.21	+	15.60	16.90	-
<i>light</i>	<i>clean</i>	70.71	73.06	+	9.90	10.60	
<i>light</i>	<i>light</i>	70.95	72.82	+	12.10	12.40	
<i>light</i>	<i>heavy</i>	36.05	38.46	+	60.90	58.10	+
<i>light</i>	<i>car</i>	64.35	63.30	-	12.30	18.00	-
<i>light</i>	<i>factory</i>	52.67	55.89	+	26.60	23.00	+
<i>heavy</i>	<i>clean</i>	49.55	50.18	+	24.50	27.50	-
<i>heavy</i>	<i>light</i>	53.41	53.30		23.80	28.10	-
<i>heavy</i>	<i>heavy</i>	55.66	57.89	+	31.60	32.80	
<i>heavy</i>	<i>car</i>	46.87	44.68	-	25.70	35.80	-
<i>heavy</i>	<i>factory</i>	40.03	40.28	+	36.50	43.00	-
<i>car</i>	<i>clean</i>	74.58	76.24	+	7.20	7.90	
<i>car</i>	<i>light</i>	60.67	62.33	+	16.30	18.40	-
<i>car</i>	<i>heavy</i>	34.12	35.36	+	73.70	71.00	+
<i>car</i>	<i>car</i>	76.02	77.58	+	7.00	7.60	
<i>car</i>	<i>factory</i>	66.86	69.83	+	12.30	11.50	
<i>factory</i>	<i>clean</i>	70.46	73.26	+	8.60	9.10	
<i>factory</i>	<i>light</i>	57.61	60.43	+	18.30	20.00	-
<i>factory</i>	<i>heavy</i>	33.55	36.32	+	69.90	69.70	
<i>factory</i>	<i>car</i>	73.72	73.10	-	8.20	10.20	-
<i>factory</i>	<i>factory</i>	71.76	74.22	+	9.10	9.90	

Table 4.4: Comparison of original MSG and MSG with LDA-derived filters. MLP trained on acoustic context of 9 frames. The +(-) annotations mark where the MSG with LDA filters is significantly better(worse) than the original MSG.

4.4 Discussion

Different feature-extraction algorithms can perform better in different classification and recognition situations. We applied the temporal processing technique using LDA to two alternate preprocessing algorithms to further improve performance. Replacing the existing temporal processing components with those derived through LDA led to a consistent improvement in frame accuracy. In contrast to results using RASTA-PLP with and without the LDA filters, however, positive results with word recognition tests were found lacking.

In explaining the discrepancy between improved frame accuracy and penalized word error, we must consider that the LDA filters were trained using context-independent monophones. The MSG envelope filters, in contrast, were adjusted empirically using word recognition error as a criterion. We can view the original filters as obtained using gradient descent based on the word error rather than on frame accuracy as was done with LDA. The original filters were consistent with the findings of Kanadera et. al. who performed numerous tests on modulation spectral components in ASR [59, 58]. They concluded that modulation spectral components below 8 Hz were most important for ASR while components up to 16 Hz yielded the best overall word recognition. It is therefore not very surprising in retrospect that the word error from the original envelope filters was lower while the frame accuracy from the LDA filters was higher; each was determined using a different criterion. Since LDA was trained with phonetic classes, they may be better suited for phone recognition. Indeed, this was shown in recent experiments by Lieb and Haeb-Umbach [71] where they replaced delta calculations with LDA filters using Mel-Frequency Cepstral Coefficients (MFCCs) rather than PLP-Cepstra. Our pilot phone recognition experiments using unconstrained grammars produced similar results.

Yet we do find the consistent frame accuracy improvement coupled with the consistent WER penalty paradoxical. We begin by observing the trends between the correct classification rates for the MSG and MSG-LDA posteriors. Figure 4.7 shows the difference between correct classification of individual phones between MSG with and without the LDA filters. We see that most of the phones are correctly classified more often with MSG-LDA than with MSG for all of the environments tested. The only consistent counterexample is the silence phone. Since the silence phone is an important element of segmentation,

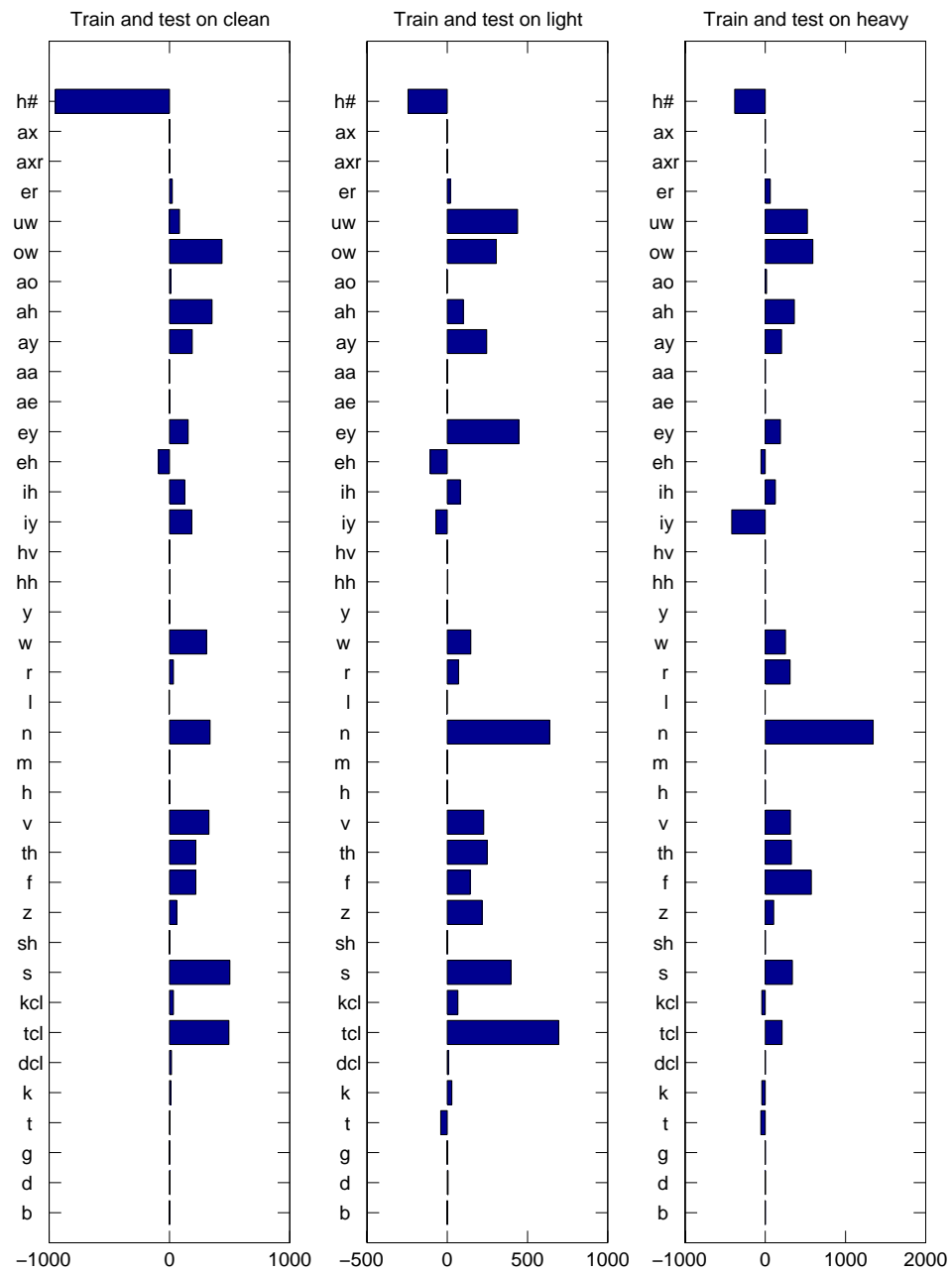


Figure 4.7: Difference between the frame accuracy of individual phones for MSG with and without LDA filters. Positive bars indicate MSG-LDA had higher frame accuracy.

Train and Test	Frame Accuracy (%)		WER (%)	
	MSG	MSG-LDA	MSG	MSG-LDA
<i>clean</i>	79.20	81.07	6.2	5.9
<i>light</i>	73.68	75.67	10.9	11.4
<i>heavy</i>	59.37	61.79	29.2	30.8

Table 4.5: Frame accuracy and WER with corrected silence phones for MSG and MSG-LDA.

cheating experiments were conducted to eliminate this difference between the two posterior streams. In the experiments, the locations of the correct silence frames were corrected in both streams, and word recognition experiments were conducted. These are listed in Table 4.5. The *clean* test yields an MSG-LDA that is slightly better than MSG but the *light* and *heavy* tests are still slightly worse (though not by a significant degree). This is despite the still improved frame accuracy. The confusion matrices do not shed much light on this result.

Classification summaries integrate out the locations and degree of all of the inaccuracies. We also computed summaries of the actual posterior values without much insight. We speculate that the timing and placement of errors is the remaining cause of the consistent disparity. Obviously, not all errors are created equal. Unfortunately, it is difficult to analyze the precise relationship between the frame-level posteriors and word recognition. Complete analyses relating frame accuracy to word error in ANN-HMM systems are not available. We conducted a preliminary empirical study, described in Appendix E, that illustrates some of the variability involved when using frame accuracy as an indicator of word error. However, these experiments did not provide an explanation for the results when using LDA augmentation to PLP-cepstra and MSG. For example, frame accuracy weighted by the posterior probabilities of the correct classes were still higher for the features with LDA augmentation. Also, the types of frames that were more often correct (other than silence) were not consistent indicators. It would seem that in some cases optimizations based on frame accuracy with frame-class discrimination as the criterion do not necessarily coincide with the optimal criterion for word accuracy. There may be an undesirable coupling between the temporal LDA computation and the Viterbi approximation used in the search, as well as an increased violation of the Markov assumptions in the underlying HMM.

Fortunately, the LDA augmentation gives a rather consistent improvement in frame accuracy that can be exploited for some tasks. Different components and methodologies are often better suited for different tasks. RASTA-PLP and MSG, for example, handle different situations better. Lieb and Haeb-Umbach found that reverberation-trained LDA filters aided MFCCs in TIMIT³ word recognition tests [71] just as we found that it aided RASTA-PLP in our NUMBERS tests. Frame-level LDA filter design presents a useful tool that can enhance performance in appropriate circumstances.

³A corpus of phonetically balanced sentences spoken by multiple male and female speakers.

Chapter 5

Multi-Stream Recognition Tests

One of the effects of a change in environmental noise is a change in the feature distribution. In order to maintain recognition performance the system must either be retrained or adapt the acoustic models to the new environment. As a complementary alternative to adaptation we investigated the option of keeping multiple system components that are trained on data in a sample of environments. Such a system will be able to partially compensate for the effects of a small set of environments. In principle, given appropriate measures of the noise characteristics, we can select the component that best matches the training condition. Hopefully, the components can also compensate one another when there is no match with any of the training conditions and a kind of interpolation between the the individual components can result.

The previous chapters demonstrated the detrimental effects that reverberation can have on recognition performance. When the system was trained on *clean* data, the presence of reverberation degraded the recognition from ca. 5% word error to as much as ca. 70%. A system trained on highly reverberated data improved such performance to ca. 30%. Unfortunately, the system had a severely degraded performance on *clean* data (degrading from 5% to ca. 30% error). Keeping two systems trained in separate environments and intelligently combined should be able to increase the range of robustness to environments that are similar or have characteristics that lie near either of the trained environments. Since reverberation presented a very difficult challenge with very discouraging word recognition scores, this chapter presents tests using the reverberant environments. Advantages in combining systems should be more apparent given the difficulty of the task.

The experiments used simple combinations of discriminatively trained probability streams from the previous chapters.

5.1 Simple Combination Strategies

Often when testing a new processing strategy, researchers have discovered that system performance is enhanced when used in combination with a mature and developed existing system. One example is using a probability stream derived from MSG features in combination with a probability stream derived from RASTA-PLP features [62, 60]. Researchers have experimented with numerous means of combining the results of two different feature processes. In summary, the feature processes may be combined at the feature level, the frame level, the HMM decoding level, and the recognition output level.

- At the feature level the feature vectors from both processes are concatenated and treated as a single feature stream from which probabilities are estimated. Feature selection algorithms (using, for example, component analysis) can be employed to mitigate the increase in dimensionality.
- At the frame level probabilities are computed for each feature process and the resulting probabilities are merged into a single stream prior to decoding. Alternatively, stacked or cascaded classifiers such as in a mixture of experts or boosting configuration (e.g. [56, 108]) can partition the probability estimation among several classifiers.
- At the HMM decoding level probabilities are obtained from each stream but the merging occurs within the HMM decoding. One example of this is HMM recombination, explored in multi-band systems [10, 11]. In this scheme, pronunciation models are expanded to include models that reflect the state of both streams. Another possibility is to use a two-pass recognition system [90]. In the first pass, word lattices are computed for each stream that are then combined prior to the second Viterbi search pass.
- Last, there is combination at the recognition output level. A full word or utterance recognition is performed on each stream generating sets of NBEST lists [95]. NBEST is a means of generating a ranked list of the most likely utterances. These NBEST lists

can be then be merged into a single NBEST list with the rankings modified using the utterance scores from both streams. Another method using a voting scheme among the recognized outputs of several ASR systems is the ROVER system [31].

Many other combination possibilities also exist. Extensive work has been conducted by researchers on using ensembles of classifiers. Many of the techniques explored involve classification decision rules from multiple knowledge sources. Soft decision versions of many of these can be used in statistical ASR systems. Since this work concentrates on the ASR front-end stage, we only explore those strategies involving combinations at the feature and frame levels. Our experiments will principally involve simple combinations of the posterior probabilities that have been employed by other researchers. These combination strategies are justified loosely on varying assumptions. Letting x_i represent the features from stream i and letting q represent classes of set C , some example combinations are listed here.

Trained probability estimation. $P(q|x_1, x_2, \dots, x_n)$ is directly estimated from a concatenation of feature vectors from all streams with x_i being the feature vectors from each of N streams. An MLP with an appropriate number of parameters is trained with “one-hot” class targets on the concatenated feature vector. A variant of this is to train $P(q|x_1, x_2, \dots, x_n)$ on the posterior probabilities $P(q|x_i)$ of each stream or a related quantity, such as the linear outputs of an MLP that has been trained with these probabilities.

Conditional independence assumption. In this method, $P(q|x_i)$ for each stream is available and the combined posterior $P(q|x_1, x_2, \dots, x_N)$ is estimated from these as

$$P(q|x_1, x_2, \dots, x_N) = \frac{P(x_1, x_2, \dots, x_N|q)p(q)}{\sum_{q' \in C} P(x_1, x_2, \dots, x_N|q')P(q')} \quad (5.1)$$

$$= \frac{\prod_{i=1}^N P(x_i|q)p(q)}{\sum_{q' \in C} \prod_{k=1}^N P(x_k|q')P(q')} \quad (5.2)$$

$$= \frac{\prod_{i=1}^N P(q|x_i) \frac{P(x_i)}{P(q)^N} P(q)}{\sum_{q' \in C} \prod_{k=1}^N P(q'|x_k) \frac{P(x_k)}{P(q')^N} P(q')} \quad (5.3)$$

$$= \frac{\prod_{i=1}^N P(q|x_i)/P(q)^{N-1}}{\sum_{q' \in C} \prod_{k=1}^N P(q'|x_k)/P(q')^{N-1}} \quad (5.4)$$

Equation 5.1 is the application of Bayes rule. In equation 5.2, the features x_i are

assumed to be conditionally independent given the state q . In the last equation 5.4, the denominator is merely the normalization of the numerator for all classes.

Mutual exclusion. Rather than a multiplicative combination of the stream posteriors, a weighted arithmetic average has also been used successfully [66]. An interpretation of this is achieved by introducing an independent switching variable $z \in 1, \dots, N$ to switch between the N streams:

$$\begin{aligned} p(q|x_1, x_2, \dots, x_N) &= \sum_{i=1}^N P(q|x_1, x_2, \dots, x_N, z = i)P(z = i|x_1, x_2, \dots, x_N) \quad (5.5) \\ &= \sum_{i=1}^N P(q|x_i, z = i)P(z = i) \quad (5.6) \end{aligned}$$

Here we assume that the state q is independent of the feature streams other than the selected stream $z = i$. In equation 5.6, we have a weighted sum of the individual posteriors from each stream where the weighting factor $P(z)$ is often taken as fixed and equal.

Independent errors. Similar to the conditional independence assumption is a strategy that assumes that the errors are independent; the error of the combination is equal to the product of the errors of the streams. The resulting posterior is then

$$P(q|x_1, x_2, \dots, x_N) = 1 - \frac{\frac{1}{(1-P(q))^{N-1}} \prod_{i=1}^N (1 - P(q|x_i))}{\sum_{q' \in C} \frac{1}{(1-P(q'))^{N-1}} \prod_{i=1}^N (1 - P(q'|x_i))}. \quad (5.7)$$

A similar formulation is the *noisy-OR* model sometime used when combining evidence in belief networks.

$$P(q|x_1, x_2, \dots, x_N) = 1 - \prod_{i=1}^N (1 - P(q|x_i)) \quad (5.8)$$

For two streams this can be rewritten as $P(q|x_1, x_2) = P(q|x_1) + P(q|x_2) - P(q|x_1)P(q|x_2)$.

Max and Min Rules. The above methods in effect implement types of *AND* and *OR* functions. Those involving products of the posteriors produce high posteriors only when all streams are high. In the other cases, larger values occur when any of the streams is high. A more direct soft combination that implements the *AND* and *OR*

are the *min* and *max* functions:

$$P(q|x_1, x_2, \dots, x_N) = \frac{\min_i P(q|x_i)}{\sum_{q' \in C} \min_i P(q'|x_i)} \quad (5.9)$$

$$P(q|x_1, x_2, \dots, x_N) = \frac{\max_i P(q|x_i)}{\sum_{q' \in C} \max_i P(q'|x_i)} \quad (5.10)$$

$$(5.11)$$

For the *min* function, the resultant posterior is high only when all of the individuals are high. With the *max* function, a high posterior occurs when any of the constituents is high.

In practice, successful frame level combinations at this level have involved some augmented versions of these methods. With the exception of training an MLP merger, the most convenient and scalable combinations involve a linear combination of the posterior probabilities or a linear combination of the log probabilities:

$$P(q|x_1, x_2, \dots, x_N) = \sum_{i=1}^N w_i P(q|x_i) \quad (5.12)$$

$$\log P(q|x_1, x_2, \dots, x_N) = \sum_{i=1}^N w_i \log P(q|x_i) \quad (5.13)$$

with $\sum_i w_i = 1$. Usually, the weights w_i are set to be equal and have yielded satisfactory results. The combination using 5.13 is tantamount to a geometric mean of the posterior probabilities when the weights are equal and is similar to the independence assumption method. Combinations with this geometric mean have often produced better results than a strict multiplication. With these combination strategies, the resulting posteriors must be renormalized to sum to one $\sum_{q \in Classes} P(q|x) = 1$ to preserve the probabilistic interpretation. These combinations have appeared in various related forms for example in [70, 66, 114] with more sample experiments in [54, 78, 51, 98].

A difference between computing averages and geometric averages is the degree of penalty that is imposed when the bulk of the assigned probability mass in both streams do not coincide. For example, when one stream is correct having a $P(q_{correct}|x_1) \approx 1$ and the other stream is incorrect with a $P(q_{correct}|x_2) \approx 0$ then the resulting probability is $P(q_{correct}|x_1, x_2) \approx 0$ after the multiplication. After renormalization, the correct posteriors can sometimes be indistinguishable from the incorrect states. Often, the posteriors are kept

at a minimum threshold to prevent numerical problems that can occur when probabilities are zero. On the other hand, coinciding probabilities are reinforced producing higher posteriors for the correct class after renormalization. The weighted average method does not as heavily penalize such disagreements among streams. However, it does not reinforce agreeing streams as much as the multiplicative method.

MLPs with concatenated feature vectors and trained mergers using MLPs have frequently yielded superior results in matched training and testing conditions. However, this comes at the cost of additional training, many more parameters, and an inconvenient means of scaling to more streams. It is also not convenient to de-select streams should additional information or constraints require it. In this work we perform most of the experiments using the simple combination strategies using the linear average method in equation 5.12 and the log-average method in equation 5.13. The linear average method is more resilient to noisy posterior estimates [66]. The log-average, however, often leads to superior word recognition [63]. In many of the results to follow we include both methods. We also frequently include an oracle frame-wise combination. The oracle combination is a cheating test that simply passes the stream that has the highest correct posterior probability to the decoder. It is used to provide a kind of upper limit as to what performance can be achieved with the probability streams¹.

5.2 Multi-Stream Experiments with RASTA-PLP

In this section, we experimented with a system that used two parallel front-end stages, each of which was trained in a different acoustic environment. We experimented only with training the MLP probability estimator to different environments. In some of the following sections, we will also experimented with training both the probability estimator and the feature extraction together. For these experiments, the feature extraction process used was RASTA-PLP. One stream was trained on *clean* data while the other was trained on *heavy* reverberation data. For comparison, tests with a bigger monolithic MLP were also included.

¹With this type of cheating combination, any additional stream, including purely random ones or a trivial one containing a high posterior in a single class, can only improve the frame accuracy; it must therefore be considered with care. However, the improvements are dependent upon the complementary utility of the streams and can therefore be useful in judging their combination potential.

Combination	Frame Acc. tests (%)			WER tests (%)		
	<i>clean</i>	<i>light</i>	<i>heavy</i>	<i>clean</i>	<i>light</i>	<i>heavy</i>
<i>clean</i> MLP alone	77.39	54.78	32.53	6.4	27.0	68.5
<i>heavy</i> MLP alone	45.14	48.80	51.95	49.0	37.1	38.0
average (eq. 5.12)	74.74	58.66 +	44.38	9.3	22.1 +	44.8
log-average (eq. 5.13)	71.82	59.36 +	43.46	10	21.3 +	49.3
indep (eq. 5.3)	70.38	59.29 +	42.59	13.1	25.5 +	54.1
noisy-OR (eq. 5.8)	74.78	58.42 +	44.30	9.5	22.7 +	43.8
oracle	80.59	66.93	57.06	4.4	11.7	29.7

Table 5.1: Results when combining two trained MLPs at the frame level. One MLP is trained with *clean* data and the other with *heavy* reverberation data. RASTA-PLP features were used for both conditions. The “+” annotations mark where the combinations in the unseen *light* reverberation testing case are significantly better than both of the singly trained MLPs.

5.2.1 Combining Heterogeneously Trained MLPs with Identical Feature Processing

As mentioned in Section 5.1, there are a large number of ways to combine the front-end stages. We begin by employing simple frame-level combination methods that have been used by other researchers. For illustrative purposes we present the results using several methods of merging the posterior probabilities. The methods we employed are *average* (equation 5.12 with equal weights), *log-average* (equation 5.13 with equal weights), *independence assumption* (equation 5.3), and *noisy-OR* (equation 5.8). These are followed by the oracle combination.

Frame accuracy and word error results from the simple combinations are shown in Table 5.1. These scores were for the development test set using an 800-hidden-unit MLP with an input context of 9 frames. Parameters for the decoder were tuned using the smaller cross-validation (CV) set. Of interest is the performance for the *light* reverberation tests. *Light* reverberation represents an *unseen condition* to the system. All tests using the simple combinations of the individual streams performed significantly better than either stream by itself. For tests in environments in which one of the streams was trained the combination scores lay in between the performance of either stream, though closer to the better of the streams. Although the performance degraded in the matched cases (*clean* or *heavy*), the unseen (*light*) case improved. Where the testing condition is uncertain or varies, the

WER (%)	1600 HU MLP training condition		
	<i>clean</i> only	<i>heavy</i> only	<i>clean+heavy</i>
<i>clean</i>	6.0	49.2	10.9
<i>light</i>	26.2	37.2	21.0
<i>heavy</i>	68.9	36.3	38.1

Table 5.2: Word error results with a single MLP with twice the number of parameters trained with *clean* data, *heavy* reverberation data, and both.

combined system can be preferable to a single-stream system. Of the combination methods listed, as well as other less promising methods not listed, the average, log-average, and the noisy-OR methods produced superior results. In this instance the noisy-OR method results were very similar to the average method. This is not surprising since it consists of a normalized addition of the posteriors lowered by a typically smaller second order term. Since the results were similar, combination results that follow list only the average and log-average scores.

5.2.2 Training an MLP on Data from Two Conditions

Using two front-end probability streams had twice as many trained parameters as either of the streams alone. It was therefore not strictly fair to compare the combined stream to a single stream. For comparison single stream tests were run with twice as many parameters. The MLP had 1600 hidden units, twice as many parameters as the single streams described above. Results are shown in Table 5.2. As before, the *light* condition was the unseen condition. The first two columns used MLPs trained solely on *clean* and *heavy* reverberation data, respectively. Increasing the number of parameters improved WER in all cases, though not to the level associated with the simple combinations or the dual-condition-trained MLP in the mismatched testing case. In this last column, the MLP was trained on data from two environments, *clean* and *heavy* reverberation, using twice as many parameters. The scores were consistent with the simple combinations. The *clean* condition did worse than the single stream trained with *clean* data but was not significantly different from the simple combinations. In the *heavy* condition, it performed better and was very close to that obtained from the stream trained solely on *heavy* reverberation. The unseen *light* condition was not significantly different from the simple combinations.

Simply increasing the number of parameters for the trained MLP improved recognition scores. However, the condition of the data used to train the MLP seemed crucial to achieving robustness to varying environments. For example, merely adding parameters to the *clean*-trained MLP did not yield scores for the *heavy* reverberation that were on par with a *heavy*-trained system. For the unseen *light* condition, good performance may eventually be achieved but not at the rate associated with adding some *heavy* reverberation training data. Training a large single net with multiple environments produced results that were at least as good as the simple combinations, though sometimes better. The interpolation power of the MLP was sufficient to handle the *light* case as a compromise between the two extreme training conditions. There are disadvantages with this approach compared to the simple combination strategy. Training large MLPs is less convenient due to training time and the fact that it must be completely retrained with every new environment we wish to add or subtract. The smaller environment-specific streams may be trained separately and in parallel. The simple frame-level multi-stream architecture also makes it possible and convenient to de-select streams or add streams if additional information about the environment is available. A monolithic MLP is not easily adapted in this way and becomes computationally expensive when we wish to train on more than two environments. These issues also arise if we consider a trained MLP as a stream merger.

Whether using a monolithic MLP or a trained MLP merger the feature streams are merged in a non-linear fashion. This is a more powerful method than the simple combination strategies and therefore has typically resulted in superior performance in tests by many researchers, for example by Sharma [100]. Trained MLPs, however, still represent a rather static means of combination. Architectural changes or extra inputs can be used to provide a more dynamic combination means that may also allow stream de-emphasis. However, we continue to use the simple combination strategies for convenience: no need for additional training data, dynamic weighting schemes are readily implementable, and simple combination results are still indicative of performance advantage.

5.3 RASTA-PLP with Different LDA Filters

We observed in Chapter 3 that different acoustic environments resulted in temporal filters with different frequency ranges. When using an MLP lacking acoustic context,

such filters offered some advantages in different acoustic environments. A further examination of the frame errors indicated certain differences in the recognized frames that could potentially be exploited. In this section we tested multi-stream combinations using LDA-RASTA-PLP with filters trained in different environments.

5.3.1 Dual LDA Filter Sets with Common MLP Training Environment

In this experiment we ascertained if improvements could be gained when using streams from two identical feature processes, LDA-RASTA-PLP, with only a difference in the frequency responses of the RASTA filters. For these tests, we used probability streams from two heterogeneously trained front-end temporal filters. The first stream used the LDA filters derived from the *clean* condition and whose principal component had an average band-pass response of 1 to 13 Hz. The second stream used the LDA filters derived from the highly reverberant condition and whose principal component had a narrower average band-pass response of 1 to 5 Hz. Since the filter sets preserved different modulation rates, this combination of feature processing was effectively a multi-rate front-end combination. The MLP probability estimator for both streams was trained on the the same environment as the LDA filters, though using data from the NUMBERS corpus rather than from the STORIES corpus. We initially allowed the MLP access to only a single frame of acoustic features in order to eliminate the possibility of redundant temporal processing that an acoustic context would provide.

Single Frame Acoustic Context

Tables 5.3, 5.4 and 5.5 contain the results where the MLP probability estimators for both streams were trained on *clean*, *light* reverberation, and *heavy* reverberation data respectively. The first two rows of the table pertain to the word error recognition results for the streams taken individually. The following two rows contain word error when the frame-level posterior probabilities were averaged prior to the decoding and where the logarithm of the posteriors were averaged. The last row contains the WER from an oracle combination of the two streams.

We see from these results that these simple combinations of the two front ends with only a difference in the temporal characteristics of the filters improved the performance

<i>Clean</i> trained MLP Combination	WER (%)		
	<i>clean</i> test	<i>light</i> test	<i>heavy</i> test
<i>clean</i> LDA filter alone	9.1	33.1	72.5
<i>heavy</i> LDA filter alone	12.0	30.2	73.4
average	8.8	28.5 +	69.7 +
log-average	8.9	27.9 +	69.1 +
oracle	4.8	16.8	60.8

Table 5.3: WER Results from a frame-level combination of LDA-RASTA-PLP with LDA filters derived under *clean* and *heavy* reverberation conditions. The MLP probability estimator was trained with *clean* data and a single frame of acoustic features. The “+” annotations mark where the combinations are better than the single streams.

<i>Light</i> trained MLP Combination	WER (%)		
	<i>clean</i> test	<i>light</i> test	<i>heavy</i> test
<i>clean</i> LDA filter alone	16.9	18.9	62.6
<i>heavy</i> LDA filter alone	20.1	18.3	63.5
average	14.6 +	16.7 +	60.0 +
log-average	13.8 +	16.3 +	60.3 +
oracle	7.70	10.10	50.2

Table 5.4: WER Results from a frame-level combination of LDA-RASTA-PLP with LDA filters derived under *clean* and *heavy* reverberation conditions. The MLP probability estimator was trained with *light reverberation* data and a single frame of acoustic features. The “+” annotations mark where the combinations are better than the single streams.

<i>Heavy</i> trained MLP Combination	WER (%)		
	<i>clean</i> test	<i>light</i> test	<i>heavy</i> test
<i>clean</i> LDA filter alone	47.0	42.7	45.5
<i>heavy</i> LDA filter alone	43.2	37.8	38.9
average	39.0 +	35.5 +	39.3
log-average	38.3 +	34.8 +	38.8
oracle	26.9	23.8	29.70

Table 5.5: WER Results from a frame-level combination of LDA-RASTA-PLP with LDA filters derived under *clean* and *heavy* heavy reverberation conditions. The MLP probability estimator was trained with *heavy reverberation* data and a single frame of acoustic features. The “+” annotations mark where the combinations are better than the single streams.

over either stream individually. This improvement occurred consistently in tests where the testing condition differed from the condition on which the MLP was trained. We see that with most improvements occurring in mismatched cases, using a combination of filters with different ranges aids in robustness in this case. In matched testing conditions, the results were not very different from those of the individual streams. The exception to this is where the MLPs were trained on *light* reverberation data, though in these instances the LDA filters that were optimized for the *light* condition were not used. Referring to Table 3.10 in Chapter 3, the combination of the *clean* and *heavy* filters with an MLP trained with *light* reverberation data yielded results that were equivalent (*light* test) or superior (*clean* and *heavy* tests) to the result where both the MLP and the LDA filters were trained on the *light* reverberation data. As mentioned previously, a direct comparison is not strictly fair given the difference in the number of parameters, though previous tests indicate that a further fair test with equal numbers of parameters would yield similar results.

9 Frame Acoustic Context

We noted in Section 3.3.3 that allowing the MLP probability estimator a context of acoustic features mitigated much of the performance differences when using separate LDA filters tuned to the matching acoustic condition. Since the filters derived under *heavy* reverberation had more selective frequency responses we observed that there were some differences in frame classification that might be exploited by using a combination. For example, the second stream using the more constrained filter may be used to reinforce those frames that were correct. We therefore repeated the experiments with MLPs that were allowed an acoustic context of approximately 100 ms. These results are shown in Tables 5.6, 5.7, and 5.8 for MLPs that were trained under *clean*, *light* reverberation, and *heavy* reverberation, respectively. We see from these scores that the simple combinations performed as well as or better than either stream alone, though significant improvements occurred in fewer test cases.

5.3.2 Matched LDA Filter and MLP Training Environments

In these tests we see if the enhancements afforded by LDA filters with RASTA-PLP also carry over to multi-stream tests with heterogeneous stream training environments.

<i>Clean</i> trained MLP Combination	WER (%)		
	<i>clean</i> test	<i>light</i> test	<i>heavy</i> test
<i>clean</i> LDA filter alone	5.2	27.2	75.1
<i>heavy</i> LDA filter alone	7.0	25.80	73.70
average	5.6	23.2 +	72 +
log-average	5.5	25.1	71.2 +
oracle	3.7	14.7	64.8

Table 5.6: WER Results from a frame-level combination of LDA-RASTA-PLP with LDA filters derived under *clean* and *heavy* reverberation conditions. The MLP probability estimator was trained with *clean* data and a context window of 9 frames. The “+” annotations mark where the combinations are better than the single streams.

<i>Light</i> trained MLP Combination	WER (%)		
	<i>clean</i> test	<i>light</i> test	<i>heavy</i> test
<i>clean</i> LDA filter alone	10.8	11.1	59.0
<i>heavy</i> LDA filter alone	14.0	12.4	60.2
average	10.3	11.0	57.5
log-average	10.5	10.7	56.7 +
oracle	6.4	7.1	49.6

Table 5.7: WER Results from a frame-level combination of LDA-RASTA-PLP with LDA filters derived under *clean* and *heavy* reverberation conditions. The MLP probability estimator was trained with *light reverberation* data and a context window of 9 frames. The “+” annotations mark where the combinations are better than the single streams.

<i>Heavy</i> trained MLP Combination	WER (%)		
	<i>clean</i> test	<i>light</i> test	<i>heavy</i> test
<i>clean</i> LDA filter alone	31.6	25.8	30.7
<i>heavy</i> LDA filter alone	37.0	31.1	30.3
average	30.1	25.1	29.3
log-average	29.9 +	26.0	28.5 +
oracle	21.0	17.9	21.1

Table 5.8: WER Results from a frame-level combination of LDA-RASTA-PLP with LDA filters derived under *clean* and *heavy* reverberation conditions. The MLP probability estimator was trained with *heavy reverberation* data and a context window of 9 frames. The “+” annotations mark where the combinations are better than the single streams.

Combination	WER (%)		
	<i>clean test</i>	<i>light test</i>	<i>heavy test</i>
<i>clean</i> LDA filter and MLP alone	9.1	33.1	72.5
<i>heavy</i> LDA filter and MLP alone	43.2	37.8	38.9
average	12.9	28.1 +	49.3
log-average	13.5	26.4 +	54.0
oracle	5.9	15.4	30.1

Table 5.9: Results from a frame-level combination of LDA-RASTA-PLP with LDA filters and an MLP trained under *clean* and *heavy* reverberation. The MLP had a single frame of acoustic features as input. The “+” annotation marks where the combination is significantly better than the single streams in the *light* reverberation test.

Combination	WER (%)		
	<i>clean test</i>	<i>light test</i>	<i>heavy test</i>
<i>clean</i> LDA filter and MLP alone	5.2	27.2	75.1
<i>heavy</i> LDA filter and MLP alone	37.0	31.1	30.3
average	7.7	22.0 +	44.5
log-average	9.4	20.2 +	44.9
oracle	4.2	12.9	24.7

Table 5.10: Results from a frame-level combination of LDA-RASTA-PLP with LDA filters and an MLP trained under *clean* and *heavy* reverberation. The MLP had an acoustic context of 9 frames. The “+” annotation marks where the combination is significantly better than the single streams in the *light* reverberation test.

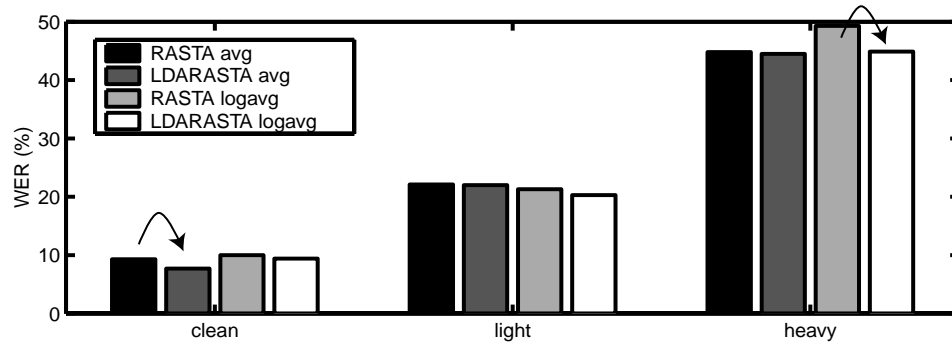


Figure 5.1: Comparison of RASTA-PLP with LDA-RASTA-PLP using average and log-average posterior combination. Significant improvement is marked with an arrow.

Figure 5.9 contains the results when two streams were trained separately in *clean* and *heavy* reverberation environments. Both the MLP and the LDA filters were derived under similar environmental conditions. In this experiment, the MLP used a single frame of acoustic features. Table 5.10 repeats the experiments using MLPs with a context of 9 frames. We see the expected result of compromised performance in the matched cases but with improvement in the unseen *light* reverberation case.

Table 5.10 is directly comparable to the scores using RASTA-PLP with the standard RASTA filter in Table 5.1 and are summarized in Figure 5.1. The LDA-RASTA error rates are all slightly lower than the standard RASTA but only two instances are statistically significant. The significant differences between corresponding RASTA and LDA-RASTA scores using the same combination method (average or log-average) are marked in the figure with an arrow. We observed that allowing a wide context window for the MLP mitigated the effectiveness of the different LDA filters. These results may therefore reflect the combination of differently trained MLPs more than the use of different LDA filters.

5.4 PLP and MSG

Experiments by other researchers have yielded some success when combining two streams that had different feature extraction properties. In many of these tests, the probability estimator from each stream was trained using the same data set and the same acoustic condition. We begin here with similar experiments in using PLP and MSG and where the MLP probability estimators were trained using the same training data. We then tested the

combined probability streams trained in heterogeneous reverberant environments.

5.4.1 Dual-stream PLP and MSG with Common MLP Training Environment

In the previous LDA-RASTA-PLP tests the feature-extraction processes for the different streams were identical except for the frequency selectivity of the temporal filters. Here we experimented with feature extraction processes that were much more distinct. Previous work by Wu and Kingsbury have demonstrated some advantage in using PLP and MSG in combination [60, 119]. Though PLP and MSG contain processing elements that are similar in function, they are computed in alternative ways that have different properties. These different properties can allow for complementary errors that may be exploited; the inabilities of one stream may be compensated for by the other stream. We replicated the experiments performed in previous sections using simple combinations of MLPs trained under the same acoustic environment to provide a baseline.

Tables 5.11, 5.12, and 5.13 contain simple combination results. The simple combinations improved the word error significantly in most cases. The combination score using the *clean* MLPs and *clean* test was the best score (to our knowledge) achieved on this task. Furthermore, the oracle combination in that case was close to the lowest possible word error². Just as the PLP and MSG features with normalization performed better than RASTA-PLP on this task, the combinations were also better. The scores were on par or better than the oracle cheating combination using RASTA-PLP and were superior to the WER scores from average and log-average combinations.

5.4.2 PLP and MSG with Heterogeneously Trained MLPs

We repeated the experiments using two streams wherein the MLPs were trained separately on *clean* and *heavy* reverberation. Since PLP had the lowest word error on *clean* tests, we used an MLP trained on *clean* data with PLP. Similarly, MSG had the lowest word error scores on reverberation tests and we therefore used an MLP trained on *heavy* reverberation with MSG. The results of this pairing are shown in Table 5.14. Again, *light* reverberation was the unseen condition.

²Decoding completely accurate frame posteriors.

<i>Clean</i> trained MLP Combination	WER (%)		
	<i>clean</i> test	<i>light</i> test	<i>heavy</i> test
PLP alone	5.1	26.7	77.6
MSG alone	6.5	15.3	77.7
average	4.3 +	14.8	71.5 +
log-average	4.3 +	14.9	70.4 +
oracle	2.5	7.2	61.1

Table 5.11: WER Results from a frame-level combination of PLP and MSG with MLP probability estimators trained with *clean* data. The “+” annotation marks where the combination is significantly better than the single streams.

<i>Light</i> trained MLP Combination	WER (%)		
	<i>clean</i> test	<i>light</i> test	<i>heavy</i> test
PLP alone	12.0	10.9	58.8
MSG alone	9.9	12.1	60.9
average	7.6 +	8.9 +	53.1 +
log-average	7.6 +	8.3 +	52.4 +
oracle	4.1	4.9	41.6

Table 5.12: WER Results from a frame-level combination of PLP and MSG with MLP probability estimators trained with *light reverberation* data. The “+” annotation marks where the combination is significantly better than the single streams.

<i>Heavy</i> trained MLP Combination	WER (%)		
	<i>clean</i> test	<i>light</i> test	<i>heavy</i> test
PLP alone	39.2	31.4	35.4
MSG alone	24.5	23.8	31.6
average	23.1	23.9	29.0 +
log-average	21.6 +	22.1 +	28.6 +
oracle	13.5	14.3	19.8

Table 5.13: WER Results from a frame-level combination of PLP and MSG with MLP probability estimators trained with *heavy reverberation* data. The “+” annotation marks where the combination is significantly better than the single streams.

Combination	WER (%)		
	<i>clean</i> test	<i>light</i> test	<i>heavy</i> test
PLP (<i>clean</i> MLP) alone	5.1	26.7	77.6
MSG (<i>heavy</i> MLP) alone	24.5	23.8	31.6
average	6.5	16.5 +	41.9
log-average	5.9	14.7 +	43.8
oracle	3.0	7.9	21.6

Table 5.14: WER Results from a frame-level combination of PLP with its MLP trained on *clean* data and MSG with its MLP probability estimators trained with *heavy reverberation* data. The “+” annotation marks where the combination is significantly better than the single streams in the *light* reverberation test.

Combination	WER (%)		
	<i>clean</i> test	<i>light</i> test	<i>heavy</i> test
PLP-LDA (<i>clean</i> LDA and MLP) alone	6.3	26.7	74.3
MSG-LDA (<i>heavy</i> LDA and MLP) alone	27.5	28.1	32.8
average	8.1	20.1 +	45.2
log-average	7.4	19.2 +	44.3
oracle	3.0	7.9	21.6

Table 5.15: WER Results from a frame-level combination of PLP-LDA with its LDA filters and MLP trained on *clean* data and MSG-LDA with its LDA filters and MLP probability estimators trained with *heavy reverberation* data. The “+” annotation marks where the combination is significantly better than the single streams in the *light* reverberation test.

As with the results when using RASTA-PLP, the combination of MLPs with different training environments seemed to compromise the scores in the matched testing conditions; the scores for *clean* and *heavy* reverberation tests lay in between the scores for the single streams, though they were closer to the better stream. The *light* reverberation tests showed a combination that was much better than the single streams by as much as 38% (relative).

Introducing temporal filters derived from LDA into PLP and MSG feature extraction process had the interesting effect of consistently improving the frame accuracy despite the higher word error. Since our combination methods were at the frame level, it was worth checking to see if the frame improvements when using LDA help when used in combination. We used PLP with both temporal LDA and MLP trained with *clean* data

Feature Combination	Frame Accuracy (%)		
	<i>clean</i> test	<i>light</i> test	<i>heavy</i> test
average PLP+MSG	76.47	62.28	47.27
average PLP+MSG LDA	78.60 +	64.13 +	51.14 +
log-average PLP+MSG	74.22	63.29	46.57
log-average PLP+MSG LDA	76.12 +	65.78 +	49.88 +

Table 5.16: Comparison of frame accuracies for PLP with MSG combinations with and without LDA. The “+” annotation marks where the frame accuracy using LDA augmentation is significantly better than the original.

Feature Combination	WER (%)		
	<i>clean</i> test	<i>light</i> test	<i>heavy</i> test
PLP (<i>clean</i> MLP) alone	5.1	26.7	77.6
PLP (<i>heavy</i> MLP) alone	39.2	31.4	35.4
MSG (<i>clean</i> MLP) alone	6.5	15.3	77.7
MSG (<i>heavy</i> MLP) alone	24.5	23.8	31.6
average	6.8	14.9	37.9
log-average	6.2	13.6 +	41.5
oracle	3.2	6.3	13.9

Table 5.17: Four stream combination: PLP and MSG using both *clean* and *heavy* reverberation trained MLPs. The “+” annotation marks where the combination is significantly better than the single streams in the *light* reverberation test.

and MSG with both temporal LDA and MLP trained on *heavy* reverberation. Word error results are shown in Table 5.15. The same frame accuracy improvement trend is witnessed in these tests. A comparison of the frame accuracies is listed in Table 5.16. Frame accuracy improved by between 3% and 8% relative. Word error, on the other hand, was still seen to be better in tests without the LDA filters. Empirical experiments have shown that frame accuracy improvements must be substantially higher to guarantee WER improvements.

5.4.3 Four Stream Combination

We notice from Tables 5.11 through 5.13 that combinations improved in all matched cases as well as in the unseen *light* reverberation case. We also notice that the scores for this *light* reverberation test using the combination of PLP and MSG with both MLPs trained on *clean* was comparable to when the PLP MLP was trained on *clean* and

the MSG MLP was trained on *heavy* reverberation. Further improvements may be obtained when using PLP and MSG trained both on *clean* and *heavy* reverberation. The simple combination method allowed us to do this readily. Results for this test are shown in Table 5.17. The best combination results for the unseen *light* condition case occurred using the log-average combination. Most of the remaining scores remained near the two stream performance.

5.5 Weighted Stream Combinations

So far, combination experiments used averaged posteriors with equal weighting. In the matched training and testing conditions, the equal weighting resulted in word error scores in between that of either stream. In such a situation, it is prudent to de-select the worst of the streams to recover the best score. It is not difficult to imagine that other circumstances exist where a non-equal weighting would also be preferable. When explicit knowledge of the environmental characteristics is available, better performance may be achieved.

In order to observe the effect of environmental characteristics on the choice of weighting we performed tests using room impulses with different reverberation characteristics. We performed tests varying relative weighting between two streams, one trained with *clean* data and the other on *heavy* reverberation. We then tested on the reverberation room impulse responses that were artificially modified to yield certain reverberation characteristics, as done in Section 3.2.2. The room impulse T60 varied between 0.25 and 2.5 seconds in 0.25-second increments while the DTR remained fixed at -8 dB. Additional tests used a DTR varying between -8 to 2 dB in 1-dB increments while holding the T60 constant at 2 seconds. These tests were performed on the smaller CV set using constant parameters for the decoder. The log-average combination method worked slightly better than the arithmetic averaging in the unseen test cases (as these tests can be considered) and was used here.

LDA-RASTA-PLP

We first tested the relative weighting using two LDA-RASTA-PLP streams using *clean* and *heavy* LDA filters separately for each stream. These streams reflected MLPs

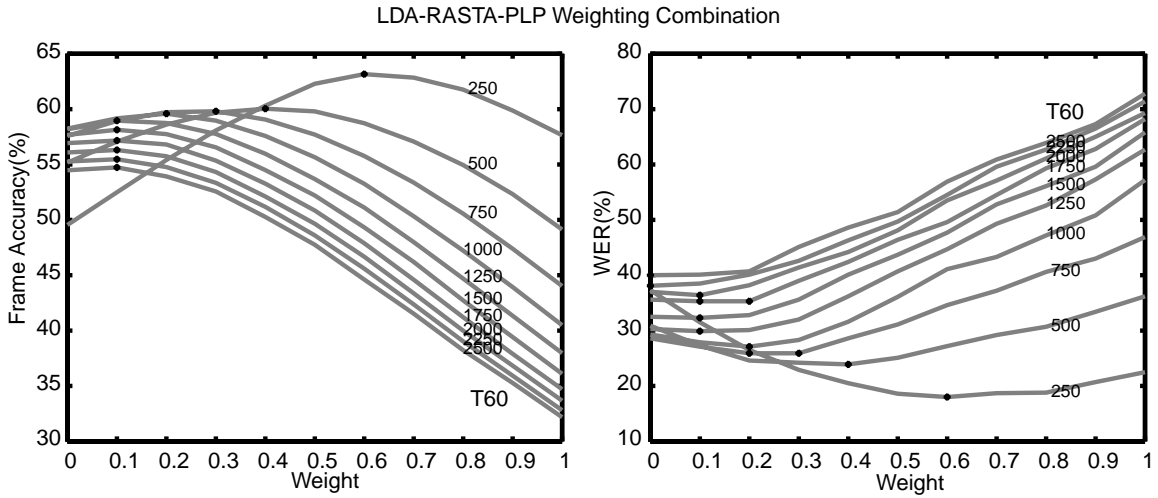


Figure 5.2: Frame accuracy and WER for a range of artificial reverberant conditions using a weighted log-average between two LDA-RASTA-PLP streams trained on *clean* and *heavy* reverberation data. Tests performed on room impulses with $DTR = -8$ dB.

using a single frame of acoustic features as input. Figure 5.2 shows frame accuracy and word error for several T60 values as the relative weighting varied between 0 and 1 in 0.1 increments. Values near 1 gave more weight to the *clean* stream and values near 0 gave more weight to the *heavy* stream. The existence of local extrema in the two plots is encouraging as it demonstrated that a weighted combination can be superior to the streams taken alone. The weight corresponding to this extreme moved depending on the severity of the reverberation T60. For the lightest case a more equal weighting was preferable. For more severe reverberation the weighting should favor the *heavy* stream and was an intuitive result.

Figure 5.3 shows similar tests where the DTR varied while holding the reverberation time to 2 seconds. The best weighting favored the *heavy* stream as in the previous tests. When the DTR increased the best weighting combination allowed more weight to the *clean* stream. This was also an intuitive result.

PLP and MSG

We repeated the tests here using PLP and MSG with the PLP stream trained on *clean* data and the MSG stream trained on *heavy* reverberation. We find similar results in Figures 5.4 and 5.5. The extrema moved closer to the stream that was trained in the

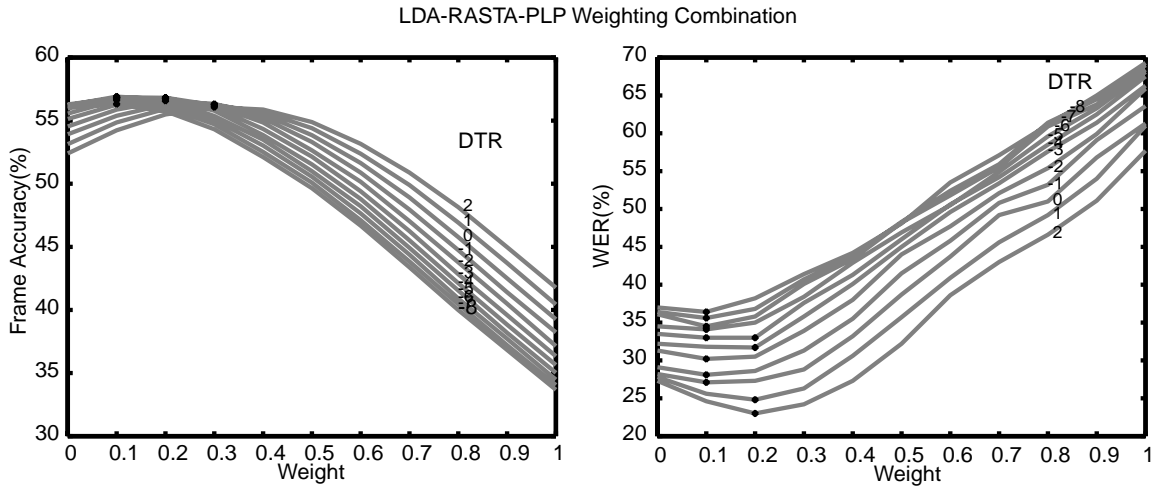


Figure 5.3: Frame accuracy and WER for a range of artificial reverberant conditions using a weighted log-average between two LDA-RASTA-PLP streams trained on *clean* and *heavy* reverberation data. Tests performed on room impulses with $T60 = 2$ sec.

reverberation condition as the $T60$ increases and DTR decreases. With DTR placed at a moderate and noticeable level, the $T60$ had more of an effect on the placement of the best weight. A very high DTR would make the room impulse closer to the *clean* condition. Should the DTR and $T60$ associated with the environment or some related indicator of the incoming speech become available then an appropriate weight can be approximated from these measurements (e.g., the best weights can be regressed onto DTR and $T60$ measurements from development data). However, since the difference in WER can be small for neighboring weights at the extrema such a precise mapping may not be necessary. Rules of thumb can be employed such as applying equal weighting for $T60$ s of 0.5 seconds or less and 0.1 or 0.2 for larger values. Previous tests indicated that the addition of LDA improved the frame accuracy using PLP and MSG. Varying the weighting between the streams also demonstrated frame accuracy improvement. WER generally would not be lower than for PLP and MSG without the LDA augmentation.

5.5.1 Weighting Based on Frame-Level Confidence

Typically, information about the acoustic environment is not available to aid in determining the appropriate weighting. It is desirable to have an automatic means of selecting the best weight between the probability streams. A number of schemes have

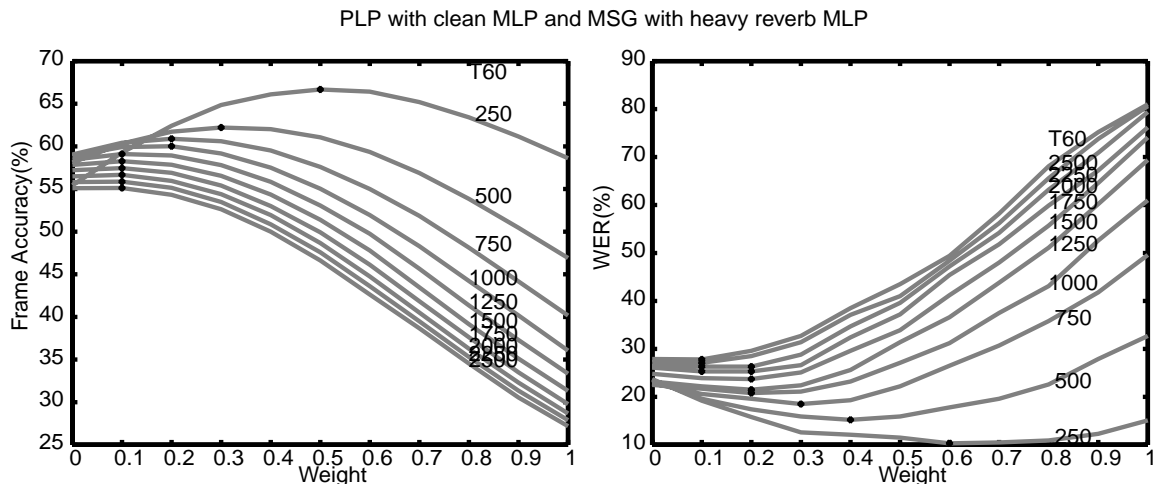


Figure 5.4: Frame accuracy and WER for a range of artificial reverberant conditions using a weighted log-average between PLP and MSG streams trained on *clean* and *heavy* reverberation data respectively. Tests performed on room impulses with $DTR = -8$ dB.

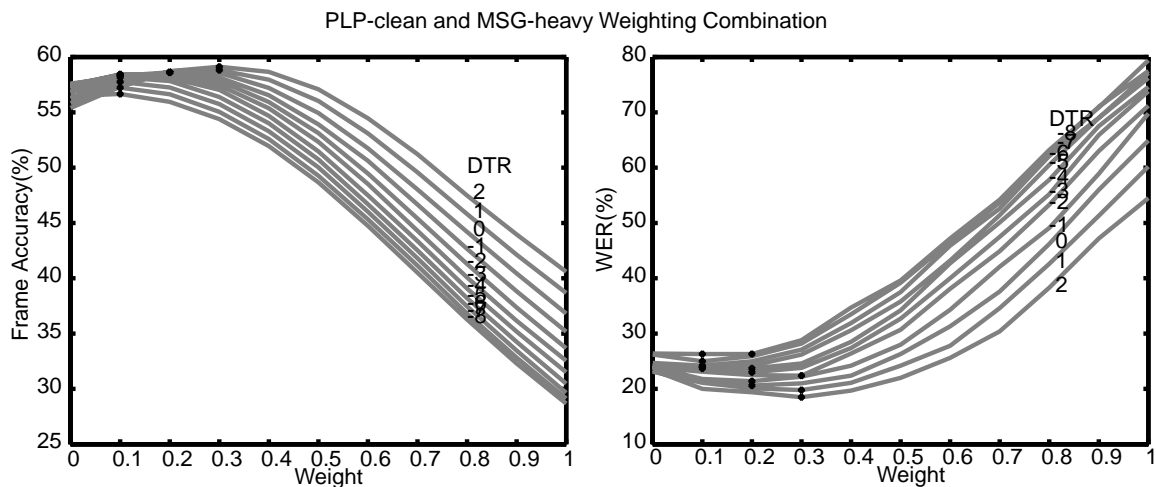


Figure 5.5: Frame accuracy and WER for a range of artificial reverberant conditions using a weighted log-average between PLP and MSG streams trained on *clean* and *heavy* reverberation data respectively. Tests performed on room impulses with $T60 = 2$ sec.

been used by researchers based on confidence measures. An excellent description of many of the confidence schemes used in speech recognition is in [92]. This summary includes higher-level non-frame-wise confidence measures as well as frame-wise ones. Though used primarily for word and utterance rejection, confidence measures may be used for stream selection. Weight is given to those streams that have higher confidence scores.

The consensus among researchers is that weighting based solely upon local frame probability measures often do not offer a significant advantage over simple equal weighting [54, 65]. Many of the tests involved combinations of different processing methods. In our case, the different streams involved different training conditions. In such a case, the difference in feature distribution due to the environment may lead to streams that have measurable differences in the posterior estimates. We therefore conducted a number of tests to investigate the appropriateness of a number of confidence measures that are based solely upon local frame-level posterior scores.

Confidence Based on Maximum Posterior Values One scheme is to interpret the actual value of the posterior as a measure of the confidence. When more probability mass is assigned to a phone, we view the stream as being more certain of its selection.

$$C_{max} = \max_q P(q|x) \quad (5.14)$$

The maximum posterior does not provide information regarding where the remaining probability mass is distributed. A related measure is the margin of the posterior values. This is the difference between the maximum posterior and the next largest posterior as a measure of confidence. A smaller margin indicates the presence of a competing class and therefore less confidence in the classification.

$$q^* = \operatorname{argmax}_q P(q|x) \quad (5.15)$$

$$C_{margin} = \max_q P(q|x) - \max_{q/q^*} P(q|x) \quad (5.16)$$

Information Theoretic Measures The entropy confidence measure of the posterior distribution is

$$C_{entropy} = - \sum_q P(q|x) \log P(q|x). \quad (5.17)$$

Entropy can be interpreted as a measure of randomness or unpredictability of a

distribution³. When most of the probability mass is concentrated at a single class then the entropy is low. When mass is more evenly distributed, the entropy is high since the class choice is more uncertain. It is maximum when the distribution is uniform ($\max C_{entropy} = \log(56)$ for 56 classes) and minimum for a delta distribution ($\min C_{entropy} = 0$). This confidence measure is in the opposite sense since lower values indicate a more peaky distribution and hence more confidence. The measure can also be defined as an entropy relative to a prior distribution $P(q)$.

$$C_{rel.entropy} = - \sum_q P(q|x) \log \frac{P(q|x)}{P(q)} \quad (5.18)$$

This is sometimes referred to as the Kullback-Liebler distance or cross-entropy [68, 23]. The symmetric counterpart to this is

$$C_{symmetric-rel.entropy} = - \sum_q P(q|x) \log \frac{P(q|x)}{P(q)} - \sum_q P(q) \log \frac{P(q)}{P(q|x)} \quad (5.19)$$

All of these measures give an indication of the flatness of the probability mass assignment and consequently the uncertainty.

Since the probability distribution is required to sum to one, all of these measures are correlated. Combination schemes can compute and normalize some function of the confidence scores for each stream as weights. The confidence could be used on a frame by frame basis or averaged over a window of frames to smooth out some of the noisiness in the estimates.

Numerous experiments were conducted with these measures and a varying width of averaged frames. Some examples using LDA-RASTA-PLP with a single frame of acoustic context for the MLPs are shown in Table 5.18. In this table, the confidence $C_{i,t}$ was computed for each stream $i \in [1, \dots, N]$ and frame t . The weighting for the entropy and relative entropy streams was determined by

$$w_{i,t} = \frac{\sum_{\tau=t-k}^t \exp(-C_{i,\tau})}{\sum_{j=1}^N \sum_{\tau=t-k}^t \exp(-C_{j,\tau})} \quad (5.20)$$

where C was from equations 5.17 and 5.18 respectively. This form makes the weights $w_{i,t}$ inversely proportional to the average number of choices from an efficiently encoded process with such a probability distribution. The margin weighting was determined using

$$w_{i,t} = \frac{\sum_{\tau=t-k}^t C_{i,\tau}}{\sum_{j=1}^N \sum_{\tau=t-k}^t C_{j,\tau}}. \quad (5.21)$$

³Entropy computed with a base 2 logarithm is measured in bits. The logarithm base merely introduces a scaling factor and is not important in this application.

Weights for the streams were directly proportional to the margin confidence computed from equation 5.16. The confidence weights were accumulated with the previous k frames; 0, 5, and 20 frames in these tests. There are, of course, an infinite number of ways of relating confidence scores to weight values. These equations were just two reasonable ways that had the desired emphasis/de-emphasis properties.

Potentially, each stream would have a consistently higher confidence in the matched training and testing conditions. Most tests, however, did not demonstrate a significant difference with the simple averaging with equal weights. In Table 5.18, the only significant improvement occurred in the *clean* test case using the relative entropy criterion averaged with 20 previous frames (demarcated by a “+”). The average entropy over the entire set for the *clean* stream is slightly lower than for the *heavy* stream. The frame-entropy measure generally did not prove reliably useful. There was some correlation between the entropy and the oracle decision, but it was small (correlation coefficient of -0.1), consistent with the findings of [92]. Overall, the posterior-based confidences used here to affect weighting did not add a consistent and significant advantage over equal weighting when using MLPs as a probability estimator. Higher-level confidence measures, such as utterance-level confidence values [65] or frame-level confidences integrated over higher-level decoding paths [115], have shown promise and may ultimately prove useful.

Knowledge of Environment

We can comfortably predict that knowledge of the room acoustics can help recognition. The simplest mechanism is to use such knowledge as a switch between the streams or as a knob to adjust the weighting. A mapping function of room acoustic measurements onto weighting values from training data can be used to obtain appropriate stream weights when testing environment measurements are available. Determining reverberation characteristics from speech samples is, unfortunately, difficult to achieve. We observed in Figures 2.11 and 2.12 that the addition of reverberation increases the mean and lowers the variance of the log-critical band trajectories and may properly be used in part for detecting noisy conditions. However, additive noise also has the same effect. The reverberation characteristics would be difficult to distinguish from additive noise simply from means and variances. The measures are also dependent on the speech energy. The modulation spectrum is a potential candidate for establishing the speech-in-noise characteristics. The modulation

Combination	WER (%)		
	<i>clean</i> test	<i>light</i> test	<i>heavy</i> test
LDA-RASTA-PLP (<i>clean</i> Filters and MLP) alone	9.1	33.1	72.5
LDA-RASTA-PLP (<i>heavy</i> Filters and MLP) alone	43.2	37.8	38.9
log-average equal	13.5	26.4	54.0
entropy	14.4	26.7	53.3
entropy +5 frame	14.5	27.0	54.4
entropy +20 frame	13.8	27.1	55.0
rel. entropy	12.5	27.2	53.6
rel. entropy +5 frame	12.4	27.3	54.2
rel. entropy +20 frame	11.9 +	27.5	54.7
margin	14.8 -	27.0	54.1
margin +5 frame	14.4	26.9	54.8
margin +20 frame	13.3	27.0	54.7

Table 5.18: WER Results from a frame-level weighted log-average combination of LDA-RASTA-PLP with *clean* and *heavy* trained MLP and LDA filters using confidence based weighting. MLPs were trained with a single input frame of features. The “+” and “-” annotations mark two cases where the weighting produced WER that was respectively significantly better and worse than the equal weighting.

spectrum of a test utterance can be computed with weight given to the stream with a “closer” modulation spectral characteristic of its training set. This method would also require further investigation. Pilot experiments reveal that the variance in the modulation spectral estimates is relatively high, especially for the short utterances in the NUMBERS corpus. Further, the room acoustics must typically be rather severe before it noticeably impedes the modulation of the speech itself. Acoustic condition detection is a topic worthy of further study.

5.6 Final Tests with Unseen Conditions and Best Stream Combination

We present some final recognition experiments using 11 additional room impulses previously unused in our experiments together with the *light* reverberation treated as the unseen case in the multi-stream tests. As before, these room impulses were collected in a varechoic chamber with reflective panels that were either opened or closed [113]. Three sets of measurements with four microphones were used. The first set had 100% of the

Room impulse test				WER %				
Panels open(%)	Mic.	DTR (dB)	T60 (s)	PLP stream		MSG stream		logavg merge
				<i>clean</i>	<i>heavy</i>	<i>clean</i>	<i>heavy</i>	
100	1	1	0.3	12.0	42.3	9.6	24.4	8.6 +
100	2	1	0.3	10.6	43.0	9.2	23.5	7.7 +
100	3	-1	0.3	12.1	39.9	10.8	24.1	8.9 +
100	4	-1	0.3	11.7	41.6	10.1	24.7	9.8
43	1	1	0.5	22.2	30.8	13.9	23.7	11.0 +
43	2	-3	0.5	21.4	33.3	15.3	23.3	11.7 +
43	3	-2	0.5	22.3	31.1	17.6	23.6	11.9 +
43	4	-5	0.5	24.2	31.4	18.9	23.5	13.5 +
0	1	-5	1	55.7	33.2	42.5	26.1	24.0 +
0	2	-7	1	55.8	31.5	45.6	25.0	24.6
0	3	-7	1	60.6	33.8	52.3	26.7	29.6 -
0	4	-9	1	59.9	35.9	53.0	26.8	29.5 -

Table 5.19: Final tests using four PLP and MSG streams trained in *clean* and *heavy* reverberation. Combination using log-average posteriors with equal weighting. The +(-) annotations mark where the log-average posterior merging produced WER that was significantly better (worse) than the single streams.

panels open, giving rise to less reflections and a less reverberant room. In the second set, 43% of the panels were open. The *light* reverberation tests used previously were of the first microphone in this set. The final set had all of the panels closed, resulting in a more reverberant environment.

Combinations using PLP and MSG yielded the best word recognition results overall. We used them here in a four stream setting where MLPs were trained using PLP and MSG data separately in both the *clean* and *heavy* reverberation environments. The combination method of log-averaging consistently produced slightly better results in tests with the unseen environment and are used here. Word error results are listed in Table 5.19.

The first 8 rows (corresponding to 100% and 43% open panels) had lower reverberation times. Equal weighting was therefore satisfactory and improved results for most of the cases, by as much as 30% relative to the best stream. MSG was constructed for robustness in reverberation and performed consistently better than PLP. The MSG stream trained on *clean* performed the best on the less reverberated conditions. The last 4 rows (no open panels) included more severe reverberation. In these cases the MSG stream trained on *heavy* reverberation performed the best. The combination for these scores had

Room impulse test				WER %				
Panels open(%)	Mic.	DTR (dB)	T60 (s)	PLP stream		MSG stream		logavg merge
				<i>clean</i>	<i>heavy</i>	<i>clean</i>	<i>heavy</i>	
0	1	0.3	1	55.7	33.2	42.5	26.1	21.1 +
0	2	0.3	1	55.8	31.5	45.6	25.0	21.3 +
0	3	0.3	1	60.6	33.8	52.3	26.7	24.4 +
0	4	0.3	1	59.9	35.9	53.0	26.8	25.2 +

Table 5.20: Combination of four PLP and MSG streams trained in *clean* and *heavy* reverberation with unequal weighting. Two *clean* streams weighted at 0.1 and *heavy* reverberation streams weighted at 0.4. The “+” annotations mark where the log-average posterior merging produced WER that was significantly lower than the single streams.

cases that were worse than the MSG *heavy* stream. The weighting for these cases was less appropriate given the severity of the reverberation. By examining Figure 5.4 we see that the ratio of *clean* to *heavy* weighting of 0.2 would have been preferable. Armed with this knowledge, we conducted a further test assigning the 0.2 weight equally between the *clean* streams (0.1 each for PLP and MSG) and 0.8 equally between the *heavy* streams (0.4 each for PLP and MSG). Word error scores are listed in Table 5.20. The combination scores with this weighting towards the *heavy* streams improved the word error to where they were significantly lower than the best of the single streams.

Additional Tests with a New Reverberation Stream

The tests in this chapter used a stream trained in the *heavy* reverberation condition in addition to the *clean* stream. The impulse response for this condition was collected independently from the impulses collected in the varechoic chamber. This room impulse had rather severe reverberation characteristics, much more than room impulses for these tests. We conducted an additional test replacing the *heavy* stream with a room impulse with less severe characteristics. This last test used the room impulse corresponding to the fourth microphone with all of the panels closed and had a DTR of -9 dB with a T60 of 1 second. Results from using the *clean* stream and the new *moderately heavy* stream are shown in Table 5.21. The weights for the streams were the same as for the previous four-stream tests: equal weighting for the first eight rows of results and un-equal weighting for the last four. The four-stream combination lowered WER in all tests by as much as 36% relative to

Room impulse test				WER %				
Panels open(%)	Mic.	DTR (dB)	T60 (s)	PLP stream		MSG stream		logavg merge
				<i>clean</i>	<i>heavy</i>	<i>clean</i>	<i>heavy</i>	
Weight \Rightarrow				0.25	0.25	0.25	0.25	
100	1	1	0.3	12.0	21.7	9.6	15.3	7.3 +
100	2	1	0.3	10.6	21.9	9.2	14.9	6.3 +
100	3	-1	0.3	12.1	21.3	10.8	15.8	7.3 +
100	4	-1	0.3	11.7	21.9	10.1	15.4	7.7 +
43	1	1	0.5	22.2	17.0	13.9	15.0	9.2 +
43	2	-3	0.5	21.4	17.2	15.3	14.9	9.6 +
43	3	-2	0.5	22.3	17.8	17.6	15.5	9.9 +
43	4	-5	0.5	24.2	18.0	18.9	15.6	10.9 +
Weight \Rightarrow				0.1	0.4	0.1	0.4	
0	1	-5	1	55.7	23.4	42.5	19.6	16.9 +
0	2	-7	1	55.8	22.7	45.6	20.2	16.8 +
0	3	-7	1	60.6	24.3	52.3	20.6	19.1 +
0	4	-9	1	59.9	22.8	53.0	18.8	17.8

Table 5.21: Final tests using four PLP and MSG streams trained in *clean* and the *moderately heavy* reverberation room impulse from the last row. Combinations used log-average posteriors with specified weighting. The + annotations mark where the log-average posterior merging produced WER that was significantly lower than the single streams.

the best of the single streams. Only the last row of results, corresponding to the condition for one of the streams, did not lower the WER significantly. Using this less severe room impulse as one of the streams yielded results that were better than when using the more severe *heavy* stream by between 15% and 40% relative. The new reverberation impulse had characteristics closer to the testing data environments with better performance among the single stream tests. This allowed for word error rates in the unseen environments that are much more usable.

5.7 Discussion

By and large the environment in which the MLP probability estimator is trained is the overriding factor on the performance in different reverberant environments. Even with robust feature extraction routines the difference in the feature distributions associated with room characteristics varies widely enough to cause severe degradation in word recognition. From the single stream tests in reverberant environments it seems likely that even given an arbitrarily large number of trained parameters, the performance of a system trained with *clean* data would not approach the performance of a system trained with *heavy* reverberation on tests with *heavy* reverberation. In fact it would be in danger of over-fitting the training data. Extrapolating, this *clean*-trained single stream system will only be effective in approximately *clean* environments. The effects of a more highly reverberant environments on the feature distributions are too great. Single streams trained on some type of reverberation can sometimes produce better results with other types of reverberation compared to the performance of the *clean*-trained stream. The feature distribution of the new reverberant environment may deviate further from the *clean* training data than from the reverberation training data and therefore can result in better probability estimates. It would then seem prudent to include in the system some measure of what the distribution might look like in such an environment.

By employing a switching algorithm a system having trained elements from two environments should broaden the range of graceful degradation due to the environment. An encouraging side-effect from the combination experiments, however, is that a combined system can perform better in a new environment than a single environment system can; this is an example where the whole can be worth more than the sum of the parts. The

probability estimates from each stream re-enforce each other when frame decisions agree while moderating the set of choices when they disagree.

The most encouraging results occurred when a two-stream system had streams that were trained in different environments and then presented with data from an unseen environment. Scores in the unseen environment were superior in the combined system than the singly trained systems. The unfortunate side effect was a penalty in either of the matched conditions. In this situation, one stream was at its best and the other stream was at its worst. In such cases, the worse stream harmed the combination more than help, though the resulting combination still performed closer to the better stream. A non-linear merging scheme or a dynamic weighting scheme may improve the results. An extra input or measure that can intelligently switch off the worse stream appropriately would rectify problems in the matched cases. When such information is not available though, the compromised performance in matched cases can still be a reasonable trade-off. Real deployed ASR systems will typically be presented with speech in an alternative environment to its training environment.

The tests here were constructed such that the two training conditions were at the more extreme ends of the reverberation spectrum: *clean* and *heavy*. This would make the unseen condition more likely to have reverberation characteristics lie in between these two extremes. This setup was chosen to broaden the range of graceful performance degradation the most. In the earlier single-stream tests, both the *clean* and *light* single stream systems performed abysmally on *heavy* reverberation. Using these two streams in combination improved results to some extent in *heavy* reverberation but were still unacceptable for use. Using the *heavy* trained stream instead yields results that are much more acceptable over a wider range of room impulses, as the final tests in the last section indicated. Using a less severe reverberation stream in lieu of the *heavy* room impulse improved results further. The characteristics of the new stream were closer to the testing environments. It would also be of interest to see the effects of adding a third stream trained with reverberation characteristics between the extreme ones used. Due to the compromised performance in matched cases arbitrarily high numbers of streams may yield diminishing performance gains.

A trend in the experiments was that the PLP and MSG streams combined more effectively than RASTA-PLP with different temporal filter sets. Intuitively, PLP and

MSG process speech much more differently and therefore should be more prone to making different kinds of errors. For example, in *clean* training and testing experiments, 71% of the misclassified frames using the *clean* LDA filters in RASTA-PLP co-occurred with the *heavy* LDA filters. However, only 67% of the frame errors made by a *clean* PLP stream co-occurred with frame errors from a *clean* MSG stream. Similarly, with *clean* and *heavy* RASTA-PLP streams and a *light* reverberation test, 72% of the frame errors of the *clean* stream were also made by the *heavy* stream while 66% of the errors of the *clean* PLP stream overlapped with the *heavy* MSG stream. This difference in the number of overlapping frame errors needs to be interpreted with a considerable degree of caution due to the complex relationship between frame accuracy and word error.

The combination experiments, as with single-stream experiments, also provided a number of examples where a system with a lower frame accuracy performed significantly better for word recognition. For example, we conducted four stream experiments using RASTA-PLP (not listed) with both *clean* and *heavy* LDA filters with MLPs trained on *clean* and *heavy* reverberation data. All of the frame accuracies were between 10% and 20% better relative to the four-stream PLP-MSG frame accuracy scores corresponding to the tests in Table 5.17. However the word errors for four-stream LDA-RASTA-PLP were up to 88% worse relative. Another example was that the frame accuracies for the four-stream PLP-MSG combinations were 20% worse relative to the two-stream PLP-MSG systems while the word error either remained constant or improved. A possible explanation for this result is that not all of the frames are equally important for word recognition. The combined system may be reinforcing the posterior scores for the frames that are crucial to word recognition. Reinforcing occurs at those frames where most or all of the streams agree while making more uncertain the remaining frames. This may be hindering the Viterbi search from following false paths caused by frames with high probability in the incorrect class. Again, further research and a more complete diagnostic would be required to arrive at a convincing explanation.

The language model scaling parameter in the CHRONOS decoder was re-tuned using the CV set for each recognition run to yield the lowest word error on that set. In many tests the best language model scaling factors were similar. In other tests (for example, between MSG and RASTA-PLP) this parameter was different. Different language-model scaling parameters were also used between the two-stream and four-stream systems; the

best language model scaling parameter was lower for the four-stream than for the two-stream system, meaning that the acoustic probabilities had more relative influence in the overall decoding. This can also be telling in that it offers some indication that the acoustic probability stream was more reliable and needed less aid by language constraints. The decoding parameter was constantly re-tuned between the tests to give an indication of the best word error achievable with the decoder and in order to remove the effect of a possibly sub-optimal selection of parameters. Different front-end components may sometimes be poorly matched to specific decoding constraints, models and parameters. Forced alignment is sometimes used to produce training data that better matches the pronunciation models to the acoustic probability training. However, pilot tests using this method did not benefit our experiments. Despite the many real and potential shortcomings, the combination of streams trained in different environments consistently improved recognition in unseen environments.

Chapter 6

Conclusion

A common problem with current ASR systems is that the performance can degrade significantly when presented with speech emanating from a different acoustic environment than was seen during training. An important cause of this is that the feature distribution to which the ASR system is trained no longer matches that of a new environment. A partial remedy is to additionally train system components on feature distributions from different environments in a multi-stream system. A benefit of the multi-stream approach is that it can capitalize on the strengths of more than one approach for maintaining robustness to acoustic degradation. Advances in any of the components of the system can be readily integrated into the multi-stream system.

Multi-stream approaches can take a number of forms. The approach used in this thesis employed multiple front-end acoustic modeling stages whose acoustic probability estimates were then merged for further processing by the word-recognition decoder. Each of the front-end stages was trained to improve phone classification in a specific acoustic environment. With multiple front-end stages trained in different conditions, the range of environments where the ASR system can maintain reasonable performance increases. Room reverberation was the principal type of acoustic distortion investigated in the experiments, though preliminary tests also included some examples of additive background noise.

The evolution of this work proceeded in two stages. The first stage involved training front-end stages to perform optimally in sample acoustic environments. A phone class discriminant criterion was used in training the front-end acoustic modeling. The second

stage tested these trained front-end modeling components in combination. Of particular interest was the performance in acoustic environments other than the ones used in training.

6.1 Discriminant Feature Extraction

We investigated a means of improving the performance of the front-end system over a range of acoustic environments. In addition to training the probability estimator we modified the speech signal processing to improve class discrimination in the degraded acoustic environment. Rather than develop a novel processing technique for each environment we modified the temporal filtering of existing preprocessing algorithms. The general approach was to apply discriminative learning to the time-frequency plane. Since the MLP probability estimator already incorporated non-linear discriminant training along the frequency-related direction, we added a discriminant component along the temporal dimension. The temporal filters were derived using Linear Discriminant Analysis. The LDA filters were derived on a task-independent data set to promote generality.

Linear Discriminant Analysis has proven to be a powerful technique in statistical data analysis. As applied in this thesis, LDA automatically generates an ordered set of discriminant linear filters that operate on the temporal trajectories of the frequency energies. The temporal filters derived with LDA bear striking similarity to the standard RASTA filter that passes the modulation frequencies between 1 and 12 Hz. Since the acoustic environment modifies the critical-band energy trajectories and since the LDA filters are computed from these modified trajectory distributions, we expected to see some modifications to the resulting temporal filters with respect to the acoustic environment. In the presence of reverberation there is a tendency for the band-pass range to narrow towards the more syllabic rate of 5 Hz. This is consistent with evidence that syllabic rates harbor some perceptual stability. In cases with added background noise, there is also some narrowing of the preferred frequency range, though not as severe.

Using the derived filters almost uniformly improves frame-classification accuracy. This is expected since LDA filters were designed to distinguish among phone classes. Tests with RASTA-PLP also indicate that this can lead to improvements in word recognition. The improvements between the different filters can be mitigated or made redundant, however, by allowing the MLP probability estimator access to a wider acoustic context of

frames. With a wider acoustic context, the MLP training implicitly includes temporal processing. Further, MLPs are discriminatively trained in a nonlinear manner that is complex and inherently more powerful than the linear filters. Word recognition improvements were also not forthcoming in tests using PLP cepstra and MSG even while the frame accuracy was maintained or improved upon.

In our experiments, a single bank of filters was derived to distinguish among all phones. The filters in the individual frequency bands were generally consistent though sometimes have different preferred modulation frequency ranges. This was due in part to the relative severity to which an acoustic environment affected different frequency ranges and in part to the differences in the temporal and frequency characteristics among subsets of phonetic classes. Future work may involve further discrimination within sets of phones for a finer discrimination, similar to the TRAPS filters derived by Sharma [99, 98, 51]. It may be useful to observe the effect of acoustic environments on these filters. Further discriminative training based upon criteria distinct from those used in LDA may also be investigated. However, due to the inconsistent gains in word recognition using filters optimized for phone classification, such an effort may result in disappointing gains. Kanedera and Arai found through repeated ASR experiments that modulation spectral components below 16 Hz yielded the highest word recognition accuracy. Components ranging from 2 and 8 Hz were the most important for ASR [58, 59, 5]. The data-driven temporal filters consistently preserve these lower modulation frequency rates where the speech information resides. Further parsing of this frequency range can give rise to improved classification between phones at the frame level but currently gives diminishing returns in word recognition tests. What remains arguably important however is that the modulation rates where the phonetically relevant components of the speech reside be preserved in some manner in the feature processing.

6.2 Multi-Stream Combinations

With front-end stages that were trained to specific acoustic environments, the ensuing work consisted of experiments with combining these stages in a multi-stream setting. A number of tests were conducted using many of the techniques found in the literature. Optimal methods of combining such probability streams remains a research issue. Con-

sistent with many research results, we found that simple averaging combinations of the log-probability streams provided reasonable and effective results, particularly when combining PLP trained on clean speech and MSG trained on reverberant speech. This simple method also allows for stream weighting that facilitates emphasizing (or de-emphasizing) streams should additional information concerning the acoustic environment warrant it.

Tests using several room impulses with various stream weights indicate that combined systems can improve upon the recognition accuracy of the system above a single stream system. Performance degradation due to the acoustic environment can be mitigated by having a system trained in more than one environment. We chose to train our combined system in the extreme cases of clean speech and heavy reverberation. Doing so broadened the range of reasonable performance when confronted with data associated with unknown reverberation characteristics. In these cases, the probability estimates from the constituent streams served to reinforce each other enough to improve performance. An apparent caveat is that a stream that performed very badly individually degraded the performance of the higher quality streams. This can be seen in the matched condition cases. In these instances, the introduction of a weighting knob or computed information about the acoustic environment could help maintain recognition rates considerably. Tests in which we adjusted these knobs and observed the results were significantly better than the evenly weighted feature streams.

The recognition tests were conducted using a hybrid ANN-HMM ASR system. It would be worthwhile to repeat many of these experiments on a GMM-HMM system. Many techniques, for example Maximum Likelihood Linear Regression [69], exist for adapting models in these systems. It would be useful to confirm that the improvements using multiple front-end acoustic modeling stages trained in different environments would also benefit systems that contain methods that attempt to account for such differences. Further, experiments using local posterior measures to adjust the relative weighting yielded mediocre gains in our tests. This was due to the noisiness in the local measures and possibly the types of errors, often pathological, that the MLP produced. Some researchers have found that frame-level posterior-based confidence measures, although useful for word and utterance rejection tasks, were less useful for stream weighting [65]. Higher-level confidence measures or frame-level measures integrated into higher-level measures, on the other hand, should be useful here and should be investigated. Many of these types of measures are

implementation or decoder specific, non-trivial to calculate, and were outside the scope of this work. Confidence measures, whether for utterance rejection or stream weighting, remains the subject of on-going research.

6.3 Contribution and Future Work

This thesis has demonstrated that combinations of front-end acoustic modeling components that have been trained in heterogeneous acoustic conditions can improve ASR robustness to untrained acoustic conditions. Discriminatively trained temporal filters, in addition to the discriminatively trained MLP probability estimator, were used to improve each streams performance in a sample acoustic condition. We found that this method consistently improved phone classification at the frame level. For the task of word recognition, a single-stream system based on this method was only useful in certain cases. On tests with unseen reverberation, the multi-stream system having components trained in both clean and heavy reverberation produced results significantly superior to the system trained solely in one condition. Combination results appeared to be best when each of the streams was based upon different preprocessing strategies.

The multi-stream approach has been rapidly gaining attention within the ASR community. Many have found that new experimental system components that sometimes yielded unsatisfactory performance in isolation would boost performance when used in combination with other approaches. Though the subject of feature-stream combination has been studied by many researchers, optimal combination methods remain elusive; empirical results often show that theoretically justifiable strategies do not necessarily perform best. The best combination method can be dependent on the kinds of streams involved, the type of system, and even the recognition task. Unfortunately, there is not yet a principled way of determining the best combinations and best streams to combine other than to perform exhaustive testing. A hindrance to this is the combinatorial explosion of the number of experiments. This factor also caused us to limit our experiments to simple combination methods with a small number of streams. Given the number of possible combination methods and the number of possible feature streams, further multi-stream work would benefit from a means of predicting which feature streams and stream combination strategies would be most successful. Ellis and Bilmes have recently tested conditional mutual information

between streams as a candidate prediction tool in this area [30]. Their results suggest that the mutual information between streams can indicate the classifier merging potential from two feature streams and provides a good starting point for further investigation into feature stream combination. For combination strategies, Bilmes and Kirchhoff have recently tested new combination methods based on specific independence assumptions with encouraging results [8]. They used directed acyclic graphical models as a tool for constructing combination methods with explicit statistical properties.

A recurring difficulty in our experiments was the complex relationship between the frame accuracy and the overall word recognition rate. There were repeated cases where an improvement in frame accuracy did not give rise to similar improvements in word recognition. This is a common observation when experimenting with complex systems where a system component is optimized separately from the entire system. Our optimization of the front-end acoustic modeling was based on phonetic classification at the frame level. This optimization neglected the complex interaction with the rest of the system, including the pronunciation and language models, as well as the decoding algorithm. Although high frame accuracy is arguably important for good word recognition, there is an apparent mismatch between the criterion we used for good phone classification and the criterion for optimal word recognition. With this contradiction facing us, it is difficult to determine proper front-end and front-end combinations without doing exhaustive testing including word recognition. Future work should analyze the interaction of the frame level posteriors and the maximum *a posteriori* decoding. Our preliminary study in Appendix E indicate that not all of the frame errors carry the same importance for the word recognition and that the locations of these errors are significant. A starting point of further work could be to conduct further diagnostic tests of the ASR system in a style similar to that which Greenberg and associates did on Switchboard ASR results [42, 41]. Tests using data with varying degrees and types of frame errors together with various indicators of location (e.g. onsets, nuclei, and coda of phones or syllables) as well as phone confusion and segmentation can be computed and compared with recognition output. Results from such analysis may become instrumental in the future design of front-end acoustic modeling methods and combinations.

Appendix A

Recognition Units

Recognition tests in this work used a subset of the Oregon Graduate Institute (OGI) NUMBERS corpus [19]. The subset used consisted of utterances that had phonetic transcriptions. Utterances that had non-number words such as “dash” were eliminated from this subset, though some filled-pauses were kept. A vocabulary of this corpus subset is listed in Table A.1.

The ICSI ASR system uses 56 context independent monophone units. These are listed in Table A.2 together with example words for pronunciation¹. Due to the small vocabulary of the NUMBERS corpus, only 32 of the 56 phonemes appear in the NUMBERS corpus. For filter derivation, the OGI STORIES corpus was used. This corpus was better suited to deriving temporal filters due to the length of the utterances and the more complete phonetic coverage. The independence of this corpus from the NUMBERS corpus also promoted testing the generality of the derived LDA filters.

¹This table was adapted from one courtesy of Su-Lin Wu, Eric Fosler-Lussier, and Charles Wooters.

[uh]	[um]	eight
eighteen	eighty	eleven
fifteen	fifty	five
forty	four	fourteen
hundred	nine	nineteen
ninety	oh	one
seven	seventeen	seventy
six	sixteen	sixty
ten	thirteen	thirty
three	twelve	twenty
two	zero	

Table A.1: Words contained in the subset of the OGI NUMBERS corpus used for word recognition experiments.

ASR Phoneme Symbols			
ICSI56set	Example	ICSI56set	Example
pcl	(p closure)	bcl	(b closure)
tcl	(t closure)	dcl	(d closure)
kcl	(k closure)	gcl	(g closure)
p	pea	b	bee
t	tea	d	day
k	key	g	gay
ch	choke	dx	dirty
f	fish	jh	joke
th	thin	v	vote
s	sound	dh	then
sh	shout	z	zoo
m	moon	zh	azure
em	bottom	n	noon
ng	sing	en	button
nx	winner	el	bottle
l	like	r	right
w	wire	y	yes
hh	hay	hv	ahead
er	bird	axr	butter
iy	beet	ih	bit
ey	bait	eh	bet
ae	bat	aa	father
ao	bought	ah	but
ow	boat	uh	book
uw	boot	ix	debit
aw	about	ay	bite
oy	boy	ax	about
h#	(silence)		

Table A.2: Set of phone classes used in ICSI recognition system.

Appendix B

Temporal LDA Filters with Phonetic Units

This appendix contains detailed plots of the LDA filters derived from log critical band trajectories. Figures B.1, B.2, and B.3 contain the three principal LDA filters derived with *clean* data, highly reverberated data and data with *factory* noise added at 10 dB SNR, respectively. These plots illustrate the similarity in impulse and frequency response between the filters using a sampling of the frequency bands for clarity. The second, fourth, eighth, and twelfth bands centered at 250, 450, 1000, and 1850 Hz respectively are presented. There are slight differences between the frequency responses of the lower bands and the others; the filters from the lower bands tend to pass slightly lower modulation frequencies for the non-clean cases. In the presence of *heavy* reverberation, for example, there is a pronounced lowering in the preferred frequency ranges of the modulation spectra. Differences between the lower and higher bands are also more evident with lower bands passing the lower frequencies. This is consistent with reverberation being most evident at the lower portions of the spectrum. *Factory* noise also demonstrates some lowering of the frequency ranges though not as much.

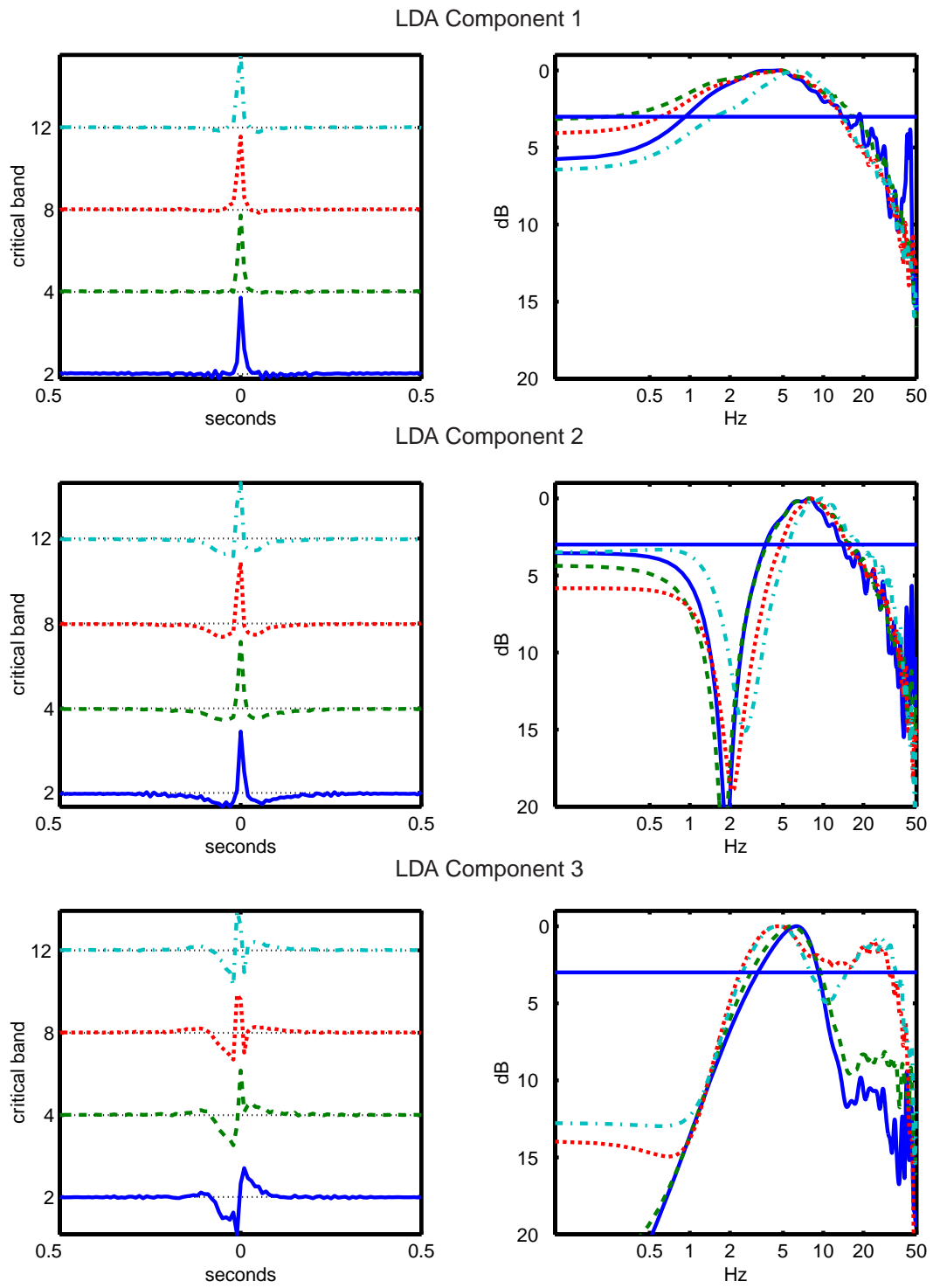


Figure B.1: Impulse and frequency responses for first three LDA filters derived with *clean* data.

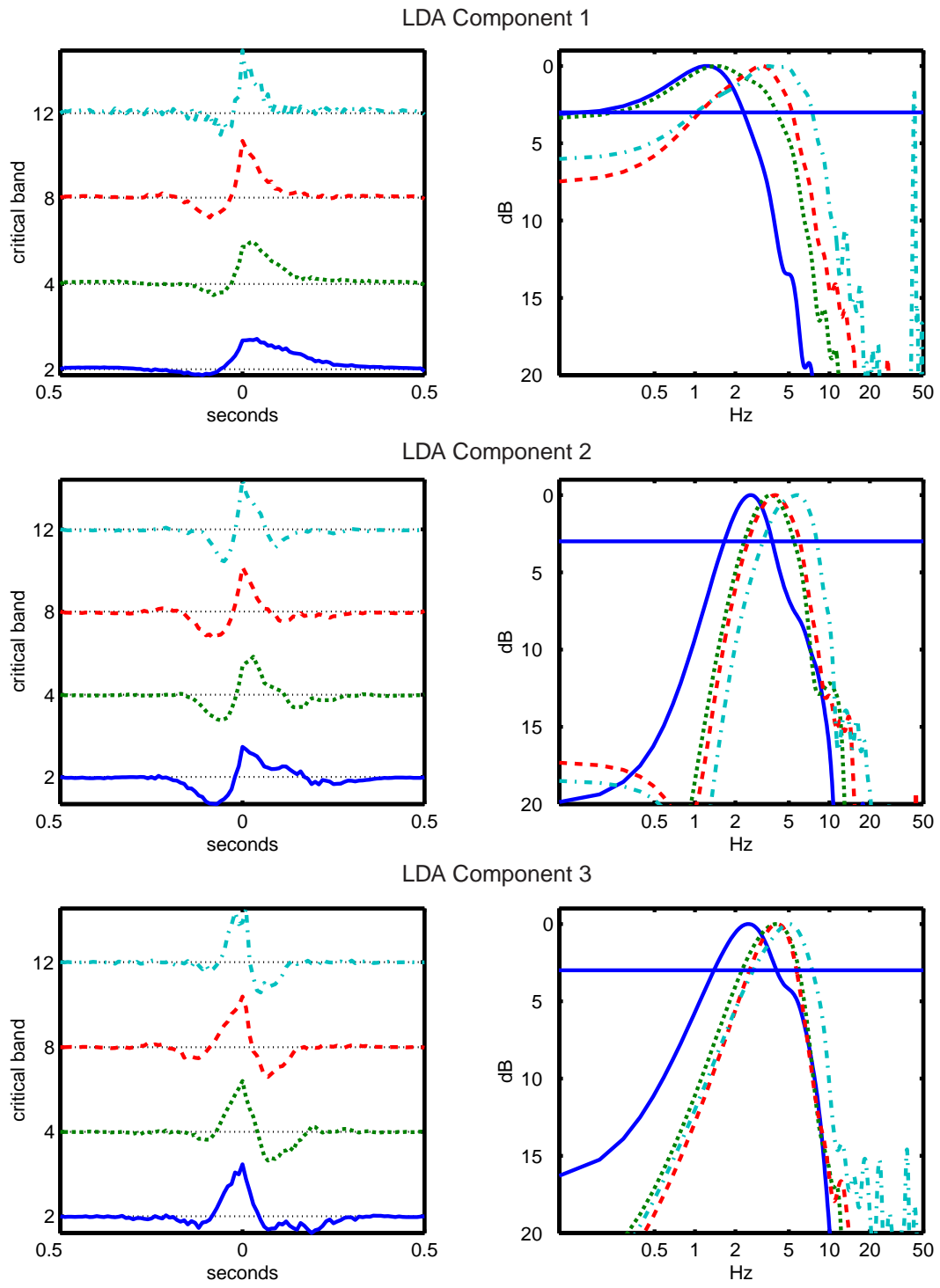


Figure B.2: Impulse and frequency responses for first three LDA filters derived with *heavy* reverberated data.

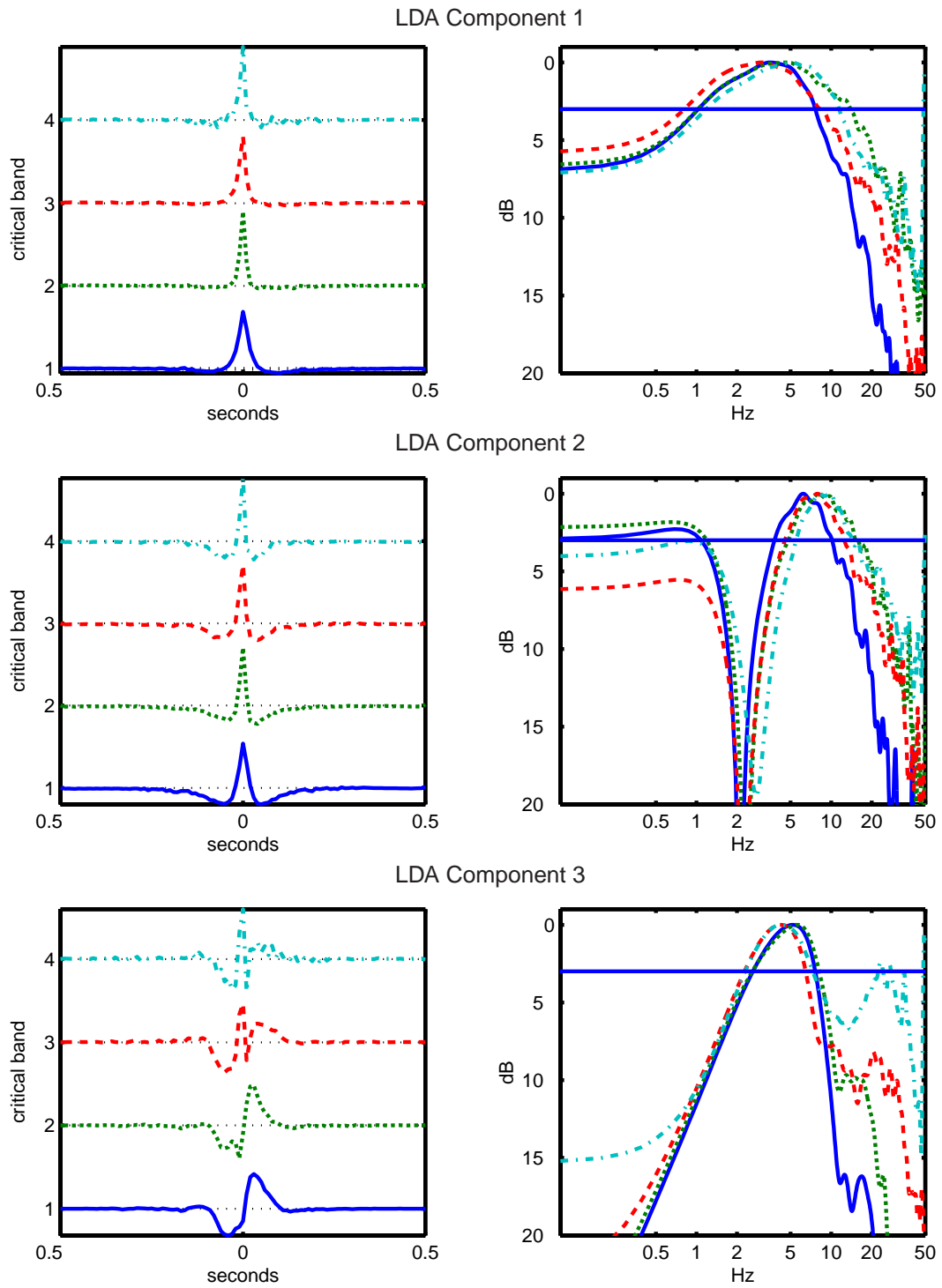


Figure B.3: Impulse and frequency responses for first three LDA filters derived with *factory* noise data at 10 dB SNR.

Appendix C

Temporal LDA Filters with Syllabic Units

Since the LDA filters derived in *heavy* reverberation tended to restrict the modulation rates to those commensurate with syllabic rates, pilot tests were conducted using syllabic targets in lieu of phonetic targets. These syllabic targets were derived from the phonetic targets using the TSYLB program written by Bill Fisher at the National Institute of Standards and Technology (NIST). The program grouped phone sequences into syllables using phonotactic and pronunciation rules. When applied to the OGI STORIES corpus, the algorithm produces 5427 distinct syllable patterns, most of which occurred very infrequently. For filter derivation, the 100 most frequent syllable patterns (comprising 42% of the total number of syllable instances) were used as class targets. Detailed plots of the three principal LDA filters derived with these targets with *clean* data is shown in Figure C.1. The preferred frequency ranges are consistent with those found in the reverberation cases using phonetic targets. A comparison of the LDA filters derived in different noise conditions using syllable targets is shown in Figure C.2. The frequency responses in this plot are of the averaged impulse responses across thirteen frequency bands (neglecting the highest and lowest ones). Whereas phonetic targets yielded band-pass ranges that changed drastically with reverberation conditions, the filters using syllable targets were noticeably consistent. This was also true when using additive noise.

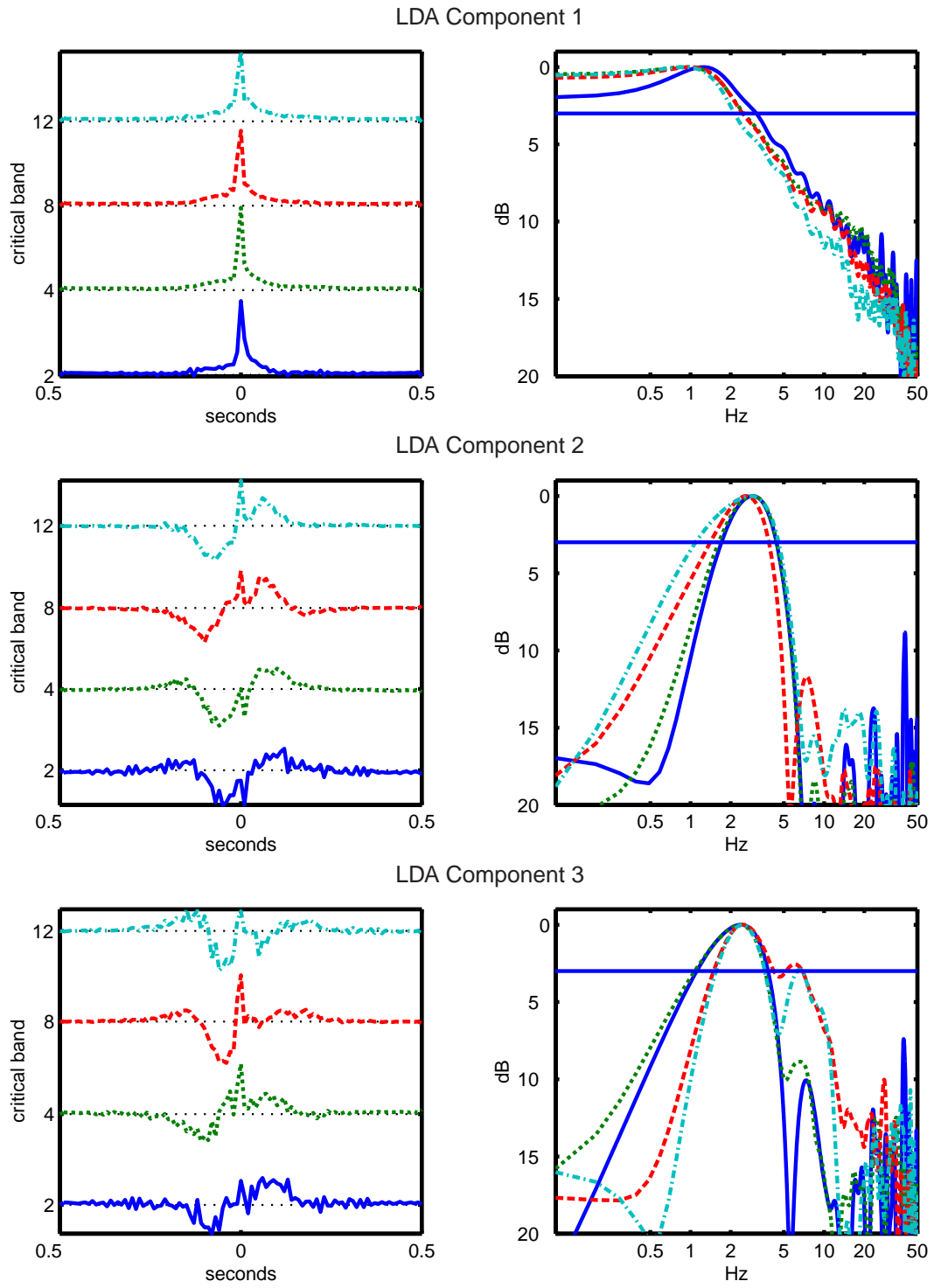


Figure C.1: First three LDA filters derived with syllabic targets on *clean* data.

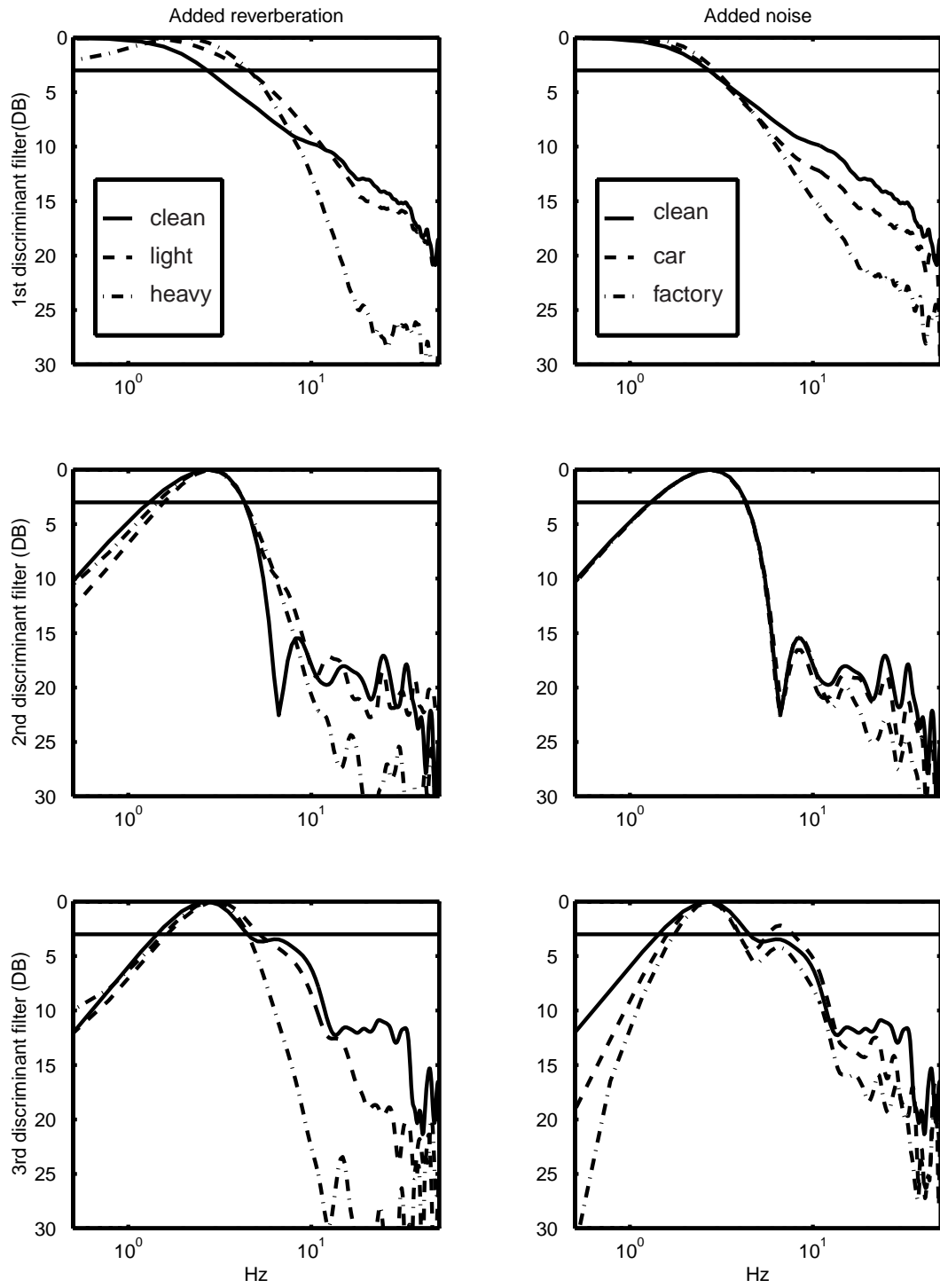


Figure C.2: Comparison of averaged filters using syllable targets in different noise conditions.

Appendix D

Temporal LDA Filters for PLP

LDA filters derived using PLP cepstral trajectories are shown in figure D.1. This plot has impulse and frequency responses from *clean* data. Only the first, fourth, and seventh of the 8 cepstral coefficients are plotted for comparison. Since the individual cepstral components are only weakly correlated there appears to be more differences among the filter responses of the different cepstral components. Despite the apparent noisiness in the responses, the filters do generally maintain a “Mexican-hat” band-pass shape.

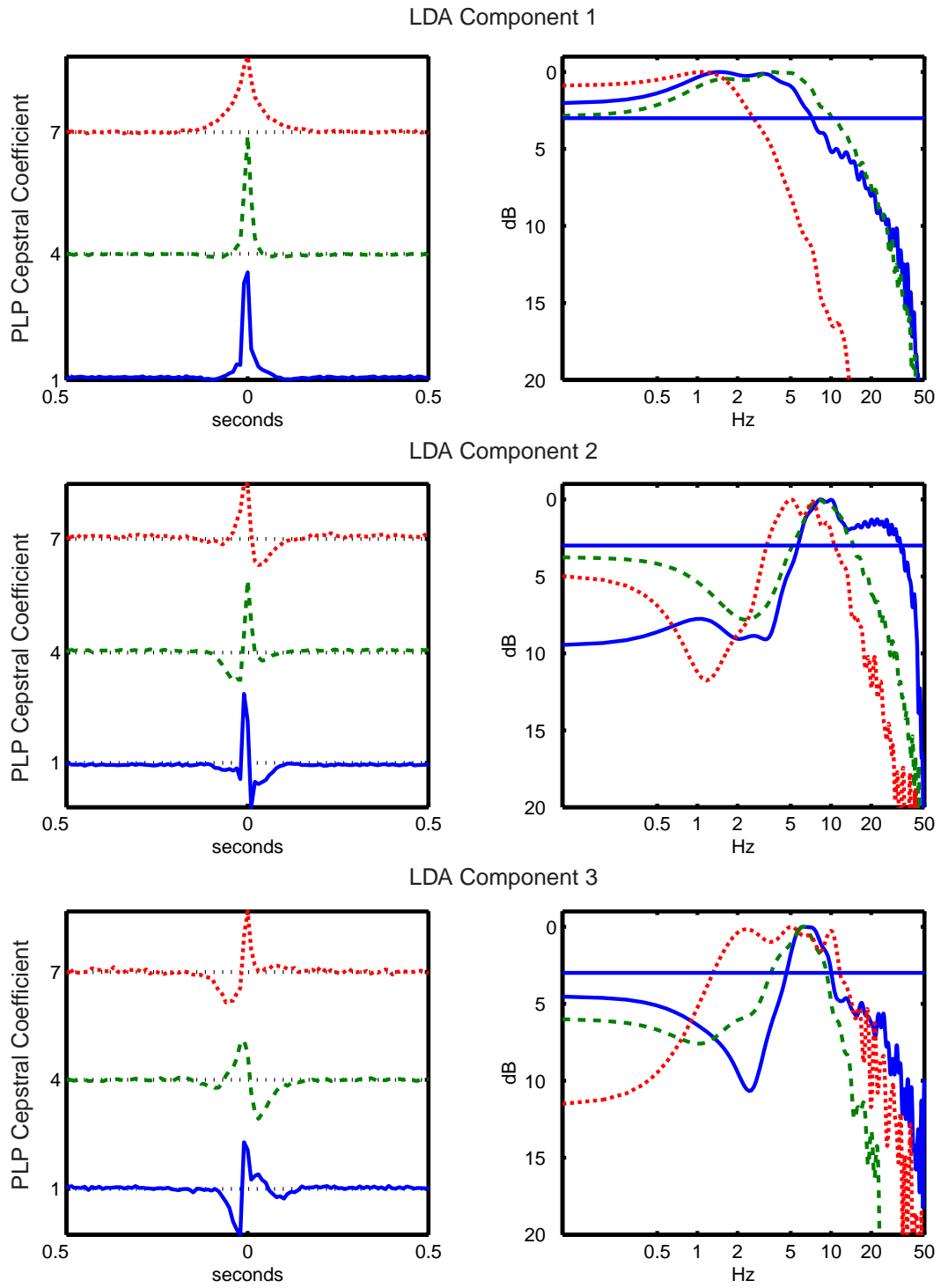


Figure D.1: First three LDA filters derived from PLP cepstra on *clean* data.

Appendix E

Correlating Frame Accuracy and Word Error

Frame accuracy is a common and natural summary statistic to use in speech classification tasks. In neural-network-based ASR it is convenient to use such a statistic when estimating sub-word-unit probabilities in the acoustic modeling stage. For example, frame accuracy gives an indication of the performance of the MLP probability estimator and is used for the stopping criterion during training. However, as with many summary statistics, it presents an incomplete and sometimes deficient indicator of performance for the overall task of word recognition. Many of our experiments with LDA temporal filters, for example, gave rise to cases where an improvement in the frame accuracy resulted in either no significant change or an increased word error. This is a problem that has been seen by many in the ASR community. Unfortunately, we are not aware of any detailed analysis or satisfactory explanation to comprehensively account for instances when frame accuracy and word error are uncorrelated. Without such an answer, many are forced to rationalize or excuse such results to complex interactions in the ASR system, as we have.

We conducted pilot experiments in an effort to illustrate some of the variability in word-recognition performance associated with frame accuracy. This preliminary study also attempts to shed light on some of the factors that might give rise to instances where frame accuracy and word error correlate (or not). Some of the results are confirmation of intuitive or commonly known trends.

E.1 Method

The method we used to perform controlled experiments was to artificially modify the frame classification rate of a probability stream from a data set prior to decoding. First a base sequence of class posterior probability estimates was obtained that had a relatively low frame accuracy. We used the probability sequence from a forward pass of PLP with delta and double-delta features through an 800-hidden-unit MLP. The training data for the MLP was the development test set from the NUMBERS corpus whose training features were artificially corrupted by *heavy* reverberation. The forward pass data was in the original clean state. The resultant probability sequence had a frame accuracy of 45% relative to the reference phonetic hand-transcription. We then corrected an additional 25% of the total number of frames (or 38% of the incorrect frames) to yield a total frame accuracy of 70%. Frames were randomly selected from a pool of all inaccurate frames and corrected by assigning a high posterior probability to the correct classes (from the reference transcription), while distributing the remaining probability mass equally among the remaining classes. Afterwards, word recognition was performed using the CHRONOS decoder with fixed decoding parameters. A summary of the original sequence is shown in the following table.

Number of utterances	1206
Number of frames	216518
Number of incorrect frames	118979 (55%)
Number of correct frames	97539 (45%)
WER (of 4673 words)	40%
Number of frames to fix to achieve 70% frame acc.	54024 (25%) (38% of incorrect)

We chose to modify a relatively poor-performing sequence of probabilities rather than constructing a purely artificial one for practical reasons. We wished to start with probabilities that were generated from real features that would contain realistic posterior values, errors, and confusions. It would be non-trivial to construct a purely artificial sequence with these characteristics. In particular, the distribution of the probability mass among the non-correct classes would be difficult to do in a principled manner. Further, it is more convenient to correct the frames that were originally inaccurate than to corrupt correct frames in a realistic fashion.

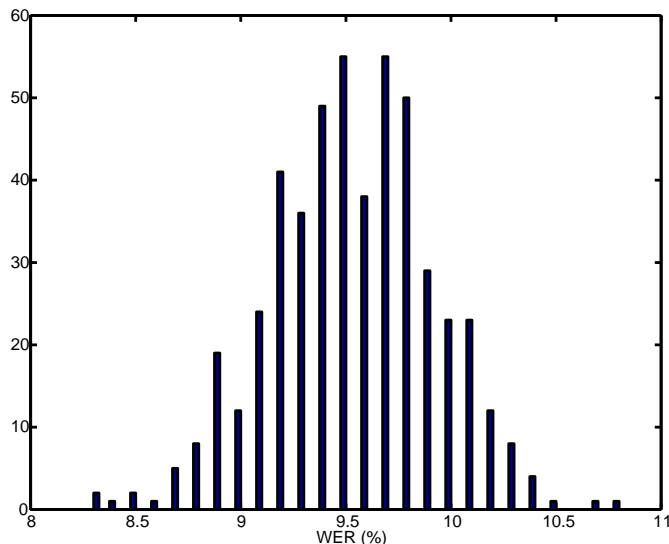


Figure E.1: Histogram of WER for 500 recognition runs. In each run random incorrect frames were corrected to yield a frame accuracy of 70%.

E.2 Experiments

In all of the following, a total of 54024 of the 118979 misclassified frames were corrected to bring the frame accuracy to 70% of the total number of frames. In each of the experiments, the frames to be corrected were randomly chosen among either the total number of incorrect frames or a subset of frames that matched a given criterion. Random frames were selected by uniformly shuffling a list of the candidate frames and selecting a portion of them. Specific random seeds were assigned to permute the random numbers and to allow random sequences to be duplicated or recovered.

Uniform Random Frame Correction

We ran 500 word-recognition experiments where the fixed number of corrected frames were randomly chosen among all of the incorrect frames. A different frame selection was chosen between recognition runs. The corrected frames were given a posterior probability of 0.99 in the correct class. A histogram of the resulting word error rates is shown in Figure E.1. With a constant frame accuracy but a difference in selected correct frames, the resulting WER varied from 8.3% to 10.8%. Those runs with a WER higher than 10% or lower than 9% are significantly different from 9.5%.

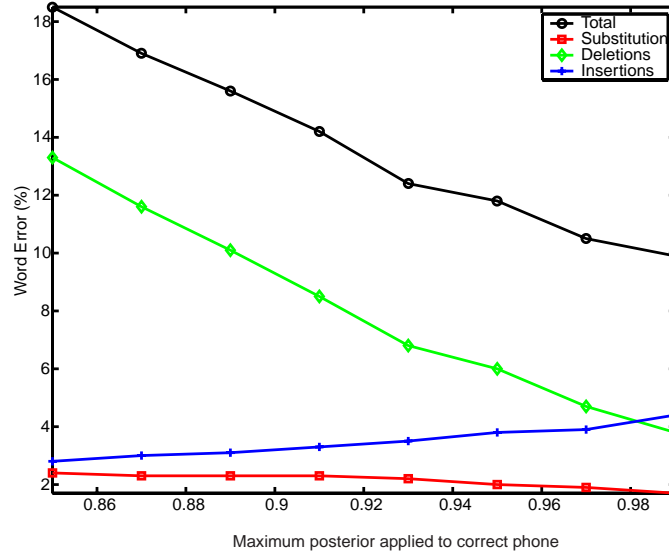


Figure E.2: WER for one recognition run of randomly chosen corrected frames where the value of the posterior placed corrected frames was varied.

Note that the original correct frames, 45% of the total frames, were the same for all runs. This test demonstrates that the placement of the correct frames can have a significant effect on the WER even though the total correct number of frames remained the same. The frame corrections were randomly chosen, equally among all incorrect frames. In subsequent tests, where certain frame types were corrected preferentially, WER scores sometimes varied by a much wider margin.

Posterior Value of Corrected Frames

In the previous tests, corrected frames had a high posterior of 0.99 assigned to the correct phone class with the remaining probability mass distributed equally among the rest of the phone classes. Frame accuracy, however, is a summary based upon the maximum posterior classification. The value of the maximum posterior can be much lower, as low as $\frac{1}{\#phones} + \epsilon$. The value has a direct bearing upon word recognition depending upon the probabilities associated with the surrounding frames. We conducted an additional test where the assigned corrected probability lowered from 0.99 to 0.85 in 0.02 decrements. Results from a single run using a fixed sequence of corrected frames is in Figure E.2.

Varying the maximum posterior to something less or more "confident" signifi-

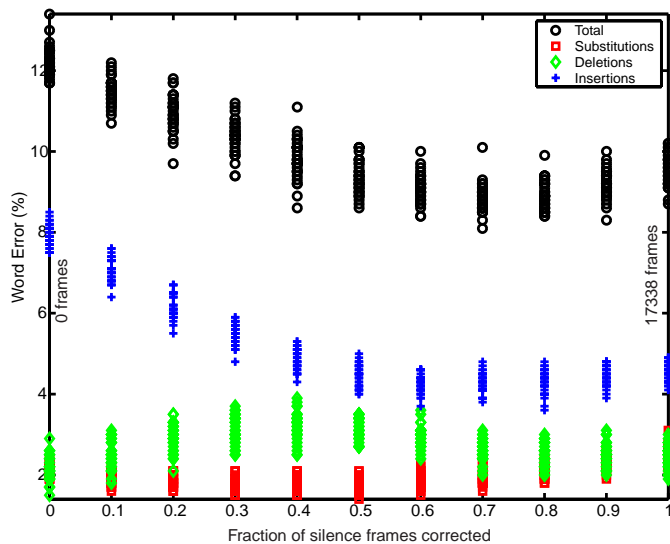


Figure E.3: WER for 20 recognition runs with a varying proportion of corrected silence frames.

cantly altered the resulting WER. Even though each data point in Figure E.2 is from a probability sequence with the exact same frame accuracy with the exact same frames classified correctly, the WER varied between 10% and 18%. This is not so difficult to believe since the decoded path must rely on the confidence of neighboring frames. Admittedly, the experiment is artificial and the pattern of frame probabilities is no longer "natural." The incorrect frames were fixed randomly with possibly many isolated among a group of incorrect frames. This is a possible shortcoming of the technique we have chosen to use here. However, correcting frames with a high posterior is necessary to force a new search path and overcome deficiencies in the surrounding frames. Correction with a high posterior allows us to observe indications of the importance of the placement of correct frames.

Corrected Silence Frames

Correctly determined locations of silence has an important function in segmentation, both of words and utterances. This next test makes a further distinction between the silence frames and the non-silence frames within the total number of incorrect frames. Proportions of the silence frames were corrected separately from the non-silence frames.

Total number incorrect frames	118979
Silence frames incorrect	17338 (15%)
Non-silence frames incorrect	101641 (85%)

In Figure E.3, the recognition tests were run with varying numbers of corrected silence frames ranging from no silence frames correct to all of the silence frames corrected. All the while, the total frame accuracy was fixed at 70% of all frames. Thus, when more silence frames were corrected then fewer non-silence frames were corrected and vice versa. This was done 20 times with a different random number seeds to select different frames. Again, corrected frames were given a posterior of 0.99 in the correct phone.

The number of insertions has the most prominence in the total word error, likely owing to restrictions silence places on word boundaries. As the number of corrected silence frames increases, the number of insertions goes down. Past a certain point (70% of the silence frames), the number of substitutions begins to rise, possibly due to less non-silence frames being corrected. In these tests, the number of corrected silence frames and the WER are strongly and negatively correlated with a coefficient of -0.86. Further, silence constitutes only 15% of the incorrect frames, but makes a significant impact. Correct detection of silence is important for low WER.

Corrected Vowel Frames

These next tests repeat the previous test except that frames corresponding to vowels are distinguished from the remaining phones (including silence). Vowels largely constitute the syllable nuclei. Therefore, these also test to some degree the importance of syllable nuclei versus non-nuclei except that silence is a competing factor.

Total number incorrect frames	118979
Vowel frames incorrect	44541 (37%)
Non-vowel frames incorrect	74438 (63%)

Results from 20 recognition runs with different randomly chosen corrected frames are shown in Figure E.4. In this test, the fraction of corrected vowels and the WER are correlated with a coefficient of 0.76. This result indicates that less attention should be paid to vowels versus all else. However, the principal error in the total is the insertions. Since silence is also important for eliminating insertions, it is possible that the reduced number of silence phones corrected overtook the corrected vowels. For this reason, further tests

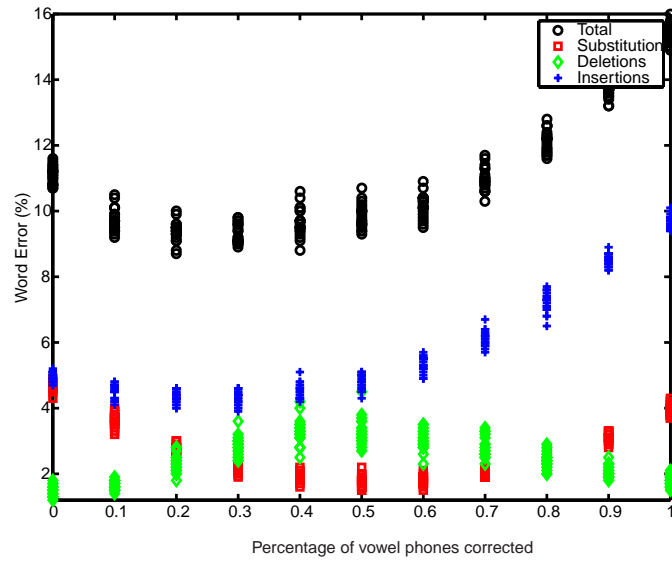


Figure E.4: WER for 20 recognition runs with a varying proportion of vowel frames corrected.

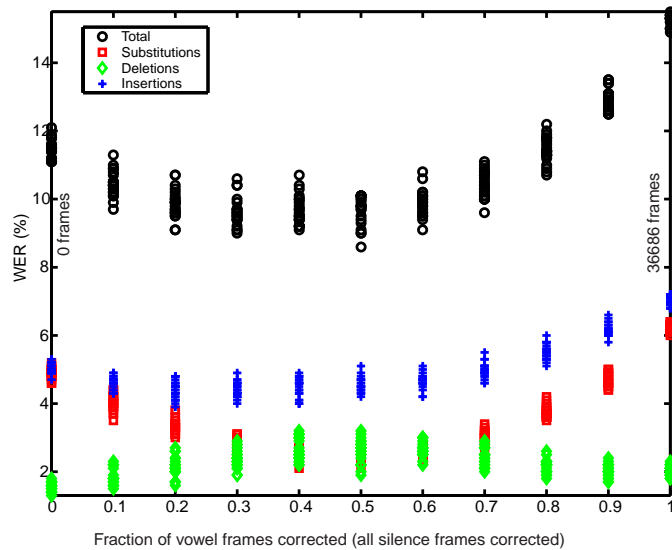


Figure E.5: WER for 20 recognition runs with a varying proportion of vowel frames corrected. All silence frames were corrected independently.

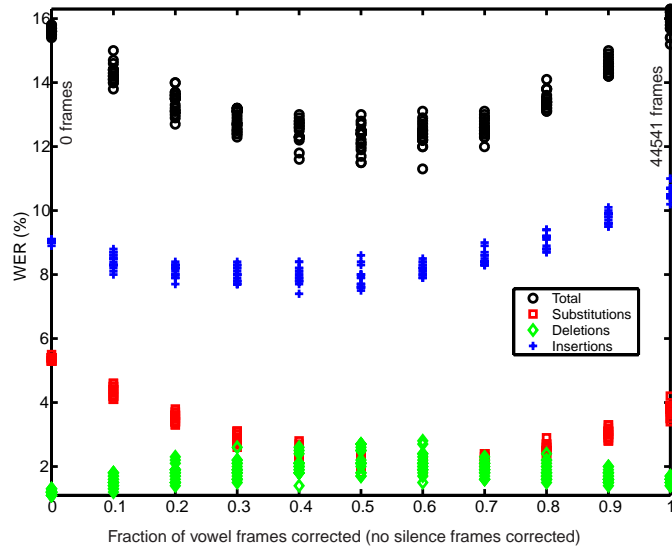


Figure E.6: WER for 20 recognition runs with a varying proportion of vowel frames corrected. All incorrect silence frames were left uncorrected.

were conducted where the silence frames were sectioned out and controlled independently. Two tests were conducted. In the first, all of the silence frames were corrected with results in Figure E.5. The fixed silence phones reduced the number of allowed corrections so only 36686 of the 44541 frames were candidates for correction. In the second, none of the silence frames were corrected with results plotted in Figure E.6.

Total number incorrect frames	118979
Vowel frames incorrect	44541 (37%)
Silence frames incorrect	17338 (15%)
Non-vowel, non-silence frames incorrect	57100 (52%)

With the silence phones corrected and somewhat removed from consideration, the fraction of vowel phones corrected has a correlation coefficient with WER of 0.56. Substitutions seem to follow the total WER best though it is not the principal error type. With none of the silence frames corrected, the correlation coefficient between the fraction of vowels and the WER is 0.05, a very weak correlation. The insertions due to the uncorrected silence frames increases the WER level to between 12% and 16%. At this level it appears that a more or less equal proportion of corrected vowels and non-vowels is needed. There seems to be a balance between vowel and non-vowel phones such that some number of each is best. However, from the extremes (none or most vowels corrected) and from the

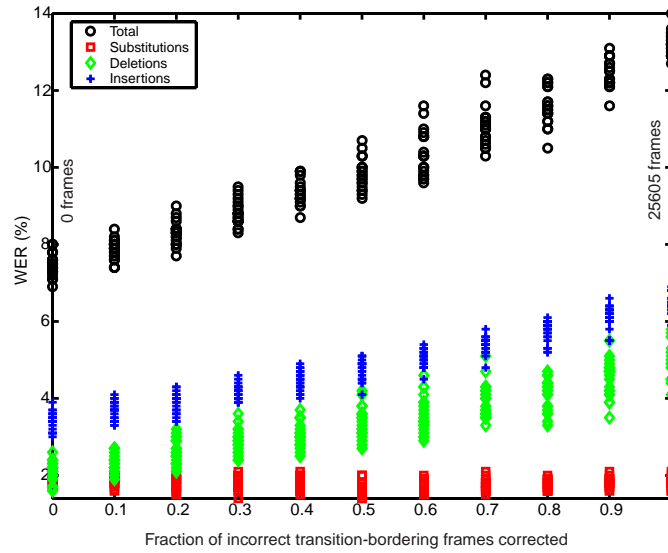


Figure E.7: WER for 20 recognition runs with a varying proportion of the corrected frames that bordered phone transitions in the hand transcription of the NUMBERS corpus.

correlation coefficients, it appears that correcting the consonants offers the greater benefit, but only slightly when the silence accuracy is good.

Frames Bordering Phone Transitions

This test examines the effect of incorrect frames near transitions from one phone to another in the reference transcription. Two tests were conducted. In the first, fractions of the number of incorrect frames that bordered phone transitions in the reference transcription were corrected. Results from this test are plotted in Figure E.7. In the second test, incorrect frames that were within 2 frames from the transition were grouped and randomly corrected, with results in Figure E.8. 20 recognition runs with different random frames selected were performed in each of the tests.

Total number incorrect frames	118979
Incorrect frames bordering transitions	25605 (22%)
Incorrect frames not bordering transitions	93374 (78%)
Incorrect frames within 2 frames from border transitions	47223 (40%)
Incorrect frames not within 2 frames from border transitions	71756 (60%)

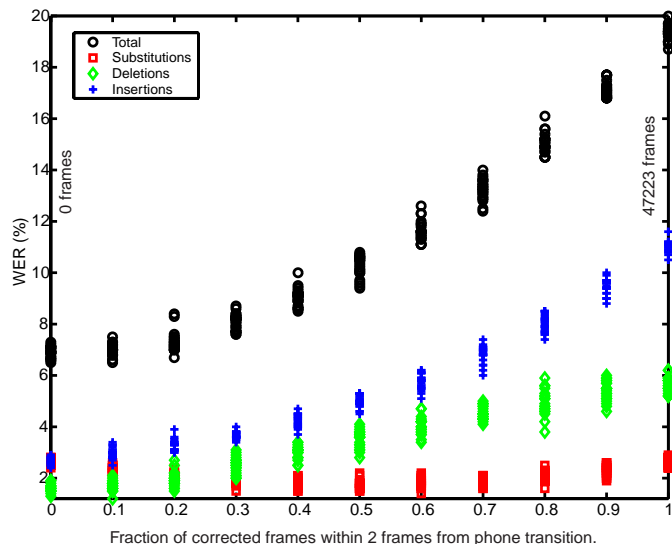


Figure E.8: WER for 20 recognition runs with a varying proportion of the corrected frames that were within 2 frames from phone transitions in the hand transcription of the NUMBERS corpus.

The fraction of corrected frames that border phone transitions is strongly correlated with WER with a coefficient of 0.97. This is true for both tests. It is interesting to see the WER in Figure E.8 rise from about 7% to almost 20%. All experiments have exactly the same frame accuracy. To the extreme right in the plot, all of the transition-bordering frames were corrected with relatively few (6801) of the remaining frames corrected. To the extreme left in the plot, only non-transition-bordering frames were corrected; incorrect transition-bordering frames were left unaltered. This resulted in the best group of WER. The WER when assigning corrected frames away from the transition borders is lower than the average WER from a uniform random assignment (Figure E.1). From these tests, it seems that corrections that are nearer the centers of the phones are more important than near the boundaries.

These tests used hand-transcribed phonetic transcriptions as the reference for both training the probability stream and classification summaries. The tests therefore rely on accurate phonetic segmentation as well as identity. Precise placement of transitions between phones can be dubious for many pairs of phones. It is therefore encouraging that precise classification at the boundaries may not be necessary.

E.3 Discussion

Word recognition error depends upon the accurate classification of the frame probabilities, the locations of the errors and the frame posterior values. A random sampling of corrected frames gives rise to a distribution of corresponding word error rates despite equal overall frame accuracy. Varying the proportion of some types of frame errors can yield results that vary in a systematic fashion. Depending upon the proportion of errors, the resulting WER can vary by a significant amount. With these complications, the frame accuracy is not necessarily a proper measure when comparing the acoustic probabilities of two or more streams. Since the value of the maximum posterior can have a strong effect on WER, we also considered a frame accuracy weighted by the posterior values for the correct class and an average of the posteriors for the correct classes. Computed measures were, however, only weakly correlated with WER, with a coefficient of -0.10. Additional weighting could be included if it is determined that certain types of frames are more important than others in the resulting decoding. For example, the silence frames are relatively important whereas the transition bordering frames may not be. Naturally, further tests are needed for a better picture.

A thorough investigation of the relationship between frame accuracy and word recognition would require a more detailed sensitivity analysis of the decoding system and the models. Such an analysis is non-trivial to construct and is dependent upon the decoding algorithm and its parameters. The random selection approach conducted here is a general empirical method that is independent of the specific decoder and can yield some indication as to factors that are important for word recognition. Our tests examined to some degree the location of frame errors depending on criteria such as silence, vowel and phone transition. Further tests associated with model states can be conducted with other decoders that provide decoding lattice information. The results may be combined and compared to related work by Chang et. al. who analyzed frame errors relative to phone position [21] and Greenberg et. al. who conducted ASR diagnostic evaluations with respect to many acoustic, linguistic and speaker characteristics [42, 41]. As this topic is tangential to this thesis, such a pursuit is left to future investigations. Results from future diagnostics may aid in selecting and training front-end acoustic modeling in a manner better suited to the overall goal of word recognition.

Bibliography

- [1] Fevzi Alimoglu and Etham Aplaydin. Combining multiple representations and classifiers for pen-based handwritten digit recognition. In *Proceedings of the Fourth International Conference on Document Analysis and Recognition*, volume 2, pages 637–40, Ulm, Germany, August 1997.
- [2] Jont B. Allen. How do humans process and recognize speech? *IEEE Transactions on Speech and Audio Processing*, 2(4):567–77, October 1994.
- [3] Christos Antoniou and Jeff Reynolds. Acoustic modelling using modular/ensemble combinations of heterogeneous neural networks. In *International Conference on Spoken Language Processing*, volume 1, pages 282–5, Beijing, China, October 2000.
- [4] Takayuki Arai and Steven Greenberg. Speech intelligibility in the presence of cross-channel spectral asynchrony. In *International Conference on Acoustics Speech and Signal Processing*, volume 2, pages 933–6, Seattle, Washington, May 1998. IEEE.
- [5] Takayuki Arai, Misha Pavel, Hynek Hermansky, and Carlos Avendano. Syllable intelligibility for temporally filtered lpc cepstral trajectories. *J. Acoust. Soc. Am.*, 105(5):2783–91, May 1999.
- [6] Carlos Avendano, Sarel van Vuuren, and Hynek Hermansky. Data based filter design for RASTA-like channel normalization in ASR. In *International Conference on Spoken Language Processing*, volume 3, pages 2087–90, Philadelphia, Pennsylvania, October 1996.
- [7] Jeff A. Bilmes. Joint distributional modeling with cross-correlation based features. In *Proc. IEEE Automatic Speech Recognition and Understanding*, pages 148–55, Santa Barbara, California, December 1997.

- [8] Jeff A. Bilmes and Katrin Kirchhoff. Directed graphical models of classifier combinations: application to phone recognition. In *International Conference on Spoken Language Processing*, volume 3, pages 921–4, Beijing, China, October 2000.
- [9] B. Bogert, M. Healy, and J. Tukey. The quefrency analysis of time series for echos. In M. Rosenblatt, editor, *Proc. Symposium on Time Series Analysis*, chapter 15, pages 209–43. Wiley, New York, 1963.
- [10] Hervé Bouchard and Stéphane Dupont. A new ASR approach based on independent processing and recombination of partial frequency bands. In *International Conference on Spoken Language Processing*, volume 1, pages 426–9, Philadelphia, Pennsylvania, October 1996.
- [11] Hervé Bouchard and Stéphane Dupont. Sub-band based speech recognition. In *International Conference on Acoustics Speech and Signal Processing*, volume 2, pages 1251–4, Munich, Germany, April 1997. IEEE.
- [12] Hervé Bouchard and Nelson Morgan. *Connectionist Speech Recognition- A Hybrid Approach*. Kluwer Academic Press, 1994.
- [13] Christoph Bregler, Herman Hild, Stephan Manke, and Alex Waibel. Improving connected letter recognition by lipreading. In *International Conference on Acoustics Speech and Signal Processing*, volume 1, pages 557–60, Minneapolis, Minnesota, April 1993.
- [14] Christoph Bregler and Yochai Konig. "Eigenlips" for robust speech recognition. In *International Conference on Acoustics Speech and Signal Processing*, volume 2, pages 669–72, Adelaide, SA, Australia, April 1994. IEEE.
- [15] Christoph Bregler, Stephan Manke, Herman Hild, and Alex Waibel. Bimodal sensor integration on the example of 'speechreading'. In *International Conference on Neural Networks*, volume 2, pages 667–71, San Francisco, California, March 1993. IEEE.
- [16] Christoph Bregler, Stephen M. Omohundro, and Yochai Konig. A hybrid approach to bimodal speech recognition. In *Conference Record of the Twenty-Eighth Asilomar Conference on Signals, Systems and Computers*, volume 1, pages 556–60, Pacific Grove, California, October 1994.

- [17] John S. Bridle. Probabilistic interpretation of feedforward classification network outputs, with relationship to statistical pattern recognition. In F. Fogelman Soulie and J. He'roult, editors, *Neurocomputing: Algorithms, Architectures, and Applications*, pages 227–36. Springer Verlag, New York, 1990.
- [18] Pierre J. Castellano, Stefan Slomka, and Sridha Sridharan. Telephone based speaker recognition using multiple binary classifier and Gaussian mixture models. In *International Conference on Acoustics Speech and Signal Processing*, volume 1, pages 1075–8, Munich, Germany, April 1997. IEEE.
- [19] Center for Spoken Language Understanding, Department of Computer Science and Engineering, Oregon Graduate Institute. Numbers corpus, release 1.0, 1995.
- [20] Center for Spoken Language Understanding, Department of Computer Science and Engineering, Oregon Graduate Institute. OGI multi-lingual corpus, 1994.
- [21] Shuangyu Chang, Lokendra Shastri, and Steven Greenberg. Automatic phonetic transcription of spontaneous speech (american english). In *International Conference on Acoustics Speech and Signal Processing*, volume 4, pages 330–3, Beijing, China, October 2000.
- [22] Michael M. Cohen and Dominic W. Massaro. What can visual speech synthesis tell visual speech recognition? In *Conference Record of the Twenty-Eighth Asilomar Conference on Signals, Systems and Computers*, volume 1, pages 566–71, Pacific Grove, California, October 1994.
- [23] Thomas M. Cover and Joy A. Thomas. *Elements of Information Theory*. Wiley, New York, 1991.
- [24] Steven B. Davis and Paul Mermelstein. Comparison of parametric representations for monosyllabic word recognition in continuously spoken sentences. *IEEE Transactions on Acoustics, Speech and Signal Processing*, 28(4):357–366, August 1980.
- [25] A. P. Dempster, N. M. Laird, and D .B. Rubin. Maximum-likelihood from incomplete data via the EM algorithm. *Journal of the Royal Statistical Society Series B*, (39):1–38, 1977.

- [26] Rob Drullman. Temporal envelope and fine structure cues for speech intelligibility. *Journal of the Acoustical Society of America*, 97(1):585–592, January 1995.
- [27] Rob Drullman, Joost M. Feston, and Reinier Plomp. Effect of temporal envelope smearing on speech reception. *Journal of the Acoustic Society of America*, 95(2):1053–64, February 1994.
- [28] Richard O. Duda and Peter E. Hart. *Pattern Classification and Scene Analysis*. John Wiley & Sons, 1973.
- [29] H. Dudley, R. Riesz, and S. Watkins. A synthetic speaker. *Journal of the Franklin Institute*, (227):739, 1939.
- [30] Daniel P. W. Ellis and Jeff A. Bilmes. Using mutual information to design feature combinations. In *International Conference on Spoken Language Processing*, volume 3, pages 79–82, Beijing, China, October 2000.
- [31] J. G. Fiscus. A post-processing system to yield reduced word error rates: Recognizer output voting error reduction (ROVER). In *IEEE Workshop on Automatic Speech Recognition and Understanding*, pages 347–54, 1997.
- [32] James L. Flanagan. *Speech Analysis Synthesis and Perception*. Springer-Verlag, New York/Berlin, 2 edition, 1972.
- [33] Harvey Fletcher. *Speech and Hearing in Communication*. Krieger, New York, 1953.
- [34] Jürgen Fritsch, Michael Finke, and Alex Waibel. Adaptively growing heirarchical mixtures of experts. In *Advances in Neural Information Processing Systems 9*, pages 459–65, Denver, Colorado, December 1994.
- [35] Keinosuke Fukunaga. *Introduction to Statistical Pattern Recognition*. Academic Press, Inc., London, 1990.
- [36] Sadaoki Furui. Speaker independent isolated word recognition using dynamic features of speech spectrum. *IEEE Transaction on Acoustics Speech and Signal Processing*, (ASSP-34):52, 1986.
- [37] Steven Greenberg. Auditory function. In Malcolm J. Crocker, editor, *Encyclopedia of Acoustics*, pages 1301–23. John Wiley, New York, 1997.

- [38] Steven Greenberg. The significance of the cochlear travelling wave for theories of frequency analysis and pitch. In E. R. Lewis and C. Steele, editors, *Diversity of Auditory Mechanics*. World Scientific Press, Singapore, 1997.
- [39] Steven Greenberg. Speaking in shorthand - A syllable-centric perspective for understanding pronunciation variation. In *Proceedings of the ESCA Workshop on Modeling Pronunciation Variation for Automatic Speech Recognition*, Kexrade, United Kingdom, May 1998. ESCA.
- [40] Steven Greenberg, Takayuki Arai, and Rosaria Silipo. Speech intelligibility derived from exceedingly sparse spectral information. In *International Conference on Spoken Language Processing*, Sydney, Australia, November 1998.
- [41] Steven Greenberg and Shuangyu Chang. Linguistic dissection of switchboard-corpus automatic speech recognition systems. In *Proceedings of the ISCA Workshop on Automatic Speech Recognition: Challenges for the New Millennium*. ICASA, Paris, France, 2000.
- [42] Steven Greenberg, Shuangyu Chang, and Joy Hollenback. An introduction to the diagnostic evaluation of Switchboard-corpus automatic speech recognition systems. In *Proceedings of the NIST Speech Transcription Workshop*, College Park, Maryland, May 2000.
- [43] Steven Greenberg and Brian E. D. Kingsbury. The modulation spectrogram: In pursuit of an invariant representation of speech. In *International Conference on Acoustics Speech and Signal Processing*, volume 3, pages 1647–50, Munich, Germany, April 1997. IEEE.
- [44] Steven Greenberg and Michael L. Shire. Temporal factors in speech perception. In *CSRE-based Teaching Modules for Courses in Speech and Hearing Sciences*, pages 91–106. AVAAZ Innovations, London, Ontario, 1997.
- [45] Donald D. Greenwood. Critical bandwidth and the frequency coordinates of the basilar membrane. *JASA*, 33:1344–1356, 1961.
- [46] John H. L. Hansen and Oscar N. Bria. Lombard effect compensation for robust automatic speech recognition in noise. In *International Conference on Spoken Language*

- Processing*, volume 1, pages 1125–8, Kobe, November 1990. The Acoustical Society of Japan.
- [47] Brian A. Hanson and Ted H. Applebaum. Robust speaker-independent word recognition using static, dynamic and acceleration features: Experiments with Lombard and noisy speech. In *International Conference on Acoustics Speech and Signal Processing*, volume 2, pages 857–60, Albuquerque, NM, April 1990. IEEE.
- [48] Hynek Hermansky. Perceptual linear predictive (PLP) analysis of speech. *Journal of the Acoustical Society of America*, 87(4):1738–1752, April 1990.
- [49] Hynek Hermansky. The modulation spectrum in the automatic recognition of speech. In *IEEE Workshop on Automatic Speech Recognition and Understanding Proceedings*, pages 140–7, Santa Barbara, CA, USA, December 1997. IEEE Signal Processing Society.
- [50] Hynek Hermansky and Nelson Morgan. RASTA processing of speech. *IEEE Transactions on Speech and Audio Processing*, 2(4):578–589, October 1994.
- [51] Hynek Hermansky and Sangita Sharma. TRAPS - classifiers for temporal patterns. In *International Conference on Spoken Language Processing*, volume 1, pages 193–7, Sydney, Australia, November 1998.
- [52] Hynek Hermansky, Sangita Tibrewala, and Misha Pavel. Towards ASR on partially corrupted speech. In *International Conference on Spoken Language Processing*, volume 1, pages 462–5, Philadelphia, Pennsylvania, October 1996.
- [53] Kai Hübener. Using multi-level segmentation coefficients to improve HMM speech recognition. In *International Conference on Spoken Language Processing*, volume 1, pages 248–51, Philadelphia, Pennsylvania, October 1996.
- [54] Adam Janin. Multi-stream speech recognition: Ready for prime time? In *EUROSPEECH*, pages 591–4, Budapest, Hungary, September 1999. ESCA.
- [55] Brian E. D. Kingsbury John Wawrzynek, Krste Asanovic and Jim Beck. Spert-ii: A vector microprocessor system and its applications. In *Advances in Neural Information Processing Systems 8*, pages 619–25, Denver, Colorado, November 1995.

- [56] M. I. Jordan and R. A. Jacobs. Hierarchical mixtures of experts and the EM algorithm. *Neural Computation*, 6(2):181–214, March 1994.
- [57] Jean-Claude Junqua, Steven Fincke, and Ken Field. The Lombard effect: a reflex to better communicate with others in noise. In *International Conference on Acoustics Speech and Signal Processing*, volume 4, pages 2083–6, Phoenix, AZ, May 1999. IEEE.
- [58] Noboru Kanedera, Takayuki Arai, Hynek Hermansky, and Misha Pavel. On the importance of modulation frequencies for speech recognition. In *EUROSPEECH*, volume 3, pages 1079–82, Rhodes, Greece, September 1997. ESCA.
- [59] Noboru Kanedera, Takayuki Arai, Hynek Hermansky, and Misha Pavel. On the relative importance of various components of the modulation spectrum for automatic speech recognition. *Speech Communication*, 28:43–55, 1999.
- [60] Brian E. D. Kingsbury. *Perceptually Inspired Signal-Processing Strategies for Robust Speech Recognition in Reverberant Environments*. PhD thesis, University of California at Berkeley, 1998.
- [61] Brian E. D. Kingsbury and Nelson Morgan. Recognizing reverberant speech with RASTA-PLP. In *International Conference on Acoustics Speech and Signal Processing*, volume 2, pages 1259–62, Munich, Germany, April 1997. IEEE.
- [62] Brian E. D. Kingsbury, Nelson Morgan, and Steven Greenberg. Robust speech recognition using the modulation spectrogram. *Speech Communication*, 25(1-3):117–32, August 1998.
- [63] Katrin Kirchhoff. Combining articulatory and acoustic information for speech recognition in noisy and reverberant environments. In *International Conference on Spoken Language Processing*, volume 1, pages 186–9, Sydney, Australia, November 1998.
- [64] Katrin Kirchhoff. *Robust Speech Recognition Using Articulatory Information*. PhD thesis, Universität Bielefeld, 1999.
- [65] Katrin Kirchhoff and Jeff A. Bilmes. Dynamic classifier combination in hybrid speech recognition systems using utterance-level confidence values. In *International Conference on Acoustics Speech and Signal Processing*, volume 2, pages 693–6, Phoenix, AZ, May 1999. IEEE.

- [66] J. Kittler, M. Hataf, R. P. W. Duin, and J. Matas. On combining classifiers. *IEEE Transactions on Pattern Analysis and Machine Intelligence*, 3(20):226–39, 1998.
- [67] Joachim Köhler and Nelson Morgan. JAH-RASTA: Approach for robust speech processing by filtering the trajectories in critical bands. Technical Report TR-93-025, International Computer Science Institute, Berkeley, California, August 1993.
- [68] S. Kullback and R. A. Leibler. On information and sufficiency. *Ann. of Math. Stat.*, (22):79–86, 1951.
- [69] C. J. Leggetter and P. C. Woodland. Speaker adaptation using HMMs using linear regression. Technical Report CUED/F-INFENG/TR.181, Cambridge University, June 1994.
- [70] Adam Krzyżak Lei Xu and Ching Y. Suen. Methods of combining multiple classifiers and their applications to handwriting recognition. *IEEE Transactions on Systems, Man, and Cybernetics*, 22(3):418–35, July-August 1992.
- [71] Markus Lieb and Reinhold Haeb-Umbach. Lda derived cepstral trajectory filters in adverse environmental conditions. In *International Conference on Acoustics Speech and Signal Processing*, volume 2, pages 1105–8, Istanbul, Turkey, June 2000. IEEE.
- [72] Richard P. Lippmann. Speech perception by humans and machines. In *Proceedings of the Workshop on the Auditory Basis of Speech Perception*, pages 309–16, Keele University, England, July 1996. ASRU.
- [73] Yi Lu. Integration of knowledge in a multiple classifier system. In *Industrial and Engineering Applications of Artificial Intelligence and Expert Systems*, pages 557–64, Austin, Texas, May 1994.
- [74] John Makhoul. Linear prediction: A tutorial review. *Proceedings of the IEEE*, (63):561–80, 1975.
- [75] Narendranath Malayath. *Data-Driven Methods for Extracting Features from Speech*. PhD thesis, Oregon Graduate Institute of Science and Technology, 2000.
- [76] K. V. Mardia, J. T. Kent, and J. M. Bibby. *Multivariate Analysis*. Academic Press, London, 1979.

- [77] Dominic W. Massaro and Michael M. Cohen. Auditory/visual speech in multimodal human interfaces. In *International Conference on Spoken Language Processing*, volume 2, pages 531–4, Yokohama, Japan, September 1994.
- [78] Nikki Mirghafori and Nelson Morgan. Combining connectionist multi-band and full-band probability streams for speech recognition of natural numbers. In *International Conference on Spoken Language Processing*, pages 743–6, Sydney, Australia, November 1998.
- [79] Nikki Mirghafori and Nelson Morgan. Transmissions and transitions: A study of two common assumptions in multi-band ASR. In *International Conference on Acoustics Speech and Signal Processing*, volume 2, pages 713–16, Seattle, Washington, May 1998. IEEE.
- [80] Nikki Mirghafori, Nelson Morgan, and Hervé Bouchard. Parallel training of MLP probability estimators for speech recognition: A gender-based approach. In *Proc. of IEEE Neural Networks for Signal Processing Workshop*, pages 140–7, Greece, September 1994. IEEE.
- [81] Nelson Morgan, 1995. Personal Communication.
- [82] Nelson Morgan and Hynek Hermansky. RASTA extensions: Robustness to additive and convolutional noise. In *Proceedings of the Workshop on Speech Processing in Adverse Conditions*, Cannes, France, November 1992.
- [83] Alan B. Oppenheim and Ronald W. Schaffer. *Discrete-Time Signal Processing*. Prentice-Hall, 1989.
- [84] Alan V. Oppenheim. Generalized linear filtering. In B. Gold and C. M. Rader, editors, *Digital Processing of Signals*, chapter 8, pages 233–64. McGraw-Hill, New York, 1969.
- [85] Douglas O’Shaughnessy. *Speech Communication*. Addison-Wesley Publishing Company, Reading, Massachusetts, 1987.
- [86] Nikos Papamarkos and Haris Baltzakis. Off-line signature verification using multiple neural network classification structures. In *13th International Conference on Digital Signal Processing Proceedings*, volume 2, pages 727–30, Santorini, Greece, July 1997.

- [87] Lawrence. R. Rabiner, Biing-Hwang Juang, Steve E. Levinson, and Mohon M. Sondhi. Recognition of isolated digits using hidden Markov Models with continuous mixture densities. *AT&T Technical Journal*, 64(6):1211–1234, July-August 1985.
- [88] Vlasta Radová and Josef Psutka. An approach to speaker identification using multiple classifiers. In *International Conference on Acoustics Speech and Signal Processing*, volume 2, pages 1135–8, Munich, Germany, April 1997. IEEE.
- [89] Tony Robinson and James Christie. Time-first search for large vocabulary speech recognition. In *International Conference on Acoustics Speech and Signal Processing*, volume 2, pages 829–32, Seattle, Washington, May 1998. IEEE.
- [90] H. Sakoe and S. Chiba. Dynamic programming algorithm optimization for spoken word recognition. *IEEE Transactions on Acoustics, Speech, and Signal Processing*, 27(1):43–49, February 1978.
- [91] George Saon, Mukund Padmanabhan, Ramesh Gopinath, and Scott Chen. Maximum likelihood discriminant feature spaces. In *International Conference on Acoustics Speech and Signal Processing*, volume 2, pages 1129–32, Istanbul, Turkey, June 2000. IEEE.
- [92] Thomas Schaaf and Thomas Kemp. Confidence measures for spontaneous speech recognition. In *International Conference on Acoustics Speech and Signal Processing*, volume 2, pages 875–8, Munich, Germany, April 1997. IEEE.
- [93] Manfred R. Schroeder. Recognition of complex acoustic signals. In T. H. Bullock, editor, *Life Sciences Research Report*, number 5, page 324. Abakon Verlag, Berlin, 1977.
- [94] Manfred R. Schroeder. *Computer Speech: Recognition, Compression, Synthesis*. Springer, 1999.
- [95] Richard Schwartz and Yen-Lu Chow. The N-BEST algorithm: an efficient and exact procedure for finding the N most likely sentence hypotheses. In *International Conference on Acoustics Speech and Signal Processing*, volume 1, pages 81–4, Albuquerque, New Mexico, April 1990. IEEE.

- [96] Shihab A. Shamma. Auditory cortical representation of complex acoustic spectra as inferred from the ripple analysis method. *Network: Computation in Neural Systems*, 7:439–77, 1996.
- [97] Robert V. Shannon, Fan-Gang Zeng, John Wyganski, V. Kamath, and Michael Ekelid. Speech recognition with primarily temporal cues. *Science*, 270:303–4, October 1995.
- [98] Sangita Sharma. *Multi-Stream Approach to Robust Speech Recognition*. PhD thesis, Oregon Graduate Institute of Science and Technology, 1999.
- [99] Sangita Sharma, Dan Ellis, Sachin Kajarekar, Pratibha Jain, and Hynek Hermansky. Feature extraction using non-linear transformations for robust speech recognition on the Aurora database. In *International Conference on Acoustics Speech and Signal Processing*, volume 2, pages 1117–20, Istanbul, Turkey, June 2000. IEEE.
- [100] Sangita Sharma, Pieter Vermeulen, and Hynek Hermansky. Combining information from multiple classifiers for speaker verification. In *Proceedings of Speaker Recognition and its Commercial and Forensic Applications*, France, 1998.
- [101] Michael L. Shire. Syllable onset detection from acoustics. Master’s thesis, University of California at Berkeley, 1997.
- [102] Michael L. Shire. Data-driven modulation filter design under adverse acoustic conditions and using phonetic and syllabic targets. In *EUROSPEECH*, pages 1123–6, Budapest, Hungary, September 1999. ESCA.
- [103] Michael L. Shire and Barry Y. Chen. Data-driven RASTA filters in reverberation. In *International Conference on Acoustics Speech and Signal Processing*, volume 3, pages 1627–30, Istanbul, Turkey, June 2000. IEEE.
- [104] Michael L. Shire and Barry Y. Chen. On data-derived temporal processing in speech feature extraction. In *International Conference on Spoken Language Processing*, volume 3, pages 71–4, Beijing, China, October 2000.
- [105] Rosaria Silipo, Steven Greenberg, and Takayuki Arai. Temporal constraints on speech intelligibility as deduced from exceedingly sparse spectral representations. In *EUROSPEECH*, volume 6, pages 2687–90, Budapest, Hungary, September 1999.

- [106] S. S. Stevens and J. Volkman. The relation of pitch to frequency. *American Journal of Psychology*, 53:329, 1940.
- [107] Sangita Tibrewala and Hynek Hermansky. Sub-band based recognition of noisy speech. In *International Conference on Acoustics Speech and Signal Processing*, volume 2, pages 1255–8, Munich, Germany, April 1997. IEEE.
- [108] Volker Tresp and Michinaki Taniguchi. Combining estimators using non-constant weighting functions. In *Advances in Neural Information Processing Systems 7*, pages 419–26, Denver, Colorado, December 1994.
- [109] Sarel van Vuuren. *Speaker Verification in a Time-Feature Space*. PhD thesis, Oregon Graduate Institute of Science and Technology, 1999.
- [110] Sarel van Vuuren and Hynek Hermansky. Data-driven design of RASTA-like filters. In *EUROSPEECH*, volume 1, pages 1607–1610, Rhodes, Greece, September 1997. ESCA.
- [111] Andrew Varga and Herman J. M. Steeneken. Assessment for automatic speech recognition: II. NOISEX-92: A database and an experiment to study the effect of additive noise on speech recognition systems. *Speech Communication*, 12:247–251, 1993.
- [112] Kuansan Wang and Shihab A. Shamma. Auditory analysis of spectro-temporal information in acoustic signals. *IEEE Engineering in Medicine and Biology Magazine*, 14:186–94, March 1995.
- [113] W. C. Ward, G. W. Elko, R. A. Kubli, and W. C. McDougald. The new varechoic chamber at AT&T Bell Labs. In *Proceedings of the Wallace Clement Sabine Centennial Symposium*, pages 343–6, Woodbury, NY, 1994. Acoustical Society of America.
- [114] Steve Waterhouse and Gary Cook. Ensemble methods for phoneme classification. In *Advances in Neural Information Processing Systems 9*, pages 800–6, Denver, Colorado, December 1996.
- [115] David Arthur Gethin Williams. *Knowing What You Don't Know: Roles for Confidence Measures in Automatic Speech Recognition*. PhD thesis, University of Sheffield, 1999.

- [116] Charles Wooters, 2000. Personal Communication.
- [117] Su-Lin Wu. *Incorporating Information from Syllable-length time scales into automatic speech recognition*. PhD thesis, University of California at Berkeley, May 1988.
- [118] Su-Lin Wu, Brian E. D. Kingsbury, Nelson Morgan, and Steven Greenberg. Incorporating information from syllable-length time scales into automatic speech recognition. In *International Conference on Acoustics Speech and Signal Processing*, volume 2, pages 721–4, Seattle, Washington, May 1998. IEEE.
- [119] Su-Lin Wu, Brian E. D. Kingsbury, Nelson Morgan, and Steven Greenberg. Performance improvements through combining phone- and syllable-scale information in automatic speech recognition. In *International Conference on Spoken Language Processing*, volume 1, pages 160–3, December 1998.
- [120] Su-Lin Wu, Michael L. Shire, Steven Greenberg, and Nelson Morgan. Integrating syllable boundary information into speech recognition. In *International Conference on Acoustics Speech and Signal Processing*, pages 987–90, Munich, Germany, April 1997. IEEE.
- [121] Howard Yang, Sarel van Vuuren, and Hynek Hermansky. Relevancy of time-frequency features for phonetic classification measured by mutual information. In *International Conference on Acoustics Speech and Signal Processing*, Phoenix, AZ, May 1999. IEEE.
- [122] Howard Hua Yang, Sarel Van Vuuren, Sangita sharma, and Hynek Hermansky. Relevance of time-frequency features in phonetic and speaker-channel classification. *Speech Communication*, 31(1):35–50, August 2000.
- [123] Liang Zhou and Satoshi Imai. Chinese all syllables recognition using combination of multiple classifiers. In *International Conference on Acoustics Speech and Signal Processing*, volume 3, pages 3494–7, Atlanta, Georgia, May 1996. IEEE.
- [124] E. Zwicker and E. Terhardt. Analytical expressions for critical-band rate and critical bandwidth as a function of frequency. *Journal of the Acoustical Society of America*, (68):1523–5, 1980.